Edith Cowan University

Research Online

2023

Investigation and development of titanium nitride solid-state potentiometric pH sensor

Shimrith Paul Shylendra
Edith Cowan University

Investigation and Development of Titanium Nitride Solid-State Potentiometric pH Sensor

A proposal for a dissertation submitted in partial fulfilment of the requirements for the degree of

Doctor of Philosophy

By: Shimrith Paul Shylendra

Student ID: ▮▮▮▮▮▮

School of Science

Edith Cowan University

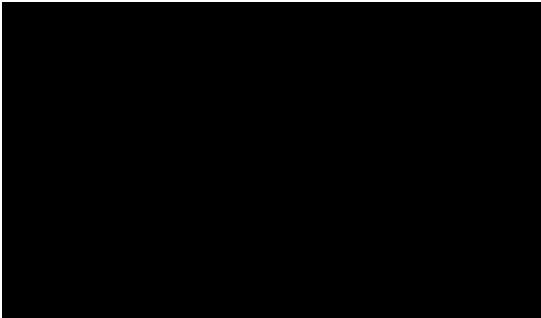**Principal Supervisor**: Professor Kamal Alameh

Associate Supervisor: Dr Magdalena Wajrak

01 March 2023

Declaration

I certify that this thesis does not, to the best of my knowledge and belief:

    I.   incorporate without acknowledgement any material previously submitted for a degree or diploma in any institution of higher education.

    II.   contain any material previously published or written by another person except where due reference is made in the text; or

    III.   contain any defamatory material

    IV.   I also grant permission for the Library at Edith Cowan University to make duplicate copies of my thesis as required.

Signature:

Date: 28/02/2023

Acknowledgements

List of Abbreviations

pH	Logarithmic Scale used to Specify Acidity and Alkalinity
ISFET	Ion Sensitive Field Effect Transistor
EGFET	Extended Gate Field Effect Transistor
PECVD	Plasma Enhanced Chemical Vapour Deposition
SEM	Scanning Electron Microscopy
AFM	Atomic Force Microscopy
ISE	Ion Selective Electrode
RFMS	Radio Frequency Magnetron Sputtering
LP-PECVD	Low Pressure Plasma Enhanced Chemical Vapour Deposition
SEGFET	Structure Extended Gate Field Effect Transistor
MOSFET	Metal Oxide Semiconductor Field Effect Transistor
CAD	Computer Aided Design
FET	Field Effect Transistor
PVD	Physical Vapour Deposition
MOCVD	Metal Organic Chemical Vapour Deposition
PANI	Polyaniline
PI	Polyimide
EDX	Energy Dispersive X-ray
XRD	X-ray Diffraction

List of Publications

1. Paul Shylendra, S., Lonsdale, W., Wajrak, M., Nur-E-Alam, M., & Alameh, K. (2021). Titanium nitride thin film based low-redox-interference potentiometric pH sensing electrodes. *Sensors, 21*(1), article 42. https://doi.org/10.3390/s21010042

2. Shylendra, S.P.; Wajrak, M.; Alameh, K.; Kang, J.J. Nafion Modified Titanium Nitride pH Sensor for Future Biomedical Applications. *Sensors* 2023, *23*, 699. https://doi.org/10.3390/s23020699

3. Paul Shylendra, S.; Wajrak, M.; Alameh, K. Fabrication and Optimization of Nafion as a Protective Membrane for TiN-Based pH Sensors. *Sensors* 2023, *23*, 2331. https://doi.org/10.3390/s23042331

DECLARATION ii

ACKNOWLEDGEMENT iii

LIST OF ABBREVATIONS iv

LIST OF PUBLICATIONS v

TABLE OF CONTENTS vi

ABSTRACT viii

ABSTRACT

The measurement of pH value is crucial parameter in various fields like, drinking water monitoring, food preparation, biomedical and environmental applications. The most common device for pH sensing is the conventional pH glass electrode. While glass electrodes have several advantages, such as Nernstian sensitivity, superior ion selectivity, excellent stability, and extensive operating range, they have several key disadvantages. pH glass electrodes need to be stored in buffer solutions, they are fragile and have limited size and shape, making them impractical for some applications, such as being potentially used as miniature pH sensors for capsule endoscopy and ambulatory esophageal pH monitoring. To address these issues of limitations of glass electrodes, various metal oxides have been investigated and proposed as potential electrode materials for the development of pH sensors. Solid metal sensors offer unique features such as insolubility, stability, mechanical strength, and possibility of miniaturization. However, the main drawback of the metal oxide pH sensors is the interference caused by oxidizing and reducing agents present in some sample solutions.

To reduce the redox interference, metal nitride solid sensors were investigated in this project with the potential for the development of high-sensitivity pH sensing electrodes. Metal nitrides are refractory, have high melting points and interstitial defects, and, at room temperature, they are chemically stable and resist hydrolysis caused by weak acids. There are many reports on different metal nitrides electrodes in literature, of which several have been previously investigated for use as pH sensors. Here, specifically, thin films of titanium nitride (TiN) were manufactured using radio frequency magnetron sputtering. The effect of sputtering parameters (e.g., thickness, sputter power, gas composition) were investigated to optimize the materials for use as pH sensor. Additionally, the underlining mechanism governing the pH sensitivity of these metal nitrides was investigated by examining the pH sensing properties (i.e., sensitivity, hysteresis, and drift) and the effect of redox agents. The successfully optimized material was then used to construct and demonstrate the concept of a solid-state pH sensor using an appropriate reference electrode.

The solid-state TiN sensor paves the way for future development of a miniaturised pH sensor capsule for biomedical applications or lab-on-a-chip pH sensor for environmental and industrial applications. Expending the realms of pH monitoring, currently limited by the glass pH electrode.

CHAPTER 1   BACKGROUND AND LITERATURE REVIEW

1.1   Introduction

The pH scale is well-known. The concept of pH was first introduced back in 1909 by Sorensen [1], and shortly after pH was defined as the negative logarithm of the hydrogen-ion activity in solution.

$$pH = -\log [H^+] \tag{1}$$

Among the various parameters that are monitored of variety of samples, pH value is the most frequently measured [2]. For example, in agriculture, it is important to control the pH of hydroponic nutrient solution supplied to the plants otherwise certain essential elements for growth of the plant will not be absorbed by the root system. pH of soil effects crop yield [3]; in nature, the pH of seawater plays a vital role in ocean's carbon cycle which must be limited to the range of 7.5 to 8.4 [4,5] then; in the brewing industry, pH is important during the brewing process [6], if the pH activity of the amylase enzymes is suboptimal, it starts to suffer significantly resulting in denaturisation of the enzyme [7]. In microbiology, in some microorganisms the metabolic activity will change the pH in cell medium, this can be used detect and quantify bacteria [8], cell biology, the degree of ionisation of intercellular compounds is affected by $[H^+]$, which in turn effects the metabolism and other cell processes. Intercellular pH is kept neutral since this is the pH at which a cell's charge becomes trapped [9]. The pH of drinking water is set forth by regulatory bodies in industrial businesses, such as portable water purification plants, so it must fall within the designated range. Accurate pH monitoring in chemical industries is essential for neutralising the effluent in pulp, steel, and paper. pH monitoring is necessary for many applications [10–12].

The glass pH electrode has been the most reliable choice due to the significance of pH measurement. The working electrode and reference electrode for glass pH electrodes are combined into a single shaft with a double connection, and they are both in contact with an electrolyte (KCl, 3 mol/L). The H^+ activity determines the potential difference that exists across the glass membrane [13]. The Nernst Equation, which is described in Section 1.2.1, is used to calculate the pH of the solution.

Glass electrodes of different sensitivities have been used for the development of specific pH sensors for various sensing applications. However, due to their fragility, large size and manufacturing cost, glass electrodes are impractical for some applications [14,15]. Metal oxide pH sensors, on the other hand, have been considered as an alternative to glass electrodes, due to their ability to be reduced in size and robustness. However, sample matrix interferences typically decrease the sensitivity of metal-oxides-based sensors [16,17], making them impractical for pH monitoring in redox matrix. Consequently, as a possible alternative to metal oxides, metal nitrides have been employed as chemical sensors since they exhibit greater electron mobility and chemical inertness in comparison to other chemical sensor materials. Additionally, nitrides have a greater energy bandgap, high melting point, are significantly hard and exhibit excellent thermal and electrical conductivity [18].

In this study, metal nitrides, specifically titanium nitride, thin films were investigated as a potential replacement for metal oxides as pH sensors. Particular attention was paid to the pH sensing capabilities as well as the impact of redox agents on the metal nitride film.

To investigate metal nitrides as a novel potentiometric sensing material, it is important to understand other materials used for pH sensing, which can be constructed using solid-state-based deposition methods. The following sections will present in detail the theory regarding solid state pH sensors and several approaches to all-solid-state electrode fabrication with mainly five kinds of sensing materials, namely:

- Liquid hydrophobic membranes
- Carbon
- Conducting polymers
- Metal oxides
- Metal nitrides

1.2   Solid State pH Sensors

Solid-state sensors work on the signal response from the processing unit (electronic device or measurement technique used) which measures the physical property sensed within the sensor structure. This physical property leads to an electrical signal that can be amplified and detected

via a voltage/current metre. There are two types of processing units particularly for solid-state pH sensors:

1.   Potentiometric
2.   Amperometric (field effect transistors)

1.2.1   Liquid hydrophobic membranes - ion sensitive electrodes

Liquid-hydrophobic membranes are potentiometric working electrodes [19]. They consist of a membrane made of hydrophobic organic material (usually plasticised PVC), loaded with an ion-selective ionophore. The concentration of the analyte ion being buffered by the ionophore determines the sensing mechanism [20,21]. The potentiometric response of polymeric membrane (organic)-based ion-selective electrodes is controlled by the sample ion's equilibrium at the sample/membrane surface, which gives rise to a phase-boundary potential as shown in Figure 1. The polymer membrane in the ISE has definite number of ionic sites as it controls the total concentration of opposite charged ions in the membrane, which are represented as impurities [22]. Note that, the addition of these sites in high concentration can be used to control the membrane properties. The phase-boundary potential arises due to the unequal distribution of ions, depending on its free energy of transfer and its activity in aqueous and organic phase boundary regions, as shown in Equation (2) [22]:

$$E = \frac{RT}{F} \ln \frac{\alpha \,(aq)}{\alpha \,(org)} \tag{2}$$

where $\alpha \,(aq)$ is the activity in aqueous phase and $\alpha \,(org)$ is the activity of the ion of interest in the hydrophobic membrane, R is the universal gas constant (8.3144 JK^{-1}mol^{-1}), T is temperature (K), F is the Faraday constant (96485 Cmol^{-1}).

A Nernstian response slope is attained because of the activity of cations on the organic membrane being kept constant and independent of its activity in aqueous phases, according to Equation (1). If no interference is experienced from other ions in the sample, then the Nernstian equation (2) of the ISE towards the ion of interest becomes:

$$E = E^0 + \frac{RT}{zF} \ln a(aq) \tag{3}$$

where, E^0 is the standard redox potential (V), z is the charge of the species (1 for H^+), which simplifies to:

$$E = E^0 - 0.0583 \log [(aq)] \tag{4}$$

The "Nernstian" response, which is defined as the output voltage for a 10-fold change in ion activity, is 58.3 mV. In liquid-hydrophobic membranes, the pH sensitive is measured due to its protonation constant, the ionophore tridodecylamine is typically used, and the working range is limited to pH 2-9 [23].

Polymeric Membrane (Organic)   Aqueous Sample
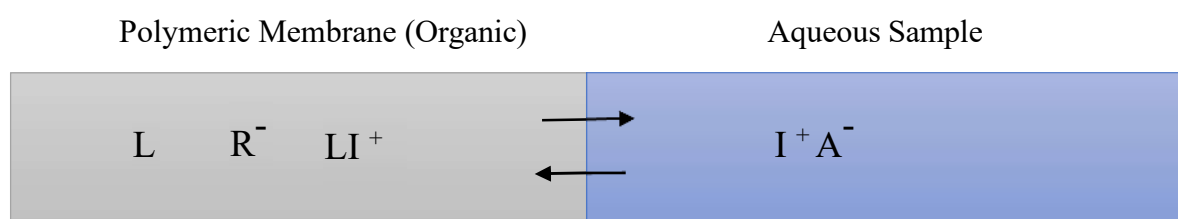
Figure 1 - Scheme for the phase-boundary potential [22]. I^+ is the analyte cation; A^- is the counter anion in the aqueous sample; L stands for the electrically neutral ionophore and R^- is the lipophilic anionic sites.

1.2.2   Carbon and conducting polymers

When the pH of a solution changes, amperometric pH sensors produce a current, while potentiometric pH sensors produce a voltage. Many materials and techniques have been used for amperometric pH sensing. However, carbon has been the widely used electrode material in electrochemistry due to its relatively large potential window, commercial availability, versatility, inertness, and low cost [24]. Oxo- groups are one of the functional groups at the carbon surface, which react with the oxygen in the atmosphere to form various surface oxo-groups, which are sites for electron transfer processes. Of the range of functional groups carbonyl, quinonyl and hydroxyl, the quinone groups, which are pH dependent, have been proposed for the measurement of pH.

Potentiometric stability can be greatly improved by using carbon materials for pH sensing, which make them more attractive as transducers [12]. Single-walled carbon nanotubes have been used as thin film for pH sensing applications [12]. Polymer-bound activated carbon

electrode has been used in super-capacitors [25]. The surface oxo-groups, such as quinones can quantify volumetric redox processes using the Nernst equation [24], which is given by:

$$Ep = E^0_{formal} - \frac{2.3\,RT}{nF}\,pH \tag{5}$$

where, T is temperature (K), R is the universal gas constant (8.3144 $JK^{-1}mol^{-1}$) and n represents the number of electrons. It is obvious from Equation (5) that there is a direct relationship between the peak potential and the pH.

Conducting polymers exhibit some properties like metals and have been implemented as pH sensors. Mainly, conducting polymers such as polypyrrole [26,27] and polyaniline [28,29] have been used as solid-state pH sensors because they exhibit high conductivity like metals, low ionization potential, low energy optical transitions and large surface area when nanostructured. Conducting polymers have alternating single and double bonds. Delocalization of electronic states lead to the formation of energy gaps. Polymer systems are typically unstable and poorly conductive. However, they can be made stable through doping, which generates and balances charge carriers in the polymer chains. For example, polaron present in polymer removes an electron from the system, forming a di-cation, which is a spin-less defect that lies within the band gap of the material, enabling conducting polymers to perform chemical sensing. Conducting polymers are also capable of providing pH sensing capability due to the protonation/deprotonation of functional groups at different pH levels [30].

Polyaniline (PANI) is the most advantageous conducting polymer as it has a variety of oxidation states that are both pH and potential dependent [31]. PANI is found in three different forms: leucoemeraldine (LEB), emeraldine (EB) and pernigraniline (PNB), and the only electrical conducting is the emeraldine salt (ES), which is the protonated form of EB [32]. The protonation process is reversible and the pH sensitivity of PANI is based on the equilibrium of EB ↔ES [32]. Hence, the strong pH sensitivity of PANI makes it a suitable membrane material for all-solid-state pH sensors. However, the main drawback of conducting polymers is that the additives (like: tridodecylmethylammonium chloride in PANI) in the membrane can affect the pH sensitivity [32].

1.2.3   Metal oxides

Metal oxides have been used to sense pH and can be grouped into three categories:

- Metal - Metal Oxide
- Metal Oxide - Metal Oxide
- Ion Sensitive Field Effect Transistor (ISFET)

1.2.3.1 Metal - Metal Oxide

Insoluble hydroxides formed from metals can be used for pH measurements, resulting in a Metal - Metal Oxide sensor. Antimony electrode is the best example, which is commonly used instead of glass electrode [16,17]. The redox potential of the antimony electrode is directly proportional to the proton activity of the solution in the range between pH 3 and 11 [13]. For example:

$$Sb_2O_3 + 6H^+ + 6e^- \leftrightarrow 2Sb + 3H_2O \tag{6}$$

$$E = E^0 \ \frac{RT}{nF} \ln\left(\frac{\alpha\,[Sb]^3.\,\alpha\,[H_2O]^3}{\alpha\,[Sb_2O_3].\alpha\,[H^+]^6}\right) \tag{7}$$

where, E^0 is the standard potential, R is the universal gas constant (8.3144 $JK^{-1}mol^{-1}$), T is the absolute temperature, F is the Faraday constant and a[Sb], a $[H_2O]$, a$[Sb_2O_3]$ and $[H^+]$ are the activities of Sb, H_2O, and H^+, respectively.

$$E = E^0 + 0.0596\log\frac{1}{\alpha\,[H^+]} \tag{8}$$

$$E = E^0 - 0.0583 \log [H^+] \tag{9}$$

Given that $E^0 = 0.512$ [38], Eq. (4) can be simplified to:

$$E = 0.152 - 0.05916 \ pH \tag{10}$$

where, E is the measured potential in Volts (V) at 25 °C.

However, hydrogen electrodes are not simple, their potential can be determined by other electrochemical processes [33,34], such as, corrosion and cathode reduction of oxygen [35]. As the ion exchanging at surface sites that does not necessarily involve a pH dependent redox transition [13]. This makes Sb-Sb$_2$O$_3$ electrodes not suitable for longer operation periods, due to drifting in potential signal.

The fact that metal - metal oxide pH electrodes are built from reasonably affordable nonprecious metals makes them advantageous. Several other metal-metal oxide systems, including those involving; Sn, W, Fe, Ag, Cu, and Zn [17], have also been described. Redox couple-based pH sensors, or metal-oxide-metal-oxide pH sensors, are a superior alternative to metal-metal-oxide sensors [13].

1.2.3.2 Metal Oxide - Metal Oxide

Reversible hydrogen electrode with oxides of Pt, Pd, Rh, Os, Ru and Ir have been investigated and used as pH sensors [14,18,36,37]. Fog and Buck [38] and Kreider *et al.* [39] have investigated these types of conductive oxides and found that they attain the best sensitivity for pH measurement compared to metal-metal-oxide sensors, with IrO$_2$ showing lowest sensitivity to redox agents and higher stability [38].

Fog and Buck [38] proposed five potential mechanisms, including (i) ion exchange of surface -OH sites, (ii) redox equilibrium between two valences, (iii) redox equilibrium involving only one phase, (iv) single phase oxygen intercalation, and (v) steady state corrosion, for the pH sensitivity of electrically conducting metal oxides. The oxygen intercalation explanation, which presupposes proton activity in the liquid phase and oxygen activity in the solid phase, was used to describe the pH sensitivity of the materials. This explanation was based on the observations that; (i) redox agents caused shifts in potential (meaning that the composition of the material influenced potential); (ii) lack of interference from cations; and (iii) the known non-stoichiometric oxygen content of these metal oxides. However, more recently, the pH sensing response of metal-oxide-metal-oxide pH systems is described by a redox equilibrium between two valences. Using Ru as an example [39,40]:

$$Ru^{(IV)}O_2 + e^- + H^+ \leftrightarrow Ru^{(III)}O(OH) \tag{11}$$

$$E = E^0 - \frac{RT}{F} \ln \frac{\alpha[\mathrm{Ru}^{\mathrm{III}}]}{\alpha[\mathrm{Ru}^{\mathrm{IV}}][\mathrm{H}^+]} = \left(E^0 - \frac{RT}{F} \ln \frac{\alpha[\mathrm{Ru}^{\mathrm{III}}]}{\alpha[\mathrm{Ru}^{\mathrm{IV}}]} \right) - \frac{RT}{F} \ln(\alpha[\mathrm{H}^+]) \qquad (12)$$

where E^0 is the standard potential, R is the universal gas constant (8.3144 JK^{-1}mol$^{-1)}$), T is the absolute temperature, F is the Faraday constant and $\alpha[\mathrm{Ru}^{\mathrm{III}}]$, $\alpha[\mathrm{Ru}^{\mathrm{IV}}]$ and $\alpha[\mathrm{H}^+]$ are the activities of $\mathrm{Ru}^{\mathrm{III}}$, $\mathrm{Ru}^{\mathrm{IV}}$ and H^+, respectively [13, 15] . Given an approximately equal proportion of $\mathrm{Ru}^{\mathrm{III}}$ and $\mathrm{Ru}^{\mathrm{IV}}$, Equation 12 is simplified to:

$$E = E_* - 58.6pH \qquad (13)$$

where, E is the measured potential in mV at 22 $^{\mathrm{O}}$C.

The main drawback of metal-oxide pH sensors [15] is their sensitivity to redox species. For example, ferri- and ferro- cyanide have been found to supress the pH response of IrO_2 pH electrodes [38, 41]. Although this could be partially overcome by the application of a Nafion membrane, interference from all redox species could not be achieved. Recently RuO_2 was shown to behave differently; Fog and Buck [38], stated that RuO_2 maintains an almost Nernstian pH response slope when exposed to redox agents, whilst Lonsdale *et al.* [42] showed that the E^0 value of RuO_2 electrodes shifts due to exposure to redox agents, whilst the pH response slope remains Nernstian.

1.2.3.3 ISFET pH-sensors

An Ion Selective Field Effect Transistor (ISFET) is basically a FET system with two electrodes (source and drain) and a semiconductor gate (as shown in Figure 2). Current flowing through the source and drain is measured [33] instead of the potential difference. A reference electrode is needed to form closed electrical circuit and maintain a fixed potential. Source-drain current changes based on the field-effect principle; the surface potential of the gate is modulated by variations in the charge at the insulator-electrolyte interface [43].

In the case of pH sensitive ISFETs the charge at the surface of the gate material (the electrolyte insulator interface) is determined by the pH of the solution and the density of active ion-exchange sites at the electrolyte-insulator interface. The active sites can be acidic, basic, or

amphoteric, to derive explicit expression for the potential ψ_o at the electrolyte-insulator interface oxides of only one type of site of Al_2O_3 is considered. Assuming the possible sites on the oxide surface are A-O⁻, A-OH and A-OH$_2^+$, the acidic and basic character of the neutral site A-OH is characterized by equilibrium constants, K_a, and K_b, as described by Bousse:

$$\text{A-OH} \leftrightarrow \text{A-O}^- + \text{H}^+, \text{ with } K_a = \frac{[A\text{-}O^-][H^+]}{[A\text{-}0]} \tag{14}$$

$$\text{A-OH} + \text{H}^+ \leftrightarrow \text{A-OH}^+, \text{ with } K_b = \frac{[A\text{-}OH_2]^+}{[A\text{-}OH][H^+]} \tag{15}$$

The potential drop at the interface in terms of pH can the written as:

$$E^0 = \left(\frac{2.323kT}{q}\right)\left(\frac{\beta}{\beta+1}\right)(\text{pH}_{\text{pzc}} - \text{pH}) \tag{16}$$

where, $[H^+]$ represents the surface concentration of H⁺ ions, T is temperature (K), q is the charge of an electron (C), k is Boltzmann's constant, pH $_{PZC}$ is the pH of the point of zero charge on the surface and β is proportional to the density of active amphoteric sites:

$$\beta = \frac{2q^2 N_s}{kTC_{DL}}\left(\frac{a_2}{K_{a1}}\right)^{1/2} \tag{17}$$

Where N_s is the number of active sites and C_{DL} is the double layer capacitance (F).
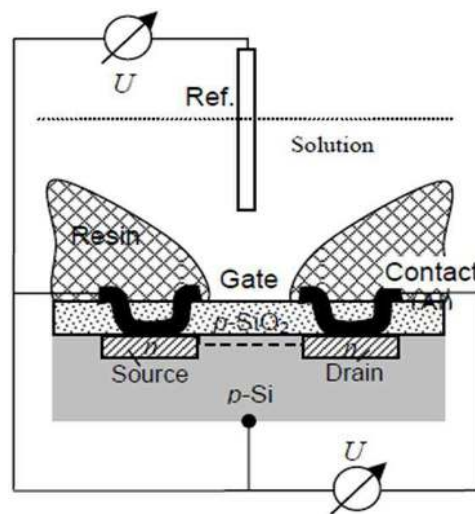

Figure 2 - A solid state ISFET based electrode. Gate is covered by SiO$_2$ layer and the potential difference U_G is between reference electrode and *n*-channel [13].

In a pH sensitive ISFET, the gate is coated with different materials some of them are metal oxides, e.g., Al_2O_3, SiO_2, Al_2O_3 and Ta_2O_5.

ISFETs show some drawbacks when used as pH measuring systems, including long term instability [13], poor stability of the reference electrode [13], inability to attain Nernstian pH sensitivity. The manufacture process plays an important role in the development of high-sensitivity ion sensing thin films as it must ensure a high density of active sites to obtain a Nernstian pH response. Many different manufacture procedures are reported specifically for ISFET-based pH sensors, e.g., sputtering, thermal evaporation, plasma enhanced chemical vapor deposition (PECVD) and sol-gel method [44].

1.2.4 Metal nitrides

The potentiometric or amperometric measurement methods are most used for electrochemical pH sensors [46]. Using either of these measurement techniques, ion selective electrodes, carbon, conducting polymers, metal oxides pH sensors and ISFETs have designed to achieve high selectivity by implementing different pH sensing mechanisms. As discussed earlier, each of these electrodes have their own drawbacks. In this work an alternative approach based on the use of metal nitride electrodes is investigated for the development of potentiometric pH sensors.

Metal nitrides have higher electron mobility and chemical inertness than other chemical sensor materials [47]. Strong metal-to-metal and metal-to-non-metal connections are thought to be promoted by the nitrogen atoms that occupy interstitial locations in the metal in metal nitrides [44]. TiN has been demonstrated to be an effective conducting membrane in applications requiring electronic devices, field emission, and electrochemical capacitors [46]. As a result, pH sensors have regularly employed them (see Table 1).

RuN [45], TiN [48], -BCxNy [49], GaN [50], and Si3N4 [51] are the primary metal nitrides employed for ISFET type pH sensors to date. The pH sensing and non-ideal properties of the sensing membrane have been studied for ruthenium nitride (RuN) [45]. Normally, the ID- VG curves of a current-voltage (I-V) measurement system in standard buffer solutions are used to determine the detecting membrane's sensitivity. ISFET type pH sensors, as illustrated in Figure 3, use MOSFET (Metal Oxide Semiconductor Field Effect Transistor) as a sensing membrane,

with the gate coupled to a RuN pH sensor and the drain and source connected to the current measurement device as shown in Figure 3. A steady potential is kept during the test, and a standard buffer solution is submerged in both the pH sensor device and an Ag/AgCl reference electrode. The VG voltage is raised while the drain-source voltage (VDS) is maintained constant. while measuring the drain-source current (IDS). The sensitivity of the RuN sensing membrane is determined using ID-VG curves [52]. The ruthenium nitride membrane's sensing properties were stable in pH buffer solutions ranging from 1 to 13, and the RuN sensor's sensitivity was 58.03 mV/pH [52]. Despite the great pH sensitivity of these devices, ISFET-based sensors have significant drawbacks, such as long-term drift, hysteresis, and thermal drift, which reduce the accuracy of pH measurement [51]. To overcome these disadvantages, in this work, the durable and non-reactive potentiometric pH sensing method is used.
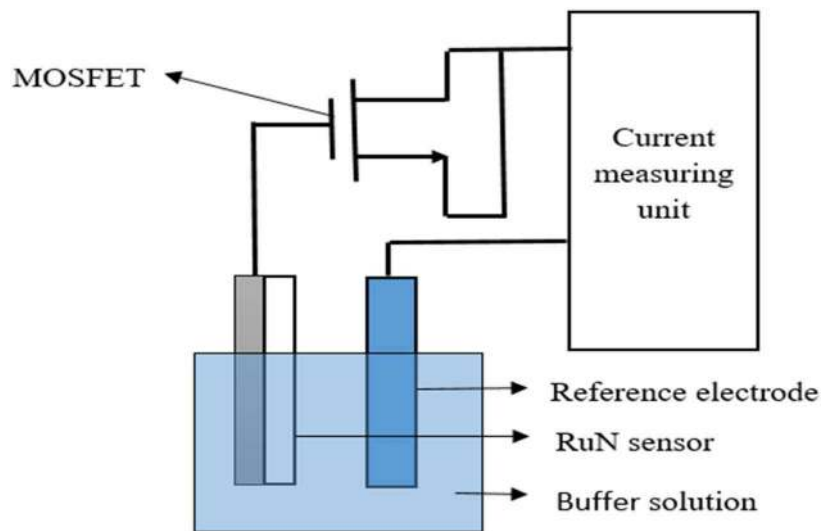
Figure 3 - Current-Voltage Measuring system of RuN pH-sensing membrane with MOSFET.

It has been demonstrated that one metal nitride, titanium nitride (TiN), possesses "super" qualities like a high melting point, substantial hardness, chemical stability, and outstanding electrical and thermal conductivities [10]. A potentiometric pH sensitive sensor made of TiN nanotube arrays [44] has a unique crystal structure where the presence of interstitial atoms causes many holes to form in the lattice. The potential difference between the inside and outside of the crystal is caused by hydrogen diffusing through these holes. This illustrates how TiN's crystal structure changed, leading to its extreme pH sensitivity. Potentiometric pH sensors have been made with TiN [23].

Zirconium nitride (ZrN) and hafnium nitride (HfN) are extremely stable due to a complex blend of covalent and ionic interactions, according to earlier research on metal nitrides from 1997 [35]. Additional research on metal nitrides in 2001 revealed sensitivity of 57 mV/pH [49] when complementary metal oxide semiconductor (CMOS) and extended gate field effect transistor (EGFET) were built on the same chip utilising TiN as a sensing membrane. GaN, AlN, InN, and their alloys were shown to be promising materials for the next generation of chemical and biological sensors by Y.H. Chang *et al.* later in 2011 [36]. Finally, in 2013, K. A. Yusof *et al.* [35] investigated a Si_3N_4 based ISFET and thin-film sensors and showed that those had sensitivities of 53.5 mV/pH and 66.9 mV/pH, respectively.

Several strategies were included for the development of the metal nitride pH electrode throughout the previous two decades (Table 1). Many gaps in the literature still exist despite the substantial research that has been done on metal nitrides as a pH sensor material. Firstly, potentiometric pH sensors have not been developed using metal nitrides; instead, ISFET-based pH sensors have. Since no research has been done on the redox sensing capabilities of metal nitrides, a detailed explanation of the potentiometric pH sensing mechanism of metal nitrides to detect pH value is missing from the literature. Secondly, only TiN [23] has been described as a metal nitride for potentiometric pH sensing; however, the sensing mechanism was never covered. TiN is a potential material for next-generation pH sensors because of its good electrical conductivity, outstanding mechanical qualities, high corrosion resistance, and biocompatibility.

Consequently, in this work the pH sensing properties of TiN will be investigated along with a potential protective membrane. In addition, the redox sensing properties of these materials will be investigated to determine if they are suitable alternatives to existing pH electrodes.

Table 1 - Chronological summary of relevant literature using metal nitrides as a pH sensitive electrode.

Author	Year	Summary
C.G. Ribbing and A. Ross [54]	1997	This work presents ZrN and HfN transition metal nitrides with extreme stability like hardness, chemical inertness, high melting point and Young's modulus. Because of intricate mixture of covalent and ionic bonds these have high stability. ZrN and HfN both are ceramic in terms of hardness, inertness and directed bonds, but metallic with high electrical and thermal conductivity.
Y. L. Chin, J. C. Chou, Z. C. Lei, T. P. Sun, W. Y. Chung, and S. K. Hsiung [55]	2001	This research has demonstrated the fabrication of Complementary metal oxide semiconductor (CMOS) together with extended gate field effect transistor (EGFET) on the same chip. EGFET Titanium nitride (TiN) a conducting material was used as sensing membrane fabricated using R.F. sputtering method. The experimental results show high linear sensitivity 57 mV/pH, hysteresis is 0.5mV cycle of buffer solution pH7→pH4→pH7→pH10→pH7.
C. L. Li, B. R. Huang, S. Chattopadhyay, K. H. Chen, and L. C. Chen [49]	2004	In this work, an extended gate field effect transistor was used for pH measurement with amorphous boron carbon nitride (a-BCxNy) as the sensing membrane. Results showed that the pH sensitivity depends on the carbon content of a-BCxNy sensing membrane, reaching 46 mV/pH for a carbon concentration of 47 at. %.
Y. Wang, H. Yuan, X. Lu, Z. Zhou, and D. Xiao [48]	2006	The fabrication and the response performance of the pH electrode was discussed in the paper. The TiN film electrode was shown to exhibit a linear response from pH range 2-12 with a near-Nernstian response (−55 mV/pH).
Y.-H. Liao and J.-C. Chou [45]	2009	Ruthenium nitride (RuN) sensing membrane non-ideal characteristics for pH sensor was investigated in this research. RuN thin films were R.F. sputtered from a 99.9% pure target on p-type silicon substrates with N_2 gas. The sensitivity of the RuN sensing membrane pH sensor was 58.03 mV/pH.

Y. H. Chang, Y. S. Lu, Y. L. Hong, S. Gwo, and J. A. Yeh [57]	2011	In this paper, authors have shown that the Group III-Nitride including GaN, AlN, InN and their alloys are promising materials for biological sensing, as they are biocompatible, have high sensitivity and robust surface properties, which guards the material from harsh chemical and thermal environments.
		In recent years, InN has become an appealing material for chemical and biological sensing applications because of its unusually strong surface electron accumulation occurring immediately under the surface.
N. S. Lawand, P. J. French, J. J. Briaire and J. H. M. Frijns [56]	2012	This paper demonstrates that TiN is more advantageous than the platinum and iridium noble metals, which are used for nerve stimulation and sensing. Generally, biomedical implants are made of TiN as they have good mechanical properties and high corrosion resistance with extreme biocompatibility.
A. Das *et al.* [50]	2013	This paper reports that gallium nitride (GaN) exhibits some excellent properties, including wide band gap, direct light emission and excellent chemical stability. In this study, pH sensitivity of the fabricated GaN-based light addressable potentiometric sensor (LAPS) was investigated. A Nernstian-like pH response with pH sensitivity of 52.29 mV/pH and linearity of 99.13% was obtained.
K. A. Yusof, N. I. M. Noh, S. H. Herman, A. Z. Abdullah, M. Zolkapli and W. F. H. Abdullah [51]	2013	This work shows the use of chemical vapour deposited silicon nitride as sensing layer. A source measure unit (SMU) was used to measure electrical properties for both Si_3N_4 thin film and Si_3N_4-based ISFET sensor. The pH sensitivity of thin film and ISFET packaged device with silicon nitride were 66.9 mV/pH and 53.6 mV/pH respectively. Both showed good linearity in the chosen pH range.
M. Liu, Y. Ma, L. Su, K. C. Chou, and X. Hou [46]	2016	In this work, TiN nanotube array (NTA) electrode open-circuit potentials were related to pH sensitivity, response time, stability, selectivity, hysteresis, and reproducibility in the pH range of 2-11 at 20°C. The TiN NTA electrode showed a near-Nernstian slope of 55.33 mV per pH with the correlation coefficient value of 0.995.

R. V. Babinova *et al.* [58]	2017	Reactive sputtered hot target titanium nitride has been investigated on the surface morphology and mechanical properties. At low nitrogen flow rate and high discharge current density showed highest hardness (up to 30 GPa) and Young's modulus (up to 300 GPa).
W M Mohammed *et al.* [53]	2017	This paper reported on the use of reactive DC magnetron sputtering to produce thin films of titanium nitride, using titanium metallic target, argon as the plasma gas and nitrogen as the reactive gas. The films were deposited on Si, fused silica and crystalline MgO substrates with various deposition conditions.

1.3 References

1. S. Yao, M. Wang, M. Madou, A pH Electrode Based on Melt-Oxidized Iridium Oxide, J.Electrochem. Soc. 148 (2001) H29. doi:10.1149/1.1353582

2. D. Maurya, A. Sardarinejad, K. Alameh, Recent Developments in R.F. Magnetron Sputtered Thin Films for pH Sensing Applications—An Overview, Coatings. 4 (2014) 756–771.doi:10.3390/coatings4040756.

3. B. Xu, W. De Zhang, Modification of vertically aligned carbon nanotubes with RuO_2 for a solid-state pH sensor, Electrochim. Acta. 55 (2010) 2859–2864.doi: 10.1016/j.electacta.2009.12.099.

4. Royal Society (2005). Ocean acidification due to increasing atmospheric carbon dioxide. www.royalsoc.ac.uk

5. D. E. Briggs, C. A. Boulton, P. A. Brookes, R. Stevens, Brewing Science and Practice, Published by Woodhead Publishing, (2004).

6. A. Fog, R. Buck, Electronic semiconducting oxides as pH sensors, Sensors, and Actuators. 5(1984) 137–146. doi:10.1016/0250-6874(84)80004-9.

7. K. Brandis, 'Acid-base pHysiology'(2015).

8. N. Uria, N. Abramova, A. Bratov, F. Munoz-Pascual, E. Baldrich, Miniaturized metal oxide pH sensors for bacteria detection, Talanta. 147 (2016) 364–369.doi: 10.1016/j.talanta.2015.10.011.

9. L. Bousse and P. Bergveld, 'The role of buried OH sites in the response mechanism of inorganic-gate pH-sensitive ISFETs', Sensors, and Actuators, (1984).

10. D. Wencel, T. Abel, and C. McDonagh, 'Optical chemical pH sensors', Analytical Chemistry. (2014).

11. J. R. Casey, S. Grinstein, and J. Orlowski, 'Sensors and regulators of intracellular pH', Nature Reviews Molecular Cell Biology. (2010).

12. M. Damaghi, J. W. Wojtkowiak and R. J. Gillies, 'pH sensing and regulation in cancer', Frontiers in Physiology. (2013).

13. P. Kurzweil, Metal Oxides, and Ion-Exchanging Surfaces as pH Sensors in Liquids: State-of-the-Art and Outlook, Sensors. 9 (2009) 4955–4985. doi:10.3390/s90604955.

14. S. Głab, A. Hulanicki, G. Edwall, F. Ingman, Metal-Metal Oxide and Metal Oxide Electrodes as pH Sensors, Crit. Rev. Anal. Chem. 21 (1989) 29–47. doi:10.1080/10408348908048815.

15.   L. Manjakkal, B. Synkiewicz, K. Zaraska, K. Cvejin, J. Kulawik, D. Szwagierczak, Development and characterization of miniaturized LTCC pH sensors with RuO2 based sensing electrodes, Sensors Actuators B Chem. 223 (2016) 641–649. doi: 10.1016/j.snb.2015.09.135.

16.   W. Lonsdale, M. Wajrak, K. Alameh, Effect of conditioning protocol, redox species and material thickness on the pH sensitivity and hysteresis of sputtered RuO_2 electrodes, Sensors Actuators B Chem. 252 (2017) 251–256.

17.   P. Kinlen, J. Heider, D. Hubbard, A solid-state pH sensor based on a nafion-coated iridium oxide indicator electrode and a polymer-based silver chloride reference electrode, Sensors Actuators B Chem. 22 (1994) 13–25, https://doi.org/10.1016/ 0925-4005(94)01254-7.

18.   L.-J. Meng and M. P. dos Santos, 'Characterization of titanium nitride films prepared by d.c. reactive magnetron sputtering at different nitrogen pressures', Surf. Coatings Technol., (1997).

19.   P. Buhlmann, L. Chen, Ion-Selective Electrodes with Ionophore-Doped Sensing Membranes, (2011-2015). doi:ISBN: 978-0-470-74640-0.

20.   E. Bakker, E. Pretsch, Potentiometric Determination of Effective Complex Formation Constants of Lipophilic Ion Carriers within Ion-Selective Electrode Membranes, J.Electrochem. Soc. 144 (1997) L125–L127. doi:Doi 10.1149/1.1837633.

21.   J. Hu, K. Ho, X. Zou, W. Smyrl, A. Stein, P. Buhlmann, All-solid-state reference electrodes based on colloid-imprinted mesoporous carbon and their application in disposable paper-based potentiometric sensing devices, Anal. Chem. 87 (2015) 2981–2987. doi:10.1021/ac504556s.

22.   E. Bakker, P. Buhlmann, E. Pretsch, The phase-boundary potential model, Talanta. 63 (2004)3–20. doi: 10.1016/j.talanta.2003.10.006.

23.   S. Anastasova-Ivanova, U. Mattinen, A. Radu, J. Bobacka, A. Lewenstam, J. Migdalski, M. Danielewski, D. Diamond, Development of miniature all-solid-state potentiometric sensing system, Sensors Actuators, B Chem. 146 (2010) 199–205. doi: 10.1016/j.snb.2010.02.044.

24.   M. Lu and R. G. Compton, 'Voltammetric pH sensing using carbon electrodes: Glassy carbon behaves similarly to EPPG', Analyst, (2014).

25.   J. S. Chae, H. N. Kwon, W. S. Yoon, K. C. Roh, Non-aqueous quasi-solid electrolyte for use in super capacitors, Journal of Industrial and Engineering Chemistry,

Volume 59, (2018).

26. F. Yue, T. Ngin, G. Hailin, A novel paper pH sensor based on polypyrrole, Sensors Actuators,B Chem. 32 (1996) 33–39. doi:10.1016/0925-4005(96)80106-7.

27. W. Prissanaroon-Ouajai, P. James Pigram, A. Sirivat, Simple Solid-state Ag/AgCl Reference Electrode, and Its Integration with Conducting Polypyrrole Electrode to produce All-solid-state pH Sensor, KMUTNB Int. J. Appl. Sci. Technol. (2016) 1–9.doi: 10.14416/j.ijast.2016.05.001.33.

28. J. Yoon, S. Hong, S. Yun, S. Lee, T. Lee, K. Lee, B. Choi, High performance flexible pH sensor based on polyaniline nano pillar array electrode, J. Colloid Interface Sci. 490 (2017) 53–58.doi: 10.1016/j.jcis.2016.11.033.

29. J. Bustillo, T. Rearick, W. Hinz and K. Fife, 'ISFET sensor array comprising titanium nitride as a sensing layer located the bottom of a micro well structure.', (2013).

30. Bergveld, P. Development of an ion sensitive solid-state device for neurophysiological Measurements. IEEE Trans. Biomed. Eng. (1970), BME-17, 70-71.

31. T. Lindfors, A. Ivaska, pH sensitivity of polyaniline and its substituted derivatives, J. Electroanal. Chem. 531 (2002) 43–52. doi:10.1016/S0022-0728(02)01005-7

32. T. Lindfors and A. Ivaska, 'pH sensitivity of polyaniline and its substituted derivatives', J. Electroanal. Chem., (2002).

33. R. Rahimi et al., 'A low-cost flexible pH sensor array for wound assessment', Sensors Actuators, B Chem., (2016).

34. W. Lonsdale, D. K. Maurya, M. Wajrak and K. Alameh. 2017. 'Effect of Ordered Mesoporous Carbon Contact Layer on the Sensing Performance of Sputtered RuO_2 thin Film PH Sensor'. Talanta 164(August 2016): 52–56. http://dx.doi.org/10.1016/j.talanta.2016.11.020

35. S. Głab, A. Hulanicki, G. Edwall, F. Ingman, Metal-Metal Oxide and Metal Oxide Electrodes as pH Sensors, Crit. Rev. Anal. Chem. 21 (1989) 29–47. doi:10.1080/10408348908048815.

36. K. A. Yusof, R. Abdul Rahman, M. A. H. Zulkefle, S. H. Herman and W. F. H. Abdullah, 'EGFET pH Sensor Performance Dependence on Sputtered TiO_2 Sensing Membrane Deposition Temperature', J. Sensors, (2016).

37. S. Chalupczok, P. Kurzweil and H. Hartmann, 'Impact of Various Acids and Bases on the Voltammetric Response of Platinum Group Metal Oxides', Int. J. Electrochem., (2018).

38. A. Fog, R. Buck, Electronic semiconducting oxides as pH sensors, Sensors and Actuators. 5(1984) 137–146. doi:10.1016/0250-6874(84)80004-9.

39. K. Kreider, M. Tarlov, J. Cline, Sputtered thin-film pH electrodes of platinum, palladium, ruthenium and iridium oxides, Sensors Actuators B. Chem. 28 (1995) 167–172.doi:10.1016/0925-4005(95)01655-4.

40. W. Lonsdale, S. P. Shylendra, S. Brouwer, M. Wajrak and K. Alameh, 'Application of ruthenium oxide pH sensitive electrode to samples with high redox interference', Sensors Actuators, B Chem., (2018).

41. S. Carroll, R. Baldwin, Self-calibrating micro fabricated iridium oxide pH electrode array for remote monitoring, Anal. Chem. 82 (2010) 878–885. doi:10.1021/ac9020374.

42. W. Lonsdale, M. Wajrak and K. Alameh, 'Manufacture and application of RuO_2 solid-state metal-oxide pH sensor to common beverages', Talanta, (2018).

43. L. Bousse, N. F. De Rood and P. Bergveld, 'Operation of Chemically Sensitive Field-Effect Sensors as a Function of the Insulator-Electrolyte Interface', IEEE Trans. Electron Devices, (1983).

44. L. Bousse, H. H. van den Vlekkert and N. F. de Rooij, 'Hysteresis in Al2O3-gate ISFETs', Sensors Actuators B. Chem., (1990).

45. Y.-H. Liao and J.-C. Chou, 'Fabrication and Characterization of a Ruthenium Nitride Membrane for Electrochemical pH Sensors', Sensors. (2009).

46. M. Liu, Y. Ma, L. Su, K. Chou, X. Hou, A titanium nitride nanotube array for potentiometric sensing of pH, Analyst. 141 (2016) 1693–1699. doi:10.1039/C5AN02675J.

47. R. Chester, T. Jickells, (2012). Marine Geochemistry. Blackwell Publishing. ISBN 978-1-118-34907-6.

48. Y. Wang, H. Yuan, X. Lu, Z. Zhou, and D. Xiao, 'All solid-state pH electrode based on titanium nitride sensitive film', Electroanalysis, (2006).

49. C. L. Li, B. R. Huang, S. Chattopadhyay, K. H. Chen, and L. C. Chen, 'Amorphous boron carbon nitride as a pH sensor', Appl. Phys. Lett., (2004).

50. A. Das Atanu Das, Anirban Da1, Liann Be Chang;, Chao Sung Lai1, Ray Ming Lin1, Fu Chuan Chu1, Yen Heng Lin1, Lee Chow, and Ming Jer Jeng., 'GaN thin film based light addressable potentiometric sensor for pH sensing application', Appl. Phys. Express, (2013).

51. K. A. Yusof, N. I. M. Noh, S. H. Herman, A. Z. Abdullah, M. Zolkapli and W. F. H. Abdullah, 'PH sensing characteristics of silicon nitride thin film and silicon nitride-based ISFET sensor', in Proceedings - 2013 IEEE 4th Control and System Graduate Research Colloquium, ICSGRC 2013, (2013).

52. S. Casans, D. R. Muñoz, A. E. Navarro, and A. Salazar, 'ISFET drawbacks minimization using a novel electronic compensation', Sensors Actuators, B Chem., (2004).

53. W M Mohammed, A I Gumarov, I R Vakhitov, I V Yanilkin, A G Kiiamov, S S Kharintsev, S I Nikitin, L R Tagirov and R V Yusupov, 'Electrical properties of titanium nitride films synthesized by reactive magnetron sputtering', in Journal of Physics: Conference Series, (2017).

54. C. G. Ribbing and A. Roos, 'Zirconium Nitride (ZrN) Hafnium Nitride (HfN)', Handb. Opt. Constants Solids, (1997).

55. Y. L. Chin, J. C. Chou, Z. C. Lei, T. P. Sun, W. Y. Chung, and S. K. Hsiung, 'Titanium nitride membrane application to extended gate field effect transistor pH sensor using VLSI technology', Japanese J. Appl. Physics, Part 1 Regul. Pap. Short Notes Rev. Pap., (2001).

56. N. S. Lawand, P. J. French, J. J. Briaire and J. H. M. Frijns, 'Thin titanium nitride films deposited using DC magnetron sputtering used for neural stimulation and sensing purposes.', in Procedia Engineering, (2012).

57. Wang, S.; Wang, X.; Chen, Z.; Wang, P.; Qi, Q.; Zheng, X.; Sheng, B.; Liu, H.; Wang, T.; Rong, X.; Li, M.; Zhang, J.; Yang, X.; Xu, F.; Shen, B. Enhanced Hydrogen Detection Based on Mg-Doped InN Epilayer. *Sensors* 2018, *18*, 2065. https://doi.org/10.3390/s18072065

58. R V Babinova, V V Smirnov, A S Useenov, K S Kravchuk, E V Gladkikh, V I Shapovalov and I L Mylnikov 'Mechanical properties of titanium nitride films obtained by reactively sputtering with hot target', in Journal of Physics: Conference Series, (2017).

CHAPTER 2   RATIONALE AND PROJECT AIMS

The aim of this project is to manufacture an all-solid-sate pH sensor with the view of developing a sensor that is more robust, flexible, smaller, and cheaper than the glass pH electrode and is capable of measuring pH in a wide range of matrices. According to literature review the interest in ion-selective electrodes (ISE) has increased due to the improved sensor selectivity. However, the pH working range is still limited to pH 2-9 for ISEs. This is where metal-metal-oxides are advantageous; their working range is between pH 2 to 12 and they are made from non-precious metals. However, unfortunately, they suffer from pronounced hysteresis. Additionally, for these electrodes, the potential measurement is also more complicated, because it is determined by other electrochemical processes, apart from hydrogen ion sensing mechanism. A redox couple-based metal-oxide-metal-oxide pH sensors were more suitable alternative to metal-metal-oxide pH sensors, however, they are still problematic, because they are sensitivity to redox species. Finally, carbon and conducting polymers were also studied to improve the potentiometric stability but, the presence of additives in synthetic metals or conducting polymers was found to significantly affect the sensitivity of such sensors. In this work an alternative approach based on the use of metal nitride electrodes is investigated for the development of potentiometric pH sensors.

In the quest for a better pH sensing material and to build on the previous work on RuO_2 sensor, the aims of this research project were:

1. To develop new type of pH sensor by R.F. magnetron sputtering of titanium-nitride (TiN) film

2. To characterise and analyse the sputtered TiN films for their sensor capabilities.

3. To investigate the mechanism of the sputtered TiN thin films in pH sensing, specifically relating to the effects of redox interference.

4. To determine the performance of TiN pH sensor in highly redox samples using potentiometric measurements.

The work here aims to fill gaps in the literature about the manufacture of potentiometric metal nitride pH sensors deposited using R.F. magnetron sputtering, understanding of the pH sensing mechanism and redox interference properties.

CHAPTER 3   METHODS AND MATERIALS

Manufacture of metal nitride pH sensitive electrodes involves sputtering using R.F. magnetron sputtering followed by characterisation to analyse the composition, crystal structure and morphology of the sensing membrane. For this project, titanium nitride has been selected, because it is electrically conducting metal nitride, making it suitable for potentiometric measurements. Also, TiN is durable and chemically resistant. TiN has been demonstrated as pH sensing material using potentiometric detection, however, to the author's knowledge, there are no reports of sputter deposited TiN in literature for pH sensing.

3.1   Manufacturing Process

The manufacturing process for the development of pH sensors comprises the following steps:

- Deposition techniques
- Electrode manufacture

3.1.1   Deposition techniques

There are several thin film deposition techniques that could be used to manufacture metal nitride electrodes for pH sensing. Some of these methods include RFMS, Plasma Enhanced Chemical Vapour Deposition (PECVD), thermal evaporation, sol-gel, Low Pressure Plasma Enhanced Chemical Vapour Deposition (LP-PECVD) and Metal Organic Chemical Vapour Deposition (MOCVD) [1]. The technique that has been chosen for metal-nitride deposition is RFMS, Korea Vacuum Tech KVS-2004L (Figure 4 left) is the system used. It will be able to sputter deposit films with known stoichiometry/composition, well-controlled thickness, high purity and crystal structure, which plays a vital role for studying the material's properties [2].

RFMS will allow the metal nitride deposition parameters like gas ratio variance, film thickness and chamber pressure and deposition power to be trialed, to optimize performance as a pH sensor. The influence of the nitrogen pressure on structural, electrical, and optical properties of TiN films [3] can also be controlled using Radio Frequency Magnetron Sputtering (RFMS). RFMS deposition of thin metal oxide films under controlled parameters have been demonstrated to produce the solid-state pH sensors with excellent performance [4]. The substrates onto which the deposition will be trialed are Alumina (Al_2O_3), glass, silicon (Si) and polyimide (PI) (plastic) to access best suitability and durability of the design.
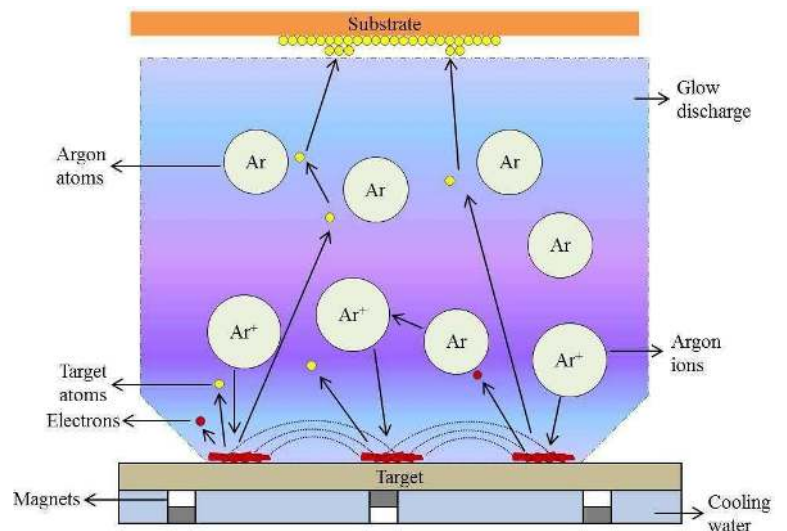
Figure 4 - RFMS system used for deposition of metal nitrides (left), schematic of the deposition process (right) [5].

3.1.2 Electrode manufacture

Electrode manufacture was carried out using the Trotec Speedy 360 flex laser cutter engraver figure 5 (left) is used to manufacture the conductive tract, electrode working area (metal nitride) and electrical connection-pad by etching the nitrides onto the substrate. Laser settings were changed according to the required cutting dimensions and is followed as per the manufacturer's instructions. Alternatively, the same laser system can be used to manufacture stencils for sputter deposition of electrodes. The electrode working area has been isolated using an insulating Gwent dielectric paste (dried at 120 °C for 20 min in air oven) and will be soaked in pH 7 buffer for a week before use, as reported previously [6]. Figure 5 (right) shows a schematic representation of the final electrode.
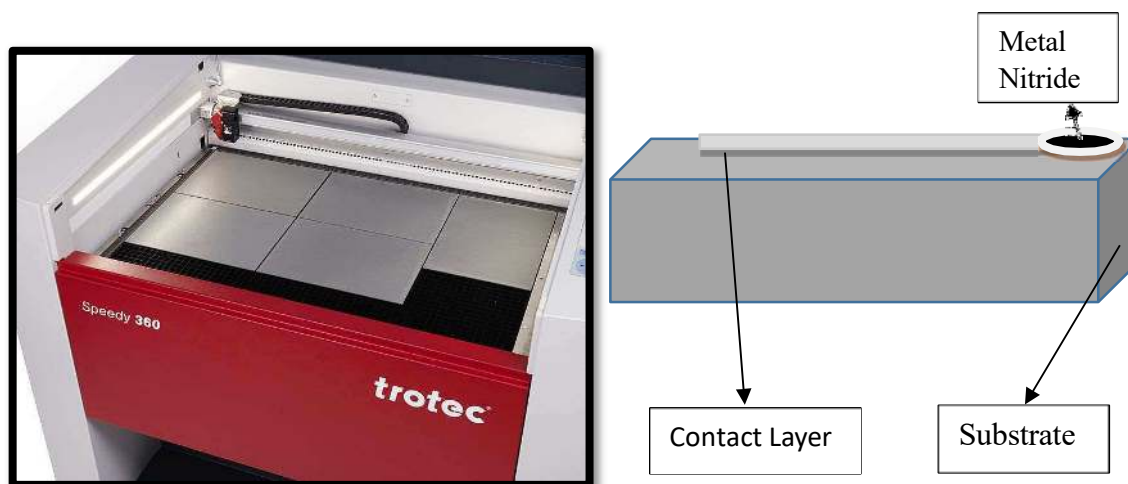
Figure 5 - Trotec Speedy 360 flex laser cutter machine (left) and schematic of the finished substrate electrode with sputtered metal nitride (right).

3.2   Characterisation

3.2.1   Physical characterisation

Sputter deposited metal nitrides will be characterised using several techniques, namely scanning electron microscopy (SEM), energy dispersive spectroscopy (EDX) and X-ray diffraction (XRD). SEM analysis was used to provide information about the material and surface morphology. EDX was used to examine the deposited materials composition, whilst XRD was used to examine crystal structure of the deposited materials. This analysis was performed to identify physical changes that may be related to the pH sensitivity of the materials.

A brief explanation of each technique is given below:

1. Morphology of the developed electrodes was examined using Scanning electron microscopy (SEM). The instrument used was Hitachi SU3500. Isopropyl alcohol was used to clean the samples and completely dried on a hotplate. A scanning electron microscope is a type of microscope that captures picture of the outer layer of the sample material. The sample's atoms meet the focused array of electrons. These connections made by the atoms and electrons produce output information regarding the sample's surface topology. This is a raster scan pattern, and the beam's position is connected to produce an image. SEM works on the resolution of 1 nm or more. Detection of secondary electrons emitted by the atoms within the sample provide specimen topology (Figure 6).
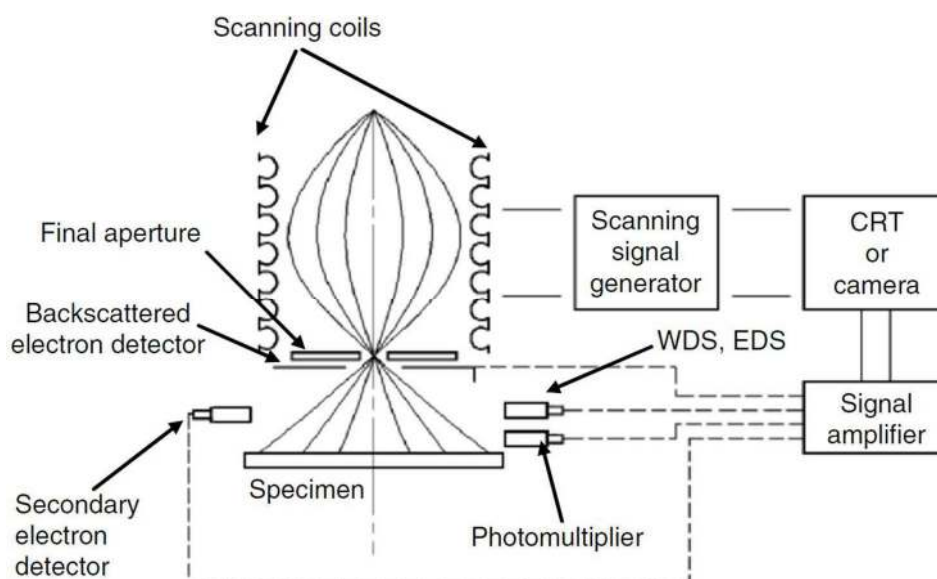
Figure 6 - Schematic representation of the SEM imaging process [73].

2. EDX (Energy Dispersive X-ray) Spectroscopy – Along with lower energy secondary electrons, backscattered electrons and X-rays are generated by primary electron bombardment. The intensity of backscattered electrons can be correlated to the atomic number of the element within the sampling volume. The analysis of characteristic X-rays (EDX or EDS analysis) emitted from the sample gives more quantitative elemental information as in composition of the bulk sample being different compositions, and rough specimens and particle [7]. SEM, accompanied by X-ray analysis, is considered a relatively rapid, inexpensive, and basically non-destructive approach to surface analysis.

3. XRD (X-ray diffraction) - XRD is the only technique that reveals structural information, such as chemical composition, crystal structure, crystallite size, strain, preferred orientation and layer thickness.

Using the above-mentioned physical characterization techniques, information is gained regarding the surface morphology, composition, and crystal structure of the designed thin film, and is used to compare with pH sensing properties.

3.2.2   Electrochemical characterization

In this project, potentiometric measurement was chosen for electrochemical characterisation since it is relatively simple to measure voltage. Many reports claim that metal oxide ISFETs can be incorporated as a measurement technique for pH sensors because of their small size, rapid response, high input impedance and low output impedance. However, according to Zhuiykov *et al.* [8], the ISFET's potential of the electrolyte-insulator interface requires a reference electrode, such that shifts in the voltage, can be measured [8]. Unfortunately, ISFET based measurements are more complex than their potentiometric counterparts, and therefore, the use of an ISFET device was undesirable for this project.

The electrochemical characterization is carried out using potentiometric method where the working (W.E.) and reference (R.E.) electrode's electrical potential is measured which are immersed in the test solution being measured (as shown in Figure 7). The reference electrode provides a stable constant reference potential while the ion selective electrode (ISE) (sensing electrode) responds to the change of the hydrogen ion (H^+) concentration in the solution. The potentiometric pH sensing set up used to access the developed metal nitride working electrodes will use an Atlas Scientific ORP EZO circuit connected to PC via an Electrically Isolated USB EZO Carrier Board (as per the manufactures instructions, to measure the potential between a double junction silver/silver chloride, potassium chloride reference electrode (Ag|AgCl|KCl) and the developed metal nitride working electrodes. Figure 7 shows a representation of the potentiometric setup that will be used.

Measurements were made using the buffer solutions (Rowe Scientific) at 20 ºC until equilibrated. By recording the potential of the buffer solution for specific amount of time until they reach equilibrium, the same was repeated for all the test solutions. The electrode was rinsed using deionised water between each test solution and any excess liquid will be removed using a blast of air. From the recorded potential over time interval a pH loop was generated, the last 30 s was averaged for each of the recordings. The pH sensor characteristics like the sensitivity, E^0, reaction time and hysteresis were analysed in MS Excel spreadsheet format. Each of these metrics is further defined in Table 2 and are summarised graphically below (Figure 8).
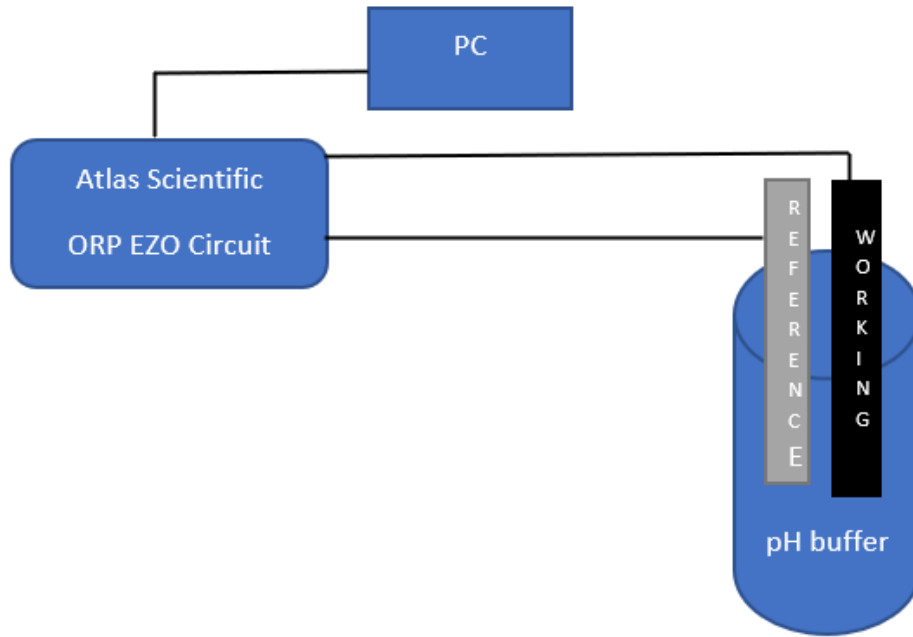
Figure 7 - A glass double-junction reference electrode and as working electrode immersed in pH buffer as a potentiometric measurement set-up.
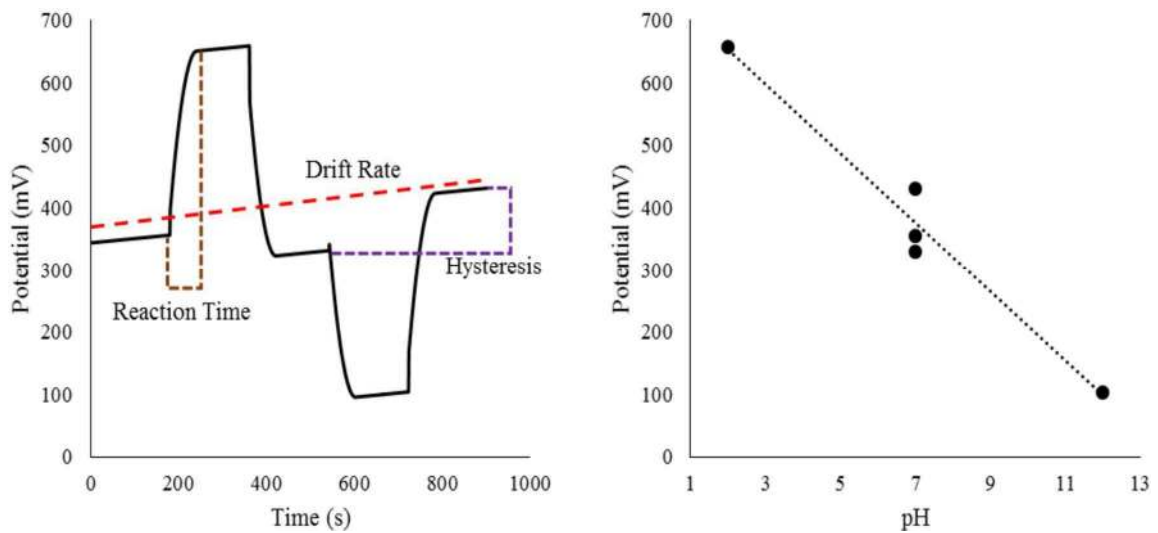
Figure 8 - Graphical representation of pH characteristics using pH data loop (left) and a linear calibration plot (right) [9].

Table 2 - List of pH characteristics tested for a designed pH sensor and their elaboration.

pH Sensor Characteristics	Definition Type
Sensitivity	The sensitivity of a pH electrode is determined by the linear slope response of the pH electrode as defined by the Nernst equation. It is represented in the unit of mV/pH [10].
Response time	The response time is defined as the time at which the pH concentration in a solution is changed on contact with a pH sensor and a reference electrode has reached 95% (or 90%) of the final value. The response time is reported as t95% or t90% in seconds or minutes [10].
Drift rate	The potential drift is defined as the difference between the peak potential value and the 90% value of the saturated potential. The potential drift measured over time is drift rate and generally represented in mV/h [10].
Hysteresis/ Reversibility	Hysteresis is defined as the difference in the electrochemical potentials measured at same pH level. The electrochemical potentials at the same pH level may be different due to various factors, such as different oxidation states and the degree of hydration on the film surfaces, which may establish a new equilibrium of ions every time in the redox reactions at different times of testing [11]. In potentiometric measurements, it is represented in mV [11].
Resolution	The resolution of a pH sensor is defined as the minimum change in pH above the noise floor that can be detected by the pH-sensor [11].

3.3   References

1.   M. B. Cortie, J. Giddings and A. Dowd, 'Optical properties and plasmon resonances of titanium nitride nanostructures', Nanotechnology, 2010. dOI 10.1088/0957-4484/21/11/115201.

2.   B. Subramanian, K. Ashok, and M. Jayachandran, 'Effect of substrate temperature on the structural properties of magnetron sputtered titanium nitride thin films with brush plated nickel interlayer on mild steel', Appl. Surf. Sci., 2008. oi.org/10.1016/j.apsusc.2008.07.083.

3.   M. B. Cortie, J. Giddings and A. Dowd, 'Optical properties and plasmon resonances of titanium nitride nanostructures', Nanotechnology, 2010.

4.   J. Yi-Hung Liaoa, Preparation and characteristics of ruthenium dioxide for pH array sensors with real-time measurement system, Sensors Actuators B Chem. 128 (2008) 603–612.doi:10.1109/ICSENS.2012.6411062.

5.   D. Maurya, A. Sardarinejad and K. Alameh, 'Recent Developments in R.F. Magnetron Sputtered Thin Films for pH Sensing Applications—An Overview', Coatings, 2014. doi.org/10.3390/coatings4040756.

6.   N. S. Lawand, P. J. French, J. J. Briaire and J. H. M. Frijns, 'Thin titanium nitride films deposited using DC magnetron sputtering used for neural stimulation and sensing purposes.', in Procedia Engineering, 2012. doi.org/10.1016/j.proeng.2012.09.250.

7.   J. I. Goldstein, D. E. Newbury, J. R. Michael, N. W. M. Ritchie, J. H. J. Scott, and D. C. Joy, Scanning electron microscopy and x-ray microanalysis. (2017).

8.   S. Zhuiykov, E. Kats, M. Breedon, N. Miura, The influence of Cu2O - doped RuO2 electrode thickness on the sensing performance of planar electrochemical pH sensors, Mater. Lett. 75 2012 165–168. doi: 10.1016/j.matlet.2012.01.107.

9.   W. Lonsdale, (2018). Development, manufacture, and application of a solid-state pH sensor using ruthenium oxide. https://ro.ecu.edu.au/theses/2095.

10.   J. Chou, W. Hsia, Study on the characteristics of the measurement system for pH array Sensors, Int. J. Chem. Biol. 3 2009 308–311. http://www.waset.org/publications/10246. doi.org/10.5281/zenodo.1074871.

11.   X. Zhang, Nitric oxide (NO) electrochemical sensors. In Electrochemical Sensors, Biosensors and Their Biomedical Applications; Zhang, X., Ju, H., Wang, J., Eds.; Academic Press: Waltham, MA, USA, 2011. doi.org/10.1021/acs.chemrev.8b00797.

CHAPTER 4 TITANIUM NITRIDE THIN FILM BASED LOW-REDOX-INTERFERENCE POTENTIOMETRIC pH SENSING ELECTRODES

This chapter was published as an article in the journal MDPI *Sensors*, 2021, Volume 21, Issue 1, 10.3390/s21010042. This article appears as it does in print, except for the abstract being removed, minor changes to the layout, changes to section numbers, font size and font style, which was implemented to maintain consistency in the formatting of this thesis.

This chapter reports on the titanium nitride as a pH sensing material and its advantages of being low-redox interferent pH material. The pilot study on titanium nitride as pH sensor and its application in redox matrices was tested.

4.1   Introduction

The pH scale is well-known, where colloquially a pH of 7 is neutral, whilst acidity increases as the number lowers and alkalinity increasing as the number gets higher. The concept of pH was first introduced back in 1909, and shortly after pH was defined as the negative logarithm of the hydrogen-ion activity in solution [1, 2], as shown in Equation (1).

$$pH = -\log [H^+] \tag{1}$$

Among the measured parameters, pH value is the most frequently measured [3, 4]. For example, in agriculture, pH of soil effects crop yield [5]; in nature, the pH of seawater plays a vital role in ocean's carbon cycle [6]; in the brewing industry, pH is important during the brewing process [7, 8,9], in microbiology [10], sweat monitoring [11]. Intercellular pH is maintained at neutrality as this is the pH at which the charge in the cell gets trapped inside [12,13, 14]. In manufacturing industries, like portable water purification plants, pH of drinking water is set forth by regulatory agencies hence, it must be within the specified range [15]. There are numerous applications which require reliable pH sensors [16].

The glass pH electrode is the most reliable option for pH measurements. Glass pH electrodes consist of a double junction single shaft combining working electrode and reference electrode

(Ag|AgCl) in contact with an electrolyte (KCl, 3 mol/L). The potential difference that occurs across the glass membrane depends on the H^+ activity [17]. The pH of the solution is determined using the Nernst Equation [18]. Glass electrodes of different sensitivities have been used for the development of specific pH sensors for various sensing applications. While glass electrodes have several advantages, such as, Nernstian sensitivity, superior ion selectivity, excellent stability and extensive operating range, they have major disadvantages, including, the requirement for storage in wet condition, fragility, manufacturing cost and limited size and shape, which make them impractical for applications like endoscopic sensor for biomedical application, soil pH testing in harsh environments [19, 21, 22], especially those requiring the pH sensor to have a small footprint. To overcome these issues of glass electrodes, various metal oxides have been investigated and proposed as potential electrode materials for the development of pH sensors, as they offer unique features, such as, insolubility, stability, mechanical strength, and the possibility of miniaturization [4, 23]. However, the main drawback of metal-oxide pH sensors is the interference caused by oxidizing and reducing agents in the sample solution. Most metal oxides are electrically conductive. Nevertheless, they are also sensitive to redox species, e.g., ferricyanide ion in the sample, which influences the pH measurements and results in significant errors, as reported in K.Brandis [8] and making them impractical for the detection of the trace levels of analytes.

To reduce such kind of error, metal nitride is considered as an alternative sensing material. Compared to other chemical sensor materials, metal nitrides exhibit higher chemical inertness, high wear, and high electron mobility [23]. Additionally, nitrides have a greater energy bandgap, high melting point, increased hardness, brittleness, and excellent thermal and electrical conductivity [23]. Nitrogen atoms in the metal nitrides occupy interstitial sites in the metal and are believed to promote strong metal-to-non-metal and metal-to-metal bonds [23]. Specifically, in applications, which require electronic devices, field emission and electrochemical capacitors, TiN has been proven as a suitable conducting membrane [22]. Therefore, in this study metal nitrides thin films were investigated as an alternative to metal oxides for the development of pH sensors. The pH sensing properties of metal nitrides, along with the effects of redox agents on metal nitrides will particularly be investigated for the development of potentiometric pH sensors. To date, metal nitrides have mainly been used for ISFET type pH sensors RuN, $\alpha\text{-}BC_xN_y$, TiN, Si_3N_4 [24-28]. For ruthenium nitride (RuN), the pH sensing and non-ideal characteristics of the sensing membrane have been investigated and

reported by Y.H. Liao *et al.* [24]. The I_D- V_G curves determine the sensitivity of the sensing membrane by a current-voltage(I-V) system in buffer solutions. According to Y.H. Liao *et al.* [24], in a MOSFET based pH sensing membrane, the gate of MOSFET is connected to RuN pH sensor and drain, source is connected to current unit. Both pH sensor device and an Ag/AgCl reference electrode are immersed in standard buffer solution, while a constant potential is maintained throughout the measurement. The drain-source voltage (V_{DS}) is kept constant and V_G voltage is increased while the drain-source current (I_{DS}) is measured. I_D –V_G curves determines the sensitivity of RuN sensing membrane. The sensing characteristics of the ruthenium nitride membrane were stable in pH buffer solution 1 to 13, sensitivity of the RuN sensor was 58.03 mV/pH. Although, these devices have high pH sensitivity, ISFET based sensors show some disadvantages including long-term drift, hysteresis and thermal drift, which limits the accuracy of the pH measurement. Previous work carried out in 1997 on metal nitrides showed that for, example, zirconium nitride (ZrN) and hafnium nitride (HfN) have exceptional surface-stability because of their interlinked mixture of covalent and ionic bonds [37]. Subsequently, research work on metal nitrides was conducted in 2001, where a pH sensor integrating complementary metal oxide semiconductor (CMOS) in conjunction with an extended gate field effect transistor (EGFET) was fabricated on the same chip using titanium nitride (TiN) as sensing membrane, demonstrating a sensitivity of 57 mV/pH [28]. Later, in 2011, Y.H Chang *et al.* [23] showed that Group-III nitrides, including GaN, AlN, InN and their alloys are promising materials for next- generation chemical and biological sensors. Finally, in 2013, K. A. Yusof *et al.* [27] developed and investigated the performances of a Si_3N_4 based ISFET (Ion Selective Field Effect Transistor) sensor and a Si_3N_4 as thin film sensor and demonstrating sensitivities of 53.5 mV/pH and 66.9 mV/pH, respectively.

Despite the work that has been reported on the use of metal nitrides as a pH sensing material, there are still several gaps in this field of research that need to be addressed for developing future-generation ultrafast and miniaturized pH sensors. Firstly, metal nitrides have mainly been used for developing ISFET-based pH sensors, not potentiometric sensors. A thorough investigation of the potentiometric pH sensing mechanism of metal nitrides to detect the pH level is lacking in the literature. Secondly, the only metal nitride reported for potentiometric pH sensing was TiN, however, no study on redox matrix was conducted. TiN is electrically conducting material, with good mechanical properties, high corrosion resistance and biocompatibility, which makes it a promising material for novel pH sensors.

In this work, titanium nitride (TiN) as a pH sensing material has been proposed as an alternative to noble metals, such as gold, platinum and iridium and for existing pH sensing materials. A comprehensive study of thin TiN films fabrication and characterization is presented here, which provides a better understanding of the behavior of TiN as a potential pH sensing layer and its redox effects. TiN layers are manufactured by using RF magnetron sputtering. The effect of sputtering process parameters, such as layer thickness, RF power density to target material and gas composition are investigated to optimize the sputtering process parameters for obtaining the best materials properties suitable for using this film as pH sensor paired up with commercial Ag|AgCl|KCl double junction reference electrode. In addition, the underlining mechanism that governs the pH sensitivity of titanium nitrides is investigated by experimentally testing the pH sensing properties of TiN films (i.e., sensitivity, hysteresis, and drift) for potentiometric sensing. The effect of redox agents on the TiN sensing material have also been experimentally tested and compared with IrO_2-based sensing materials to broaden the sensor applications.

4.2   Materials and Methods

4.2.1   Working electrodes fabrication

Titanium nitride pH working-electrodes were prepared using a RF Magnetron sputtering system on various substrates such as alumina (Al_2O_3), glass, silicon (Si) and polyimide (PI) (plastic). Sputtered-deposition process parameters used for fabrication of metal-nitride thin-films under controlled process to produce the solid-state pH sensors with excellent performance are summarized in Table 1.

Table 1 - Summary of the process parameters and conditions used to prepare thin TiN film layers on various substrates.

Process Parameters	Values
Sputtering target stoichiometry	Titanium Nitride (TiN, 99.95%)
Base pressure (Torr)	$4\text{-}5 \times 10^{-6}$
Argon (Ar) and Nitrogen (Ni) pressure (during deposition)	≈ 2 mTorr
Argon (Ar) and Nitrogen (Ni) gas flow ration	Ar:10 sccm and N_2; 2 sccm
RF power densities	300 W
Substrate stage temperature (°C)	Room Temperature (21 - 23 °C)
Substrate stage rotation rate (rpm)	10-11
Substrates to target distance	15.5 - 16 cm

The substrates were cleaned using acetone and isopropyl alcohol in an ultrasonic bath for 15-30 minutes, after which they were completely dried on a hot plate at 120 ^{0}C. Titanium nitride layer of thickness about 85 nm, was sputtered from a 4-inch diameter titanium target (99.95% purity). Figure 1 shows a schematic diagram of RF magnetron sputtering system where a Titanium (Ti) metallic target of 4-inch (10.16 cm) diameter has been installed inside the chamber. TiN thin films about 85 nm were deposited by allowing nitrogen during the deposition process. The gold-colored titanium nitride coated films on glass substrate confirmed the presence of TiN layer on the substrates as can be seen in the insert of Figure 1.
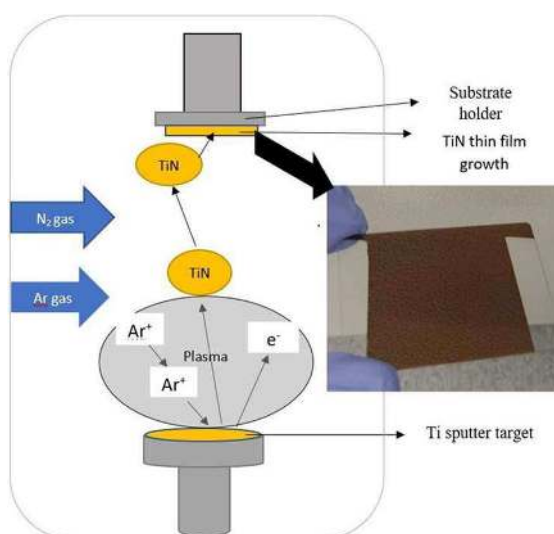

Figure 1 - Schematic diagram of RF Magnetron sputtering system used to prepare the TiN thin-film layers**.** Insert showing the image of deposited TiN film on glass substrate.

4.2.2 pH characteristics by potentiometric method

An Atlas Scientific ORP EZO circuit was used to record potential differences between the pH electrodes (reference and working electrodes) in real time, connected to a PC via an electrically isolated USB EZO carrier board, as a potentiometric setup. The working electrodes were cleaned with blasts of air at each measurement. The electrode was equilibrated in pH 7 overnight before the actual test to obtain stable potential readings. The potential was recorded with 70s interval in Rowe Scientific commercial pH 2, pH 4, pH 7, pH 10 and pH 12 buffer solutions at 22 ºC, coupled with a commercial Ag|AgCl|KCl double junction glass reference electrode. The pH acidic and alkaline loop cycles of 7-4-7-10-7 and 7-2-7-12-7 were used for testing and repeated three times, of which the last 30s potential values were averaged to calculate the sensitivity, E^0 and hysteresis, which represents the difference of consecutive measurements at pH 7, and drift, which represents the shift in potential at pH 7 over the entire test period.

4.3   Results and Discussion

4.3.1 Characteristics results of sputtered TiN films

TiN films were prepared on four different substrates; alumina (Al_2O_3), glass, silicon (Si) and polyimide (PI) (plastic) to investigate the adhesion behavior of TiN film. Each substrate was treated with deionized water for one hour in an ultrasonic bath prior to sputtering. Sputtering parameters, such as, gas ratio, chamber pressure and deposition power were varied to optimize sensor performance. Several trails of deposition runs have been conducted in various (nitrogen-deficient and nitrogen-rich) conditions and confirmed that the argon flow rate influenced the grain size, whilst the argon and nitrogen gas ratio determined the structural and electrical properties of the TiN films [29, 30]. It was noted that the color of the TiN films (as shown in Figure 2) was related to the sputtering process parameters.

Figure 2 - Sputtering parameters variation resulting in three different colored TiN films; green, gold and grey (from left to right).

The pH sensing properties of green, gold, and grey colored TiN films are tabulated in Table 2. The pH sensitivity is determined by the slope of the potential difference(mV) versus time (seconds), the intercept of the slope is the E^0 potential, hysteresis is the difference in the electrochemical potentials measured at same pH level and drift is difference between the peak potential value and the 90% value of the saturated potential. The gold film exhibited Nernstian sensitivity of -59 mV/pH while, both the green and grey films had a sub-Nernstian pH sensitivity of -55 mV/pH. The gold film exhibited the best characteristics with the least hysteresis and drift of 1.2 mV and 3.9 mv/hr, respectively. Consequently, the gold-colored film was adopted as the optimal material and its color chromaticity and sensing properties were subsequently investigated.

Table 2 – pH sensitive properties of coloured TiN films

Film color	Sensitivity (mV/pH)	Hysteresis (mV)	Drift (mV/Hr)	E^0 (Potential) (mV)
Green	-59.0	2.8	8.0	476
Gold	-59.1	1.2	3.9	483
Grey	-55.2	9.1	3.4	423

4.3.2 Color chromaticity properties of as-deposited TiN films

The color chromaticity properties of as-deposited TiN thin films were characterized using a Konica Minolta 508D colorimeter. The chromaticity values of the gold thin TiN film were characterized based on the Hunter *L, a, b* color scale. The explanation of the Hunter Lab color space is presented K. P. Lovetskiy *et al.* [31] and Nur-E-Alam *et al.* [32]. The *L* value represents the black and white color depending on the values (0 - 100) and *a* and *b* values represent red to green and yellow to blue, respectively. Table 3 reports the correlation between the film color and the process parameters.

Table 3 - Sputtering parameters for titanium Nitride different colored thin film deposition.

Film colors	Gas ratio (Ar: N$_2$) (sccm)	Sputter pressure (Milli Torr)	Sputter power (watts)
Green	09:01	10	200
Gold	10:02	2	350
Grey	10:10	10	350

The measured Hunter Lab values of two gold TiN film samples (sputtered time was around 60 mins +/- 1 min) are shown in Table 4. In this work, to analyze the color of thin TiN film, L value was considered rather than the **a** and **b** values, as the specific film's color will mostly be determined by the color evaluated by the human eye. The accuracy of measured **L** values to the simulated values was between 0.07 - 0.1% and indicated by the grey colored film. However, the measured **a** and **b** values for both samples were found to be positive, and that agreed with the simulated values indicating red and yellow color respectively as shown in Figure 3 and thus confirms the gold color of the TiN film.

Table 4 - Measured and simulated color values of TiN films.

TiN film	Simulated hunter values			Measured hunter values		
	L	*a*	*b*	*L*	*a*	*b*
Gold film 1	43.85	5.1	12.43	43.75	7.23	8.69
Gold film 2	40.67	7.8	6.07	40.60	6.68	6.96

4.3.3 Effect of TiN film thickness

It is well known that film or layer thickness of the pH sensing materials has a significant effect on the pH sensitivity [38]. We have measured the TiN film thicknesses during the deposition process using a quartz microbalance sensor which was installed inside the sputtering chamber and reconfirmed by repetitive multiple sputtering trails. The thickness of electrodes was varied from 25 nm to 500 nm and hydrated in a pH 7 buffer for one week to eliminate any effects of aging. Electrodes were then equilibrated for 1 hour at pH 7 and looped from pH 12 to 2 with pH 7 between each step in 90 s intervals. The thickness results, displayed in Table 5, show that

the sensitivity remains close to Nernstian (-58.6 mV/pH at 22^0 C) values for all thicknesses, except 20nm. A precision value (defined as hysteresis to sensitivity ratio) of 0.05 is deemed acceptable for many pH applications. An 85 nm thick TiN layer provides a precision of 0.06 pH, which represents the minimum adequate thickness for most pH applications. Notwithstanding, it can also be seen from Table 4 that electrodes with thicknesses of 100 and 200 nm would be incorporated in applications that require a precision value better than 0.05. There was no consistent trend observed for electrode hysteresis with the increment of the TiN layer thickness. However, a notable increase in the drift parameter was observed when the layer thickness increased from 85 nm to 500 nm. An 85nm thick TiN electrode was selected as the optimal, since it exhibited the least amount of drift, with a Nernstian sensitivity of -59.1 mV/pH and a precision of 0.06 pH.

Table 4 - Summary of 25 to 500 nm TiN film sensor properties in the 2-12 pH range, equilibrated at pH 7.

Thickness (nm)	Sensitivity (mV/pH)	E^0 (mV)	R^2	Hysteresis (mV)	Drift (mV/h)	Precision (pH)
20nm	-49.2	498	0.9972	5.8	18	0.1
50nm	-57.5	335.1	0.9991	5.5	9	0.1
85nm	-59.1	483	0.9997	1.2	3.9	0.06
100nm	-58.3	450	0.9996	1.8	4.8	0.03
200nm	-57.5	411.3	0.9999	0.8	5.4	0.01
300nm	-58.2	399.4	0.9998	1.3	11.8	0.2
500nm	-58.5	442.8	0.9995	2.4	15.5	0.2

4.3.4 Measurement of the TiN film thickness

The optical transmission spectra of as-deposited TiN films were measured using an Agilent Cary 5000 spectrometer. As discussed in Section 4.3.3, thickness of 50nm to 100nm showed consistent increase in drift and hysteresis as the thickness escalated. Figure 3 shows that the film thickness exhibited a transmission band in visible region (380 - 750nm) and as the thickness decreases the transmission percentage and width of the wavelength band increased. These findings agree with those reported by Y.L. Jeyachandran *et al.* [40]. The 85nm thick film was tested twice to reassure the thickness reading from the microbalance sensor. As shown in Figure 3, the optical spectrum of both 85 nm TiN films overlaps each other confirming the accuracy of the film thickness readings obtained in Section 4.3.3.
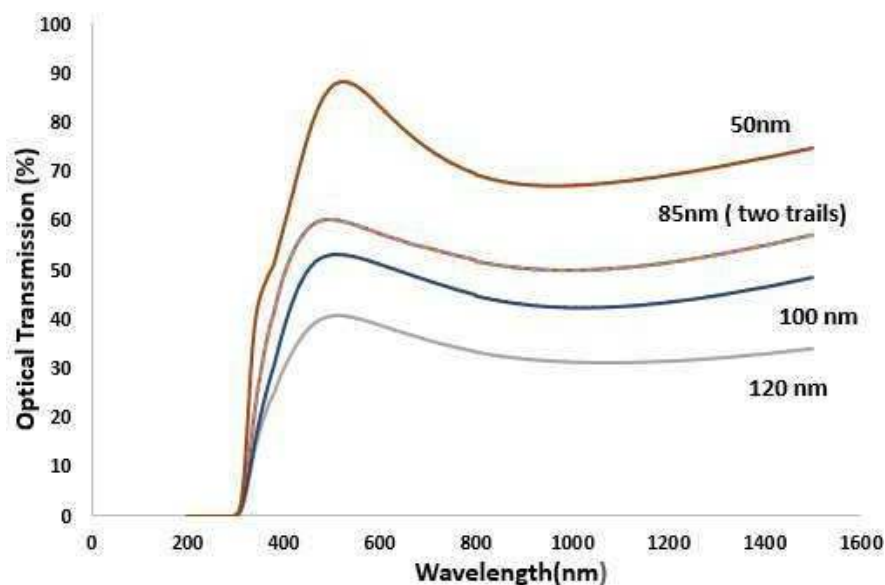
Figure 3 - Transmission spectra of TiN films deposited onto clear glass substrate, using 350 watts RF power to the Ti target under 2mT pressure with the Ar (10 sccm) and N_2 (2 sccm) gas flow.

4.3.5 Microstructure characterization of the sputtered TiN film

Hitachi SU3500 SEM was used to understand the microstructural development of TiN films on glass substrate prepared by R.F magnetron sputtering. The samples are cleaned with isopropyl alcohol and dried on hot place completely before analysis. Figure 4 shows the SEM images of the as obtained 85nm TiN films deposited with different Ar/N_2 ratios resulting in green, grey and gold films. The microstructural growth of TiN films is completely dependent on the sputtering gas ratio and different nitrogen ratios flowing into the sputtering chamber results in different roughness of the surface and electrical conductivities. It is observed that as the nitrogen concentration is low ($Ar/N_2 = 9:1$, 10:2) the surface appears rough with crystalline TiN formations uniformly distributed, Fig.5 (a,c), whereas when the nitrogen concentration is increased ($Ar/N_2 = 10:10$) the surface becomes smoother and there are no crystalline TiN formations, Fig.5(c). There is a relationship between the structural characteristics observed with the SEM and the sensing capabilities of these electrodes. The electrodes deposited with ratios $Ar/N_2 = 9:1$ and 10:2 exhibit Nernstian sensitivity while the $Ar/N_2=10:10$ sputtered electrode gave sub-Nernstian sensitivity. The gas flow inside the sputtering chamber during deposition (Ar:10, N_2:2 sccm) resulted in a Nernstian sensitivity with low hysteresis and drift, as discussed in Section 4.3.3). TiN has a special crystal structure, where the presence of interstitial atoms creates many holes within the lattice. Nitrogen atoms in the metal nitrides occupy the interstitial sites in the metal and promote stronger metal-to-non-metal and metal-
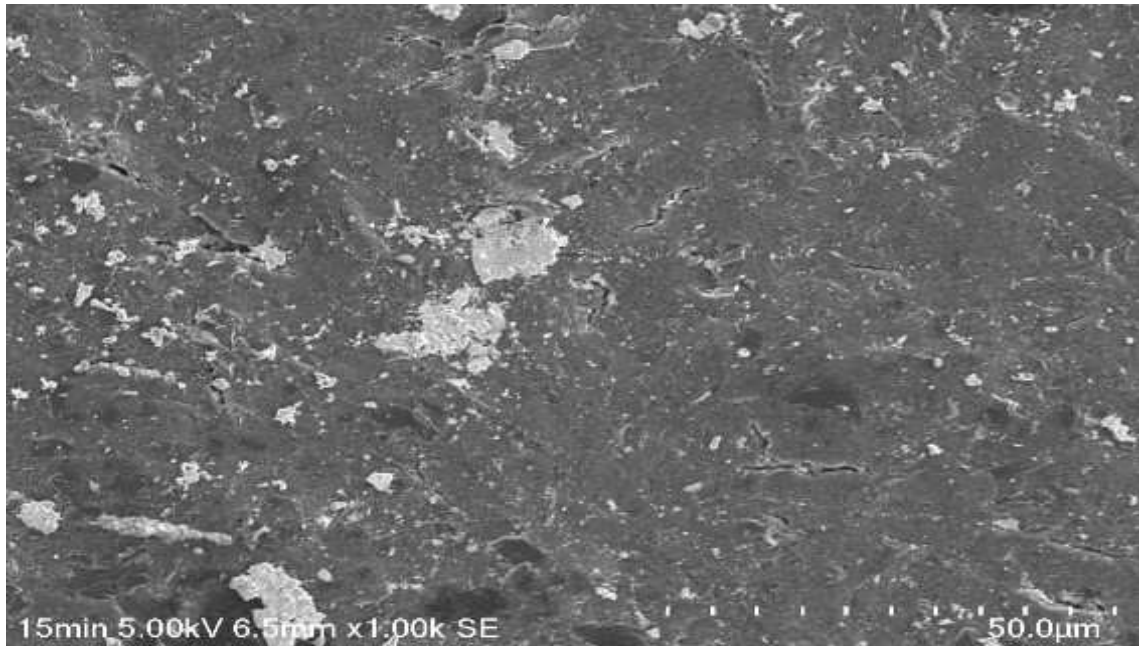
to-metal bonding. Also, hydrogen ions can diffuse between these holes, resulting in a potential difference inside and outside the crystal as reported in S. Bellucci *et al.* [33], thus increasing the pH sensitivity of the TiN film.
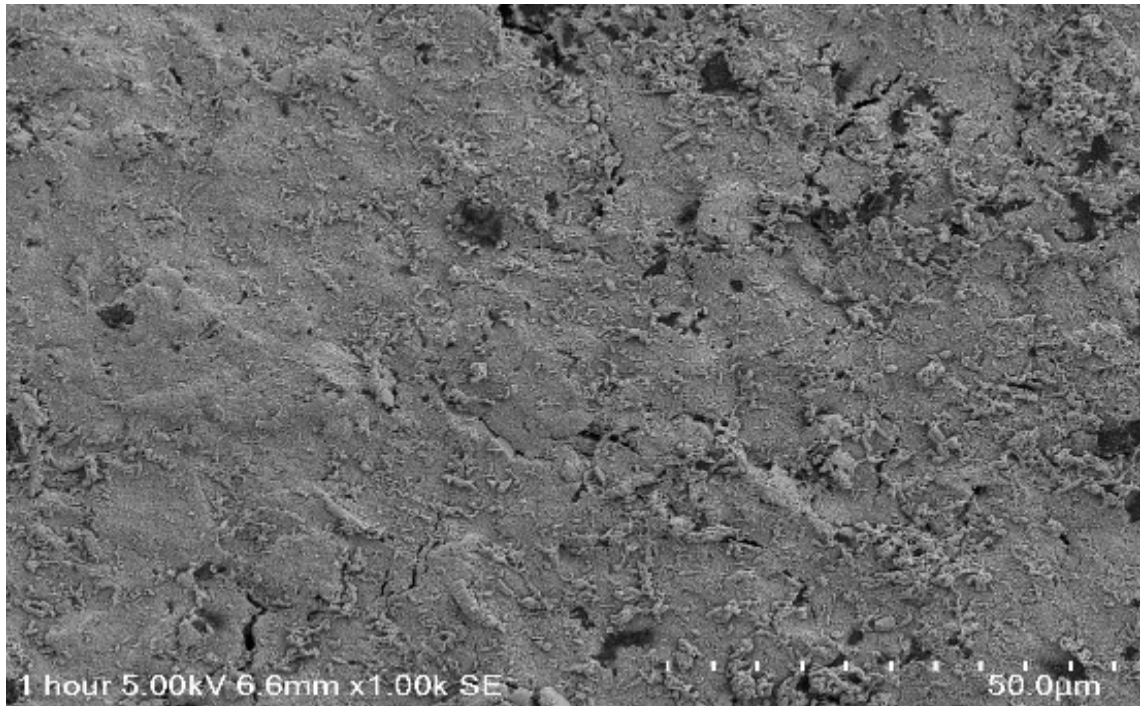
(a)
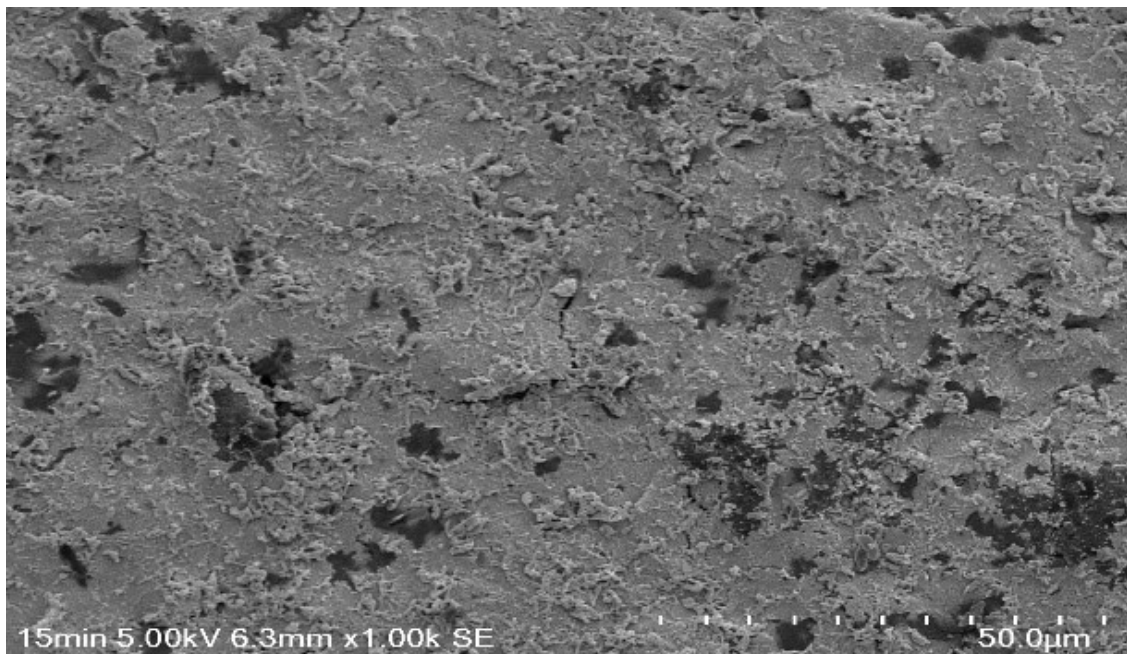
(b)

(c)

Figure 4 - SEM images of TiN films deposited on the glass substrates using different process parameters: (a) TiN surface magnified x 1000 prepared at 9:1 (Ar:N_2)gas ratio, (b) surface showing smooth morphology prepared at 10:10 (Ar:N_2) gas ratio, (c) TiN surface at 10:2 (Ar:N_2) gas ratio.

4.3.6 X-ray photoelectron spectroscopy analysis

The XPS survey spectra of unetched 85nm thick TiN prepared at 2mT sputter pressure and Ar: 10, N_2:2 sccm showed that the chemical compositon of the surface of the film was: carbon, oxygen, titanium and nitrogen as shown in Figure 5. The precise characteristic studies of these main elements reaveals Ti2p,O 1s and N1s peaks as shown in Figure 5 (b),(c),(d) respectively. The C 1s peaks seen in the spectra could be the contribution from organic carbon, Si 2p and Na 1s is from the unetched TiN surface on a glass substrate as Na atoms can easily diffuse onto the surface because of its increased mobility factor.
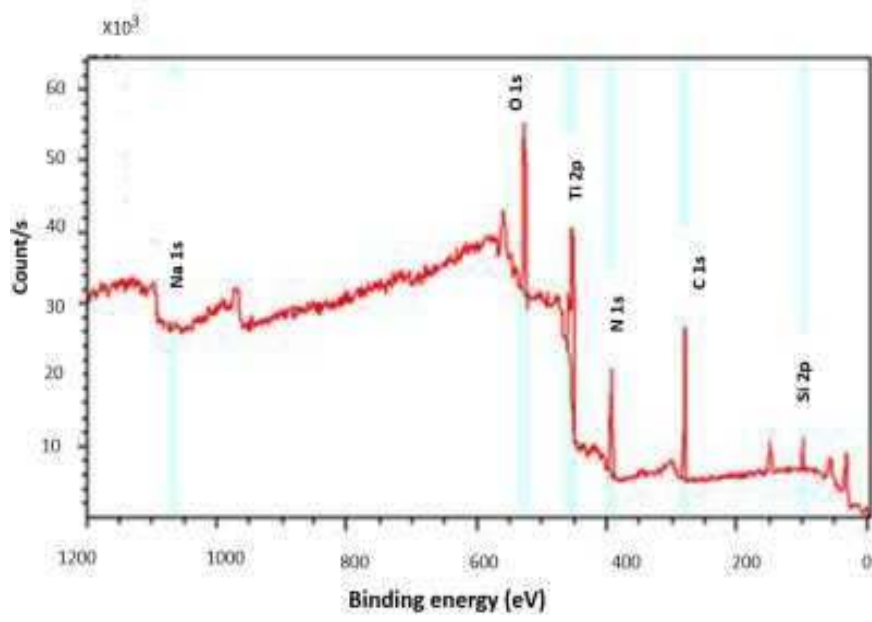
(a)
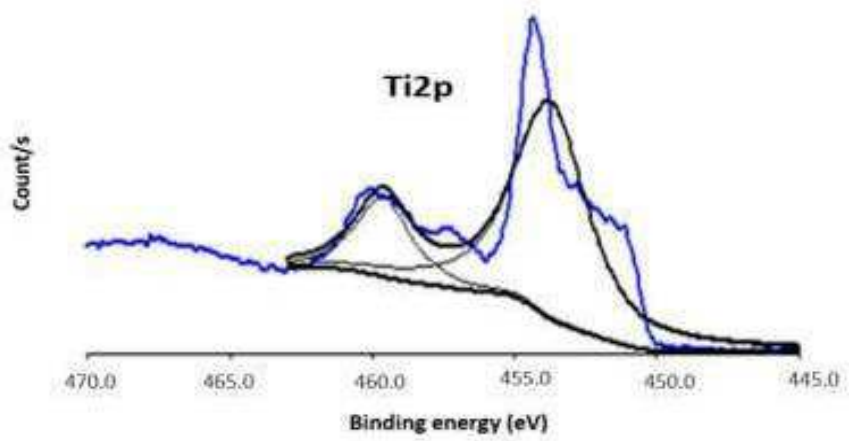
(b)
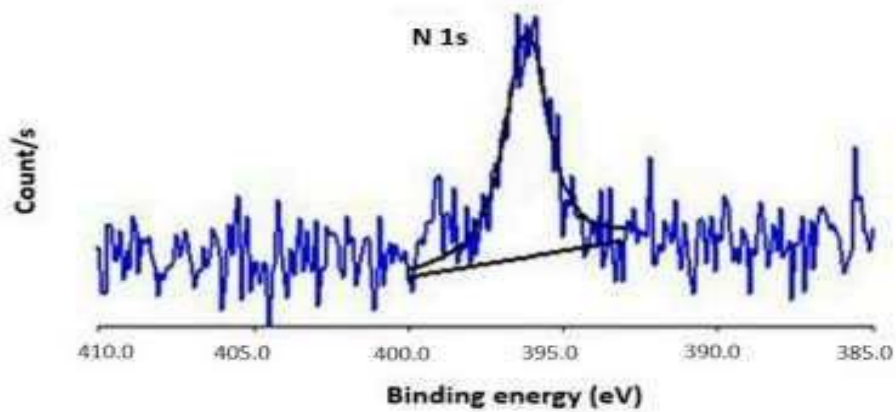
(c)
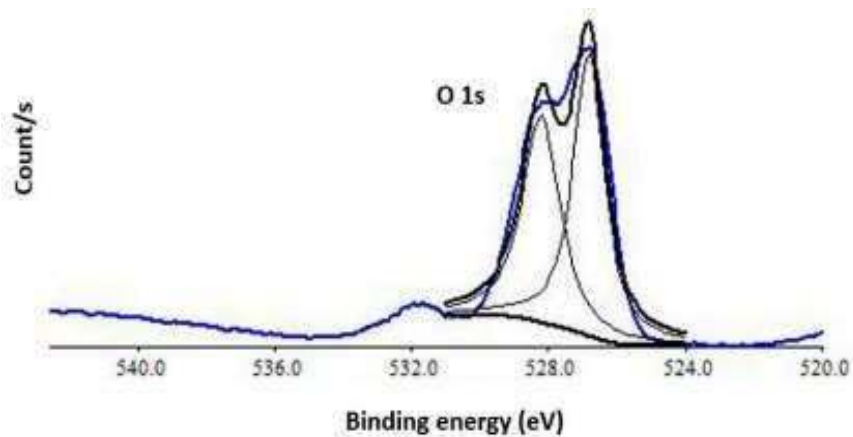
(d)

Figure 5 - XPS characterization of 85nm TiN film: (a) XPS survey spectra of the unetched 85nm sputtered TiN film (b) XPS spectrum of 2p states of titanium (c) XPS spectrum of 1s states of nitrogen (d) XPS spectrum of oxygen.

Figure 5(b) shows two peaks at binding energies of 458.9 eV and 454.5 eV. These peaks correspond to the presence of TiO_2 (Ti^{4+}) and TiN (Ti^{3+}) (2p3/2) compounds [36, 37]. The atomic percentages of Ti2p and N1s are 39.85% and 60.1%, respectively. There was no evidence of metallic titanium present on the surface since no peak was observed at 459.7 eV [38]. The N1s peak at 396.1 eV corresponds to TiN and the O1s peak at 529.1 eV belongs to TiO_2 [39, 40]. No hydroxide compounds were found in O1s spectra, and the source of oxygen

seen in the spectra can be from the gas medium in the sputtering chamber or from atmospheric contamination. The surface analysis of TiN shows that titanium in the oxide form is actually thermodynamically more favorable to form than titanium nitride in this sputtering environment. This explains the presence of TiO_2 in the titanium spectra.

4.3.7 Sensor performance

The sensitivity of the developed TiN-based pH sensor was evaluated by immersing it in a test buffer from 2 to 12 at 22 ºC. The Nernstian sensitivity of -59.1 mV/pH was obtained by incorporating a glass electrode as the reference electrode. The developed pH sensor was evaluated by looping pH from 2 to 12, as shown in Figure 6. The developed sensor shows close to Nernstian sensitivity (-59.1 mV/pH). Table 5 and Figure 8 show the main properties and the pH response (potential versus pH value) of the developed TiN pH sensor. As seen in Figure 7, the pH response of the sensor is linear (R^2=0.9997).

Table 5 - Summary of the pH sensing performance of the developed TiN pH sensor. The data is extracted from Table 5.

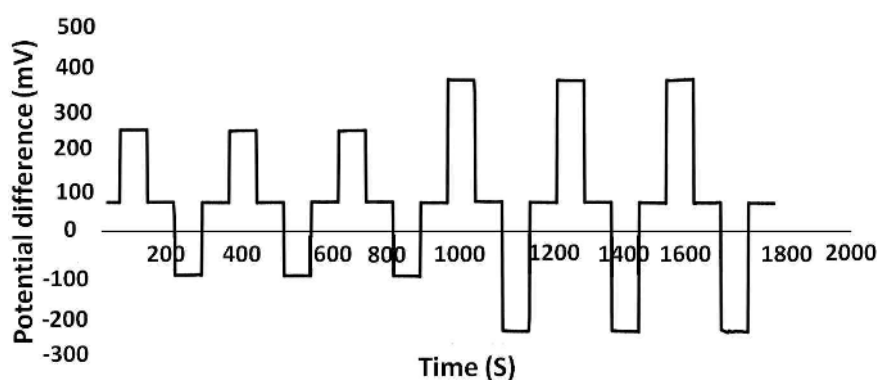| Slope (mV/pH)	E^0 (mV)	R^2	Hysteresis (mV)	Drift (mV/h)	Resolution (pH)
-59.1 ± 0.1	483 ± 2	0.9997	1.2 ± 0	3.9	0.06

Figure 6 - Potential recording for the developed pH sensor in pH buffers 7-2-7-12, and 7-4-7-10-7 three times.
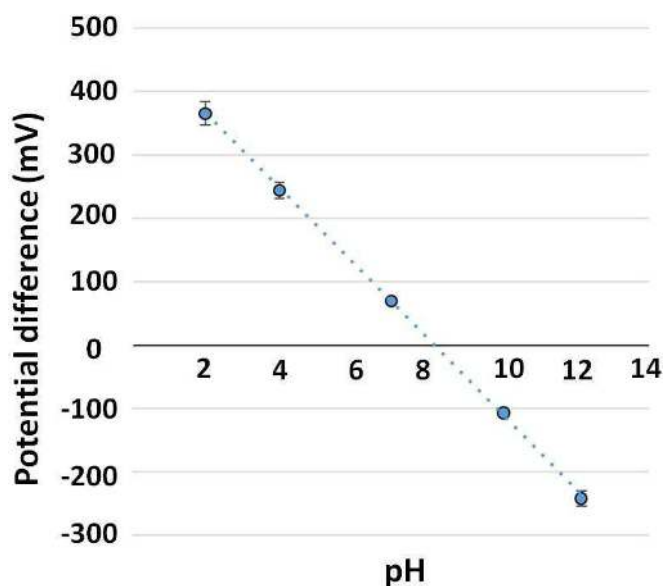
Figure 7 - Linear calibration plot for pH sensor from pH 2 to 12, using data from Table 5.

4.3.8 Redox effects

The redox effects in a pH sensor involve oxidation or reduction of redox species interfering with the response the sensor. The designed TiN electrode were left in pH 7 to equilibrate for one week. Later, the pH loops were repeated from 2 to 12 in oxidizing agent (1 mM $KMnO_4$) and reducing agent (1 mM ascorbic acid) for 20 mins duration each. The sensitivity and E^0 values of both TiN (85nm) and IrO2 (100nm) under redox conditions are recorded in Table 6. It should be noted that after oxidation there was a decrease in sensitivity and approximately 450 mV increase in the E^0 value for both TiN and IrO_2 electrodes as noted in Table 6. Immersing the TiN electrode in a reducing solution, the sensitivity remained Nernstian with a slight decrease of ±33 mV in E^0 value when the electrode was equilibrated at both pH 7 and pH 7 with reducing agent for 15min before the pH was looped from 7-4-7-10 and 7-2-7-12-7 three times, as illustrated in Figure 10. On the other hand, for the same conditions, the IrO2 electrode, exhibited a sub-Nernstian sensitivity with a significant decrease of ±114 mV in E^0 value.

W. Lonsdale *et al*. [34] reported that for a RuO_2 electrode, the E^0 value can shift by approximately ±350 mV when "fully" oxidized/reduced. To address this issue, modification of RuO_2 electrodes with a thin layer of Ta_2O_5 (150 nm) was shown to be effective in eliminating the interference caused by dissolved oxygen. Whilst electrode modification using a thin layer of Nafion reduced the interference from redox agents [35], it increased the reaction times at

neutral and basic pH values. The RuO_2 electrode modified with $Ta_2O_5|$Nafion was not immune to all redox species. It is more stable in potential when compared to an unprotected electrode in matrices such as, beer. Consequently, the presence of ascorbic acid in samples like white wine and fresh orange juice makes the modified RuO_2 working electrode still inapplicable [18]. Hence, the lower potential shift of the developed TiN in reducing species, as shown in Figures 9(a and b), makes the developed TiN films more suitable for accurate pH sensing in complex matrices.

Table 6 - Sensitivity and E0 values for 85 nm TiN electrode, after exposure to pH 7 buffer, 1 mM $KMnO_4$ (oxidized) and 1 mM ascorbic acid (reduced).

Matrix	Titanium Nitride			Iridium oxide		
	Sensitivity (mV/pH)	E^0 (mV)	R^2	Sensitivity (mV/pH)	E^0 (mV)	R^2
pH 7	-59.1	483	0.9997	-57.9	590	0.9997
Reduced (ascorbic acid)	-56.9	451	0.9992	-55.2	444	0.9965
Oxidized ($KMnO_4$)	-54.0	902	0.9974	-55.0	889	0.9683
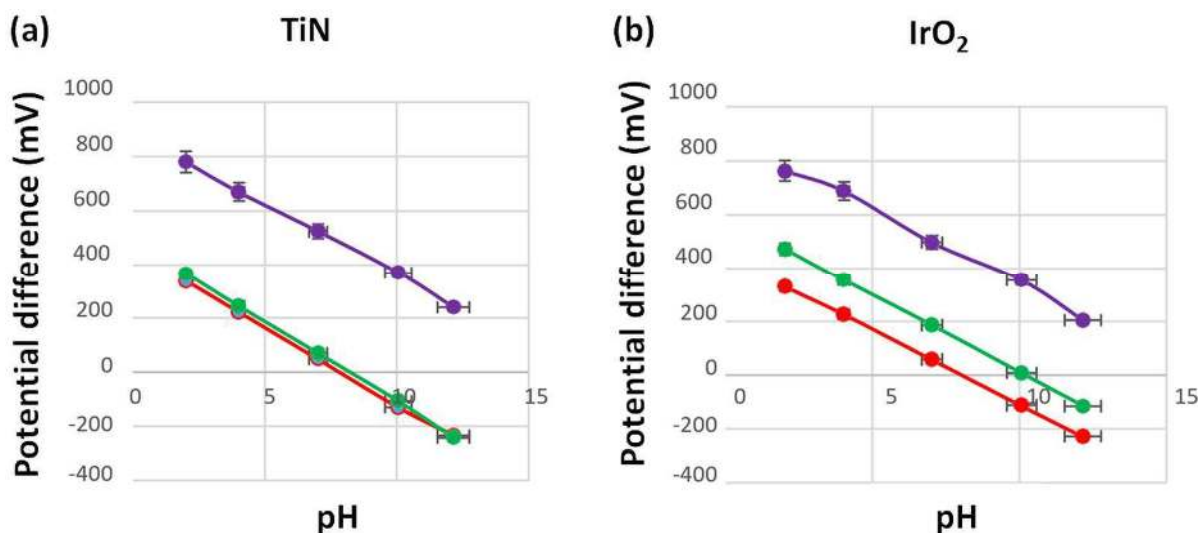
Figure 8 - Potential versus pH value for TiN working electrode when oxidized (purple); (a) pH 7 equilibrated (green) and reduced (red), (b) Linear calibration plot, when oxidized (purple), pH 7 equilibrated (green) and reduced (red) for RuO_2 and IrO_2 working electrodes.
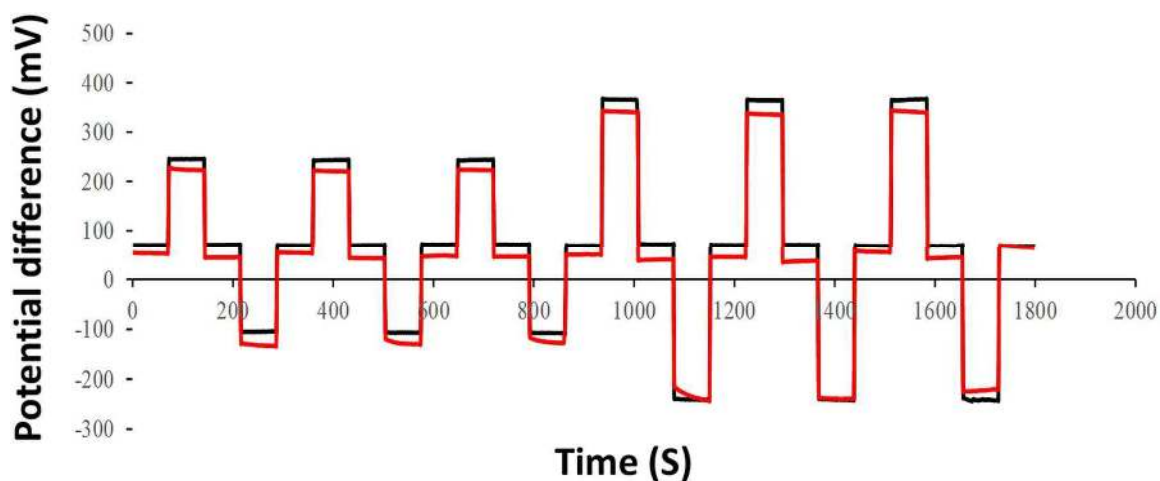
Figure 9 - Potential versus time recording for TiN working electrode in pH 7 buffer (black), reducing agent (red) vs. glass reference electrode, pH cycled 7-4-7-10-7 and 7-2-7-12-7 three times.

In summary, the experiments conducted with the developed TiN sensing electrode confirm that TiN based pH sensors exhibit lower redox interference and accurate pH readings in reducing matrix, such as wine and fresh citrus juice in comparison with the widely used metal-oxide pH sensors, such as the RuO_2 [34 - 36] and IrO_2 based pH sensors.

4.3.9 Sample application and analysis

Section 3.5 shows that the TiN film has a significantly lower redox shift of only ±33mV, as compared to metal oxides and thus it could be applied as a potential pH sensor in strong redox samples like white wine and fresh orange juice. Hence, a unprotected 85nm TiN working electrode was tested in redox samples with different substrates such as alumina (Al_2O_3), glass, silicon (Si) and polyimide (PI) (plastic). The electrode showed a 10min reaction time initially to equilibrate until the potential difference (E^0) was consistent. When the equilibration time was repeated a few times to check for reproducibility, unfortunately, it was noticed that the TiN layer peeled off from the glass, Si and PI substrates, but not from the 1mm thick Al_2O_3.
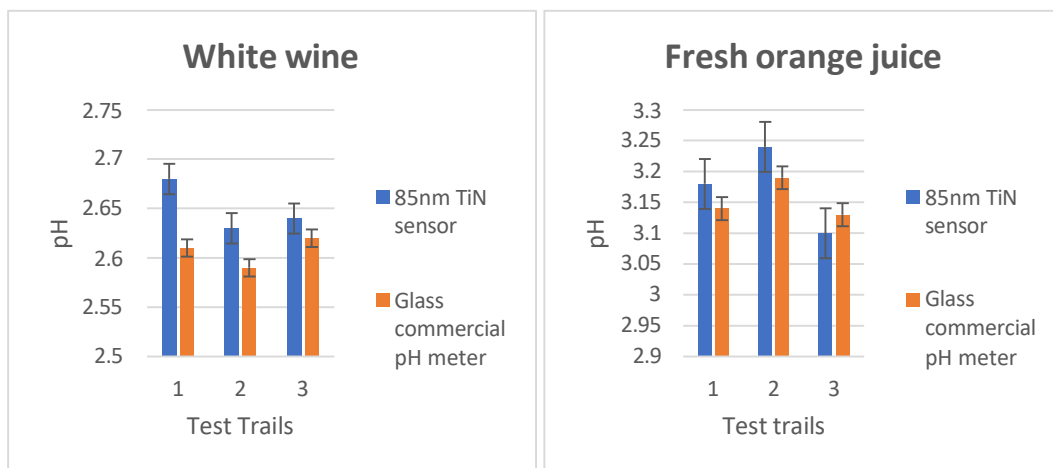
Figure 10 - The pH values of 85 nm TiN cycled three times, and the pH values determined by a commercial pH meter in white wine and fresh orange juice matrix.

The pH values in each of the sample was calculated in pH 4 buffer and with the sensitivity of -59.1mV/pH. Figure 10 shows the pH values recorded using a 85nm TiN unmodified electrode and a commercial glass pH sensor (EU Tech) are on averate spot on within experimental errors. In addition, the response time is shorter with TiN then with RuO_2 and IrO_2 (approxmately 20mins) and the equilibration duration could be reduced further by modifying the TiN layer with redox blocking membranes which will broaden the application field where fast response time is required. These modifications not only improve the sensors reaction time, but also increase the proton exchange activity in the cell, adhesion and overall performance [44, 45].

4.4   Conclusions

In this study, solid-state potentiometric TiN working electrodes have been developed and used in conjunction with a glass reference electrode to realize a pH sensor. Experimental results have shown that an 85 nm-thick TiN pH electrode exhibits a Nernstian response (-59.1 mV/pH, R^2 =0.9997) and excellent reproducibility (hysteresis 1.2 mV). The TiN electrode has demonstrated excellent durability with a stable Nernstian response over a 6-month period. The colorimeter values and transmission spectrum confirmed the stochiometric thickness (85 nm) and gold colored of the optimal TiN thin film electrode. SEM images showing the change in the TiN crystal structure due to different gas ratio trails have been presented, which enable the development of highly durable pH sensors with Nernstian sensitivity. Furthermore, experimental results have shown that the zero potential (E^0) shift for the developed TiN

electrode in reducing agents is only 30mV, compared to 115 mV for a IrO$_2$ counterpart, making the TiN pH sensor more viable for monitoring sample matrices that have reducing agents, e.g., wine, and fresh citrus juice.

4.5　References

1.　A. S. Yao, M. Wang, M. A Madou, pH Electrode Based on Melt-Oxidized Iridium Oxide, *J.Electrochem. Soc.* 2001, 148, H29. doi:10.1149/1.1353582.

2.　S. T. Han, H Peng, Sun, Q.; Venkatesh, S.; Chung, K. S.; Lau, S. C.; Roy, V. A. L. An Overview of the Development of Flexible Sensors. *Advanced Materials*. 2017. https://doi.org/10.1002/adma.201700375.

3.　Y. Wang; H. Yuan, X Lu.; Z. Zhou, D Xiao, all solid-state pH electrode based on titanium nitride sensitive film. *Electroanalysis*, 2006. https://doi.org/10.1002/elan.200603547.

4.　A. Fog; R. P Buck. Electronic semiconducting oxides as pH sensors. *Sensors and Actuators*. 1984. https://doi.org/10.1016/0250-6874(84)80004-9.

5.　M. Schirrmann; R Gebbers; E Kramer; J. Seidel, Soil pH mapping with an on-the-go sensor. *Sensors*, 2011, *11*(1), 573–598. https://doi.org/10.3390/s110100573.

6.　R. P. Kelly, A. Biastoch, F. Joos, & K. J. Kroeker, (2013). Causes and consequences of ocean acidification.

7.　E. Briggs Denni.; A Chris.; Boulton, A Peter. Brookes, Roger Stevens, Brewing Science and Practice, Published by Woodhead Publishing, 2004.

8.　K. Brandis, Acid-base pHysiology, 2015.

9.　Y. Tian, Y.; Su, F.; Weber, W.; Nandakumar, V.; Shumway, B. R.; Jin, Y.; Meldrum, D. R. A series of naphthalimide derivatives as intra and extracellular pH sensors. *Biomaterials*. 2010. https://doi.org/10.1016/j.biomaterials.2010.06.023.

10.　P. Salvo Vidin, A. Kirchhain, A. Janowska, T. Oranges, A. Chiricozzi, M. Romanelli, Sensors and biosensors for C-reactive protein, temperature and pH, and their applications for monitoring wound healing: A review. *Sensors (Switzerland)*. 2017. https://doi.org/10.3390/s17122952.

11.　D. Morris, S. Coyle, Y. Wu, K. T. Lau, G. Wallace, D. Diamond, Bio-sensing textile-based patch with integrated optical detection system for sweat monitoring. *Sensors and Actuators, B: Chemical*. 2009. https://doi.org/10.1016/j.snb.2009.02.032.

12.　M. Benčina, Illumination of the spatial order of intracellular pH by genetically encoded pH-sensitive sensors. *Sensors (Basel)*. 2013;13(12):16736-16758. Published 2013 Dec 5. doi:10.3390/s131216736.

13.　L. Bousse, P. Bergveld, The role of buried OH sites in the response mechanism of inorganic-gate pH-sensitive ISFETs. *Sensors and Actuators*, 1984.

14. A. Richter, G. Paschew, G. S. Klatt, J. Lienig, K. F. Arndt, H. J. P. Adler, Review on Hydrogel-based pH Sensors and Microsensors. *Sensors* 2008, *8*, 561-581.

15. P. Jiang, H. Xia, Z. He, Z. Wang, Design of a water environment monitoring system based on wireless sensor networks. *Sensors*. 2009. https://doi.org/10.3390/s90806411.

16. M. I. Khan, K. Mukherjee, R. Shoukat, H. Dong, A review on pH sensitive materials for sensors and detection methods. *Microsystem Technologies*. 2017. https://doi.org/10.1007/s00542-017-3495-5.

17. N. S. Lawand, P. J. French, J. J. Briaire, J. H. M. Frijns, Thin titanium nitride films deposited using DC magnetron sputtering used for neural stimulation and sensing purposes. *Procedia Engineering*, 2012. https://doi.org/10.1016/j.proeng.2012.09.250.

18. W. Lonsdale, M. Wajrak, K. Alameh, Manufacture and application of RuO_2 solid-state metal-oxide pH sensor to common beverages. *Talanta*. 2018. https://doi.org/10.1016/j.talanta.2017.12.070.

19. N. Uria, N. Abramova, A. Bratov, F. X. Muñoz-Pascual, E. Baldrich, Miniaturized metal oxide pH sensors for bacteria detection. *Talanta*. 2016. https://doi.org/10.1016/j.talanta.2015.10.011.

20. M. Liu, Y. Ma, L. Su, K. C. Chou, X, Hou, A titanium nitride depotube array for potentiometric sensing of pH. *Analyst*. 2016. https://doi.org/10.1039/c5an02675j.

21. L. J. Meng, M. P. Santos, dos., Characterization of titanium nitride films prepared by d.c. reactive magnetron sputtering at different nitrogen pressures. *Surf. Coatings Technol*., 1997. https://doi.org/10.1016/S0257-8972(96)03094-0.

22. D. K. Maurya, A. Sardarinejad, K. Alameh, Recent developments in R.F. magnetron sputtered thin films for pH sensing applications-an overview. *Coatings*. 2014. https://doi.org/10.3390/coatings4040756.

23. Y. H. Chang, Y. S. Lu, Y. L. Hong, S. Gwo, J. A. Yeh, highly sensitive pH sensing using an indium nitride ion-sensitive field-effect transistor, IEEE Sensors Journal, 2011. https://doi.org/10.1109/JSEN.2010.2080317.

24. Y. H. Liao, J. C. Chou, Fabrication and Characterization of a Ruthenium Nitride Membrane for Electrochemical pH Sensors., *Sensors*. 2009.

25. C. L. Li, B. R. Huang, S. Chattopadhyay, K. H Chen, L. C Chen, Amorphous boron carbon nitride as a pH sensor. *Appl. Phys. Lett*., 2004.

26. Y. Wang, H. Yuan, X. Lu, Z. Zhou, D. Xiao, All solid-state pH electrode based on titanium nitride sensitive film. *Electroanalysis*, 2006.

27. K. A. Yusof, N. I. M. Noh, S. H. Herman, A. Z. Abdullah, M. Zolkapli, W. F. Abdullah, pH sensing characteristics of silicon nitride thin film and silicon nitride-based ISFET sensor', in Proceedings - IEEE 4th Control and System Graduate Research Colloquium, ICSGRC 2013.

28. Y. L. Chin, J. C. Chou, J. C. Lei, T. P. Sun, W. Y. Chung, S. K. Hsiung, Titanium nitride membrane application to extended gate field effect transistor pH sensor using VLSI technology, Japanese J. Appl. Physics, Part 1 Regul. *Pap. Short Notes Rev. Pap.*, 2001. https://doi.org/10.1143/jjap.40.6311.

29. R. V. Babinova, V. V. Smirnov, A. S. Useenov, K. S. Kravchuk, E. V. Gladkikh, V. I. Shapovalov, I. L. Mylnokov, Mechanical properties of titanium nitride films obtained by reactively sputtering with hot target. Journal of Physics: Conference Series, Volume 872, 24th International Conference on Vacuum Technique and Technology 6–8 June 2017, St. Petersburg, Russian Federation 2017.

30. C. M. Zgrabik, E. L. Hu, Optimization of sputtered titanium nitride as a tunable metal for plasmonic applications. *Opt. Mater. Express*, 2015, 5, 2786-2797.

31. K. P. Lovetskiy, L. A. Sevastianov, N. E. Nikolaev, Numerical modeling of color perception of optical radiation. Math. Model. Geom. (2018). https://doi.org/10.26456/mmg/2018-612.

32. M. Nur-E-Alam, M. M. Rahman, M. K. Basher, M. Vasiliev, K. Alameh, Optical and chromaticity properties of metal-dielectric composite-based multilayer thin-film structures prepared by rf magnetron sputtering. *Coatings*. 2020. https://doi.org/10.3390/coatings10030251.

33. S. Bellucci, S. Bini, F. Micciulla, A. Dinescu, M. Danila, Synthesis of Titanium nitride film by RF sputtering. *Nanoscience and Nanotechnology Letters*. 2011.

34. W. Lonsdale, M. Wajrak, K. Alameh, Effect of conditioning protocol, redox species and material thickness on the pH sensitivity and hysteresis of sputtered RuO_2 electrodes. *Sensors and Actuators, B: Chemical*. 2017. https://doi.org/10.1016/j.snb.2017.05.171.

35. W. Lonsdale, S. P. Shylendra, S. Brouwer, M. Wajrak, K. Alameh, Application of ruthenium oxide pH sensitive electrode to samples with high redox interference. *Sensors and Actuators, B: Chemical*. 2018. https://doi.org/10.1016/j.snb.2018.07.022.

36. E. Tanumihardja, W. Olthuis, A. Van den Berg, Ruthenium oxide nanorods as potentiometric pH sensor for organs-on-chip purposes. *Sensors,* 2018. https://doi.org/10.3390/s18092901.

37.   C. G. Ribbing and A. Roos, 'Zirconium Nitride (ZrN) Hafnium Nitride (HfN)', Handb. Opt. Constants Solids, (1997).

38.   O. Korostynska, K. Arshak, E. Gill, A. Arshak, State Key Laboratory of Nonlinear Mechanics (LNM), Institute of Mechanics, Chinese Academy of Sciences, Beijing 100080, China. *Sensors (Basel)*. 2007;7(12):3027-3042. Published 2007 Nov 30. doi:10.3390/s7123027.

CHAPTER 5 FABRICATION AND OPTIMISATION OF NAFION AS PROTECTIVE MEMBRANE FOR TiN BASED pH SENSORS

This chapter was published as an article in the journal MDPI Sensors 2023, Volume 23, Issue 4,10.3390/s23042331. This article appears as it does in print, except for the abstract being removed, minor changes to the layout, section numbers, font size and font style, which was implemented to maintain consistency in the formatting of this thesis.

This chapter reports the investigation of Nafion as a protective membrane to block the interference from the redox species in the test medium. Nafion fabrication and optimization to achieve optimal pH sensitivity and linearity has also been reported in this chapter.

5.1   Introduction

pH is an important parameter in a wide range of industrial and medical applications. Several recent studies have concentrated on the formation of novel solid-state pH sensors and accurate pH measurement techniques, particularly with the development of micro/nanotechnology and innovation (Li et al. 2014; Nagy and Nagy 2015). A common way to measure pH is with a potentiometric sensor with a glass electrode. The first report on the use of a glass electrode as a pH sensor was by Max Cremer in 1906, where it was shown that an electrical potential across a glass membrane is proportional to the pH difference across that membrane. Since then, glass electrodes are routinely used in variety of situations where accurate and reliable pH measurement is required. Glass electrodes these days can identify and quantify H+ ions in many systems and a variety of samples with high precision (Li et al. 2014; Romanenko et al. 2016).

However, despite their accuracy, great sensitivity and good reliability, pH glass electrodes are too fragile and bulky in size for them to be used as miniaturized sensors for in vivo applications (Li et al. 2014). In addition, glass pH electrodes decompose over time leading to a decrease in pH sensitivity (Li et al. 2014; Romanenko et al. 2016) and the deposits on the electrode membrane can affect pH measurements. It is also very important to always store the pH glass electrodes in an aqueous solution, most usually in 3 $molL^{-1}$ KCl buffer solution when not in use and perform regular maintenance (Guler et al., 2013).

Solid-state potentiometric pH sensors are composed mainly of metal oxides and have several benefits over glass electrodes, such as variable shapes, the possibility of miniaturization, high selectivity (Manjarrés et al., 2016), low manufacturing cost with high production rate, and possibility of integration of the sensor with real-time microelectronic monitoring components. Among iron oxides, RuO_2 is highly prized for its attractive properties, such as high sensitivity (Patil, Kulkarni, & Jadhav, 2022), selectivity (Uddin et al., 2013), good reaction even in the presence of highly oxidizing and reducing species (Wedege, Draževič, Konya, & Bentien, 2016), and stable performance in various samples (Pálla, Mirzahosseini, & Noszál, 2020). However, there are still problems with the RuO_2 solid-state metal oxide electrode regarding pH measurements in complex biological, environmental, and industrial media due to redox interference. For example, proteins and other macromolecules adsorb in the electrode area can also interfere with electrode function; this limits the use of RuO_2 sensors in the measurement of pH in food matrixes (e.g., meat, fish, dairy products) and complex samples (wine and orange juice). To address this issue, the literature reports three main ways to block the electron movement between the metal-oxide sensor and solution being measured while maintaining proton conduction in the electrode area. The first method is a single point measurement protocol with an accuracy of ±0.2 pH obtained. The second method involves a matrix- compliant measurement protocol, which shows improved accuracy of ±0.1 pH compared to commercial pH sensors. The third method by Lonsdale *et al.* (Lonsdale, Wajrak, and Alameh 2018) uses sputter-deposit of a thin layer of Ta_2O_5 and drop-cast Nafion to reduce redox interference. Unfortunately, these methods are limited by their low accuracy, requirement for highly skilled operators (Maurya, Sardarinejad, & Alameh, 2014) and inability to apply to more problematic matrices, such as wine and orange juice. Aimed at expanding the application area of solid-state sensors and developing and validating additional sample- standard compounds, this work investigated another type of solid-state sensors employing active electrodes based on titanium nitride (TiN) combined with Nafion films.

A TiN-based pH electrode has been previously investigated (Chin et al., 2001), showing efficacy in more problematic matrices containing redox species. However, the potential shift due to the presence of redox species for the TiN electrode was up to 30 mV. This shift is not acceptable and, therefore, further work was needed to minimize the redox problems of this

sensor. To reduce this potential shift and make the sensor work more efficiently in challenging matrices, such as biological media, a Nafion film was applied to the TiN sensor. Nafion is an inactive substance that inhibits macromolecules, but at the same time facilitates the electron transfer between the sensor and the media (Berlinger, McCloskey, and Weber 2018; S. Li, Terao, and Sato 2018). Nafion consists of perfluorinated ionomer, which is a proton-conducting polymer. The structure of the perfluoro vinyl ether composite groups is terminated by sulfonate groups in the backbone of tetrafluoroethylene (PTFE), as shown in Figure 1, which enables Nafion to offer unique properties, such as high proton exchange, chemistry, and temperature stability (Yang et al., 2016, 2017).

$$\left[\!\left[CF_2CF_2\right]_m\!\left[CFCF_2\right]\!\right]$$
$$OCF_2CFOCF_2CF_2SO_3H$$
$$CF_3$$
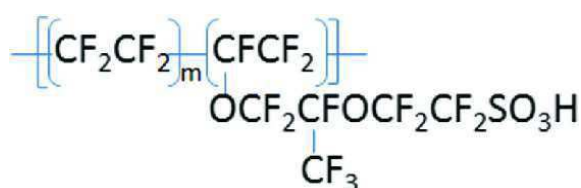
Figure 1 - Chemical structure of Nafion (Miranda et al., 2022).

Nafion's strong ionic conductivity, cation selectivity, chemical inertness and thermal stability make it a well-known ionic polymer (Miranda et al., 2022). Significant interest in the special features of Nafion has been shown in numerous research fields and applications, such as fuel cells and batteries (Zhu et al., 2022), chemical sensors (Buzid, McGlacken, Glennon, & Luong, 2018), biosensors (Awasthi, Mukherjee, O Kare, & Das, 2016; Chen et al., 2022; Tsai, Li, & Chen, 2005) and medical diagnosis technologies (Stozhko, Bukharinova, Galperin, & Brainina, 2018; Turner, Harrison, & Rojotte, 1991). Nafion has received a lot of attention recently in the context of electrochemical sensors for biomedical and environmental applications as a membrane or electrode modification (Mettakoonpitak, Mehaffy, Volckens, & Henry, 2017; Myndrul, Iatsunskyi, Babayevska, Jarek, & Jesionowski, 2022; White, Leddy, & Bard, 1982). The chemical structure of Nafion allows it to behave as a semipermeable membrane, where only protons can reach the electrode and all other types of ions are blocked. However, the Nafion protective layer embedded in previously studied metal oxide electrodes showed significant limitations in sensory use, as it significantly increased the reaction time, by up to 20 min in neutral pH environments and on average by 3 to 5 min in acidic and basic conditions (Guimerà et al., 2019). The Grotthuss explanation (Miyake & Rolandi, 2016), proposes that structural diffusion is responsible for the proton conductivity of fully hydrated Nafion. By rotating and reorienting water molecules, protons travel across the hydrogen bond within the

water 3D network inside the polymer membrane (Sofronov & Bakker, 2020). According to Gierke's model (Paul Majsztrik, 2008), hydrophilic sulfone groups coupled into channels keep water molecules in polymer clusters, allowing protons to flow continuously across the polymer membrane. When the SO_3-H connection is broken, protons dissociate, which is the first step in the transfer of protons. Dissociated protons subsequently combine with water to generate the hydronium (H_3O^+), Eigen ($H_9O_4^+$) and Zundel ($H_5O_2^+$) ions, which move through the water network. This behavior of Nafion is due to its cationic nature, as demonstrated by Kinlen *et al.* (Kinlen, Heider, & Hubbard, 1994), in which Nafion slightly inhibited the redox sensation of the IrO_2 pH sensor at the expense of the sub-Nernstian slope sensor. Nafion has also been used by other research groups (Ryder, 2003 & Yang, 2016); however, in these cases, Nafion was used to improve iron- oxide sensitivity by preventing its degradation or degradation. Manjakkal *et al.* (Manjakkal, Zaraska, Cvejin, Kulawik, & Szwagierczak, 2016) have reported another way to eliminate redox interference by placing a thin (76 nm) Ta_2O_5 layer on the sensitive electrode of the IrO_2 pH sensor. Pre-concentrating target analytes and minimizing interference from anionic species have both been accomplished using Nafion membranes (Bo Wang, 2016; Lazouskaya et al., 2021; Vaidya, Atanasov, & Wilkins, 1995; Wang, Koo, & Monbouquette, 2017). The membrane adheres well to most electrode surfaces and can prevent fouling and surface deterioration (Flimban, Hassan, Rahman, & Oh, 2020). Anodic stripping voltammetry (ASV) and a Nafion-modified bismuth film sensor were used by Akl *et al.* to determine the levels of Pb (II) and Cd (II) in lake water in the presence of surfactants (Akl, 2006). Nafion solution was drop cast onto the working electrode to create a 0.4 m thick membrane, with the detection threshold being approximately 0.5 g/L. In this work, it was discovered that the Nafion membrane's thickness significantly affected both the sensor's sensitivity and resistance to surfactants. Those studies confirmed that Nafion remains an effective redox inhibitor, and as a result, in this work, Nafion was applied to TiN as it is more cost-effective, and durable, compared to metal-oxides. Membrane deposition and treatment parameters, such as deposition process and annealing/boiling temperature, affect the proton conductivity of Nafion. The Nafion membrane was deposited on the electrode surface by drop-casting a commercially available solution and sensing mechanism of the developed layers was reported previously (Shylendra, Wajrak, Alameh, & Kang, 2023). However, methods presented in various research papers varied in the quantity of Nafion layers and in the method of drying the Nafion. There is also a lack of evidence in the literature on how TiN with Nafion layer works to prevent redox species in the sample solution. For that reason, this work aims to investigate Nafion coating on

the performance of TiN electrodes in the form of RFMS using metal-oxide pH electrodes as counterparts. Cationic Nafion research was performed in this study to determine the effect of Nafion during the reaction of the TiN sensor and its pH sensitivity with the aim of using this sensor in industrial, environmental, and medical applications.

5.2   Methodology

5.2.1. Production of TiN electrodes and Nafion deposition

Active TiN pH electrodes were made using RF magnetron spray producing 85 nm of TiN layer on the underlying 2 inch × 2-inch 0.5 mm thick alumina substrate. As previously reported [43], the parameters of the sputtered-deposition process used for the manufacture of small metal nitride films under controlled conditions to produce the most effective solid pH sensor are Ti target of 99.95% purity with a power of 350 W sputter at 10:2 Ar: N_2 at 2 mTorr pressure at room temperature. The TiN film electrode was then further refined with Nafion layer, by incorporating a 5 µL spin of 5% Nafion (Sigma) solution onto the active electrode, which was then fired at 210 °C for one hour under a vacuum of <10 mTorr using rapid thermal annealing (RTA). The RF magnetron exploded the 85 nm thick Nafion modified TiN electrode, as shown in Figure 2 (left) and Figure 2 (right) of the actual electrode.
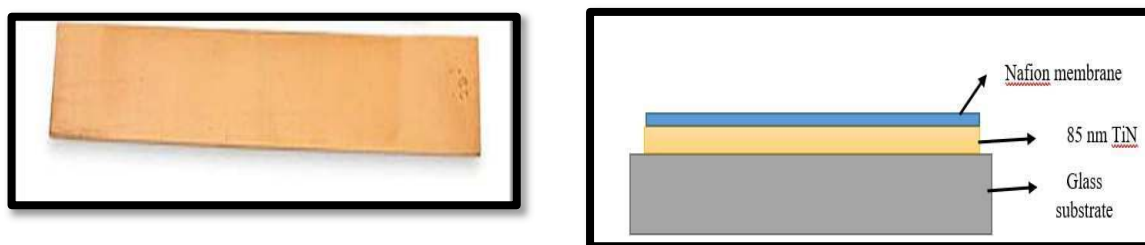
Figure 2 - Schematic representation of 85 nm thick TiN electrode with Nafion layer (**right**) and an image of the actual Nafion modified electrode (**left**).

5.2.2   Nafion deposition and annealing

The Nafion was deposited on sputter-fabricated 85 nm TiN. A total of 5 µL of 5% Nafion (Sigma)was spin coated on the pH sensitive TiN electrode. The Korea Vacuum Tech KVR-4000 Rapid thermal annealing (RTA) was used to cure Nafion to obtain good adhesion. After spin coating the modified electrode was annealed at 150 °C for 25 min.

5.2.3 SEM characterization

Scanning electron microscopy (SEM) was used to examine the morphology of modified electrodes. The instrument Hitachi SU3500 was used for analysis. Samples were cleaned using isopropyl alcohol and completely dried on a hotplate before being mounted with carbon tape to the specimen stub. Images were captured using secondary electron detection, and settings (beam power and magnification) are displayed on individual images, as discussed in Section 5.3.2.

5.2.4 Sensing protocol

Real-time recording between sensory TiN electrodes was performed using a high impedance Agilent 34410A digital multimeter, as well as a double-aging Ag | AgCl | KCl reference electrode (Sigma-Aldrich, St. Louis, MI, USA) connected to (-ve terminal) multimeter. Except for the reaction time, all measurements were taken at intervals of 20 s. To increase the signal-to-audio sensor ratio, an improved unity benefit booster was employed. All measurements were carried out at 22 °C with magnetic stirring after the electrodes had been soaked in a pH 7 buffer for an hour before calibration. Each potential recording had 30 data points, which were averaged to create individual measurement (this avoided the rapid shift that typically occurs during the first 30 s of recording due to electrode equilibration). The sensitivity, E^0, hysteresis and drift of the sensors were then determined using these results. While electrode drift was determined using the slope of the line-of-best-fit for the data at pH 12 across the measurement period, hysteresis was calculated using the difference between successive measurements at pH 12 (Lonsdale et al., 2017). The amount of time needed to bring an electrode within 3 mV (or 0.05 pH) of the stable potential was called the electrode reaction time (Shylendra, et al. 2023).

The Hanna instruments commercial pH 4.7 and 10 buffers were used to test the performance of the TiN sensor by pH looping of 7-4-7-10-7 and 7-10-7-4-7 for three minutes. Between each measurement, an air burst was used to clean the electrodes. Sensitivity, E^0, and sensory hysteresis were calculated from data points, and error bars with a 95% confidence interval were recorded. Using pH 7 buffer readings, short-term flow rate was calculated during the experimental period. The erosion level was represented by the best equity line from this data, and the errors of this measure were calculated using the worst equity line. Each sensor's response time was calculated by exposing the active TiN electrode to pH 4 or 10 for 3 min,

then monitoring the potential change for 60 s after the sensor was exposed to pH 10. The reaction time is defined as the time required to obtain 1 mV of steady power.

5.2.5 Response time, sensitivity and stability

The response time was calculated as the time required for the electrode potential to increase by 90% from its stable value. Electrodes were submerged in DI water overnight to track the stability of electrode responsiveness over time. The drift rate (in mV/h) was calculated using the line-of-best-fit approach's slope. The TiN/Nafion electrodes were subjected to a variety of pH buffer solutions to evaluate the hysteresis, or memory effect, of an electrode. Firstly, pH was altered from 1.1 to 4.1 and then from 7.0 to 10.0, i.e., acidic to basic, and then in the reverse direction from basic to acid. The electrode response was observed for three minutes after being dipped into a new buffer solution, and between each buffer the electrodes were washed with distilled water and dried with pressure gun.

5.3 Results and Discussions

5.3.1 Nafion deposition and annealing

A study by Kinlen *et al*. (Kinlen, Heider, & Hubbard, 1994) showed that many electrodes acting electrically as metal oxides react to a type of redox in a test solution. This problem was solved by using a heat-treated Nafion layer to shield the IrO_2 electrode from redox species, such as interference from ferri/ferrocyanide. Iodide and permanganate ions could still damage the IrO_2 sensor, since the Nafion layer could not completely shield all the active redox species. Additionally, the Nafion film added to the IrO_2 electrode significantly lengthened the sensor's reaction time in neutral pH, acidic and basic regions. This increase in reaction time can be explained by the presence of inaccessible sulfonic acid areas, which consequently leads to a lower level of hydration, due to higher hydrophobicity. These sulfonic sites have low acidity (6–9 pKa values) resulting in slow proton transfer rates. Lonsdale *et al*. (Lonsdale, Wajrak, and Alameh, 2017) have reported an unprotected (excluding any layer of electrode conversion) active RuO_2 electrode to exhibit up to 300 mV fluctuations when exposed to redox agents. The addition of a Ta_2O_5 layer and Nafion onto the RuO_2 electrode did show improvement and reduced the shift due to some redox species. However, it still failed to prevent disruption from stronger redox agents, such as those in wine and citrus juices. Nevertheless, since previous research demonstrated that Nafion does display characteristics of a redox inhibitor, it is

therefore, worth investigating it to improve the previously reported 30 mV shift of the TiN sensor (Shylendra, Lonsdale, Wajrak, Nur-E-Alam, & Alameh, 2020).

The TiN electrodes were prepared as explained in Section 5.2.1, and 5 µL of Nafion was spin-coated on top of 85 nm of TiN, as shown in Figure 3.
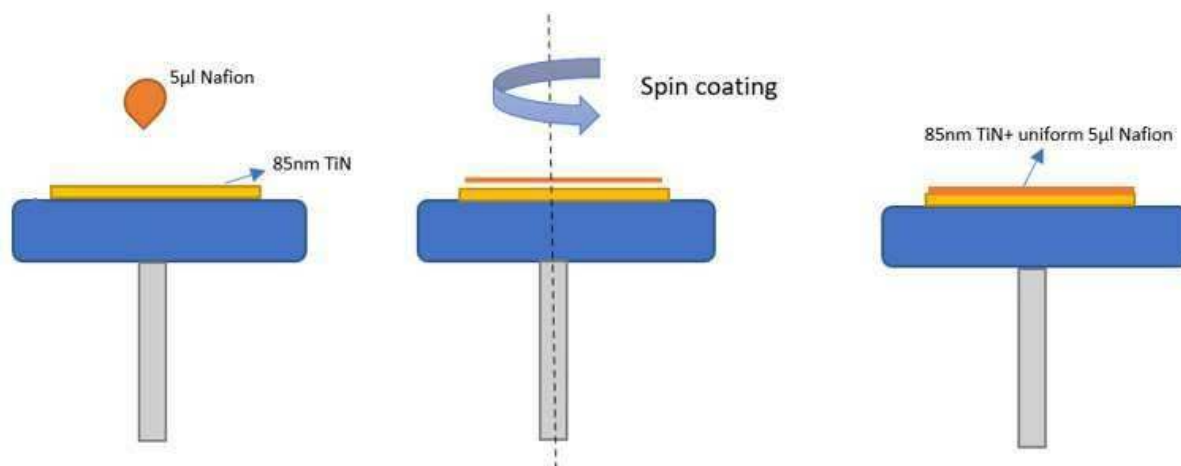
Figure 3 - Schematic showing deposition of Nafion membrane on 85 nm TiN electrode using spin coating.

After applying Nafion to the surface of the electrode, the electrode was treated with an annealing process to improve the adhesion of the film. Previous studies have shown that annealing of RuO_2 at elevated temperatures results in increased crystallinity, lower electrical resistance and decreased capacitance (Shylendra et al., 2020); however, the effect of annealing on pH sensitivity is not specifically reported in the literature. Therefore, the effect of post-deposition annealing temperature on the pH-sensing properties of thin TiN film sputtered with Nafion modification was investigated here. The effect of annealing temperature and time for Nafion was investigated and is reported in Table 1. The effects of annealing conditioning on the effectiveness of the solution-cast Nafion membranes were investigated experimentally. Annealing alters water distribution within films. Modified Nafion electrodes were subjected to a ramped thermal annealing (RTA) process that produced Nernstian sensitivity for 25 min at 150 °C in a vacuum (10 mTorr) (rating 5). Drying time and humidity affect the final resistance and, thus, the performance of the formed membrane and the retention of the membrane composition. The inclusion of thermal annealing appears to 'normalize' transport structures of various sizes and clusters of Nafion, reducing the number of modified transport structures between the thin and thick layers (Hensley, Way, Dec, & Abney, 2007).

Table 1 - (a) Nafion annealing (in vacuum) time and temperature optimization based on pH sensitivity ranking. (b) pH Sensitivity ranking criteria.

(a)				
Time (min)	**Temperature (°C)**			
	25	50	100	150
10	1	1	2	2
15	2	2	2	2
20	2	3	3	4
25	4	4	4	5

(b)	
Ranking	**Sensitivity (mV/pH)**
1	30–35
2	35–40
3	40–45
4	45–55
5	55–58 (Close to Nernstian)

The addition of Nafion altered the sensitivity of the pH sensor of the TiN electrode, as shown in Table 2. The thicknesses of the Nafion film had a direct effect on sensory function, i.e., pH sensitivity, redox inhibitory capacity and duration of the sensory response. The thickness of the Nafion protective layer was optimized considering the concentration (5%) and amount of Nafion. Both thick layers (50 µL) and thin (5 µL) layers of Nafion were investigated: the 50 µL layer, which was the maximum amount of Nafion required to block the 30-mV redox shift, while remaining sensitive to pH, and the 5 µL layer, which was the minimum amount of Nafion needed to prevent 30 mV/h redox switching in the short reaction time. The thicker Nafion layers (15 µL, 25 µL and 50 µL) demonstrated an increase in both hysteresis and drift, whereas the thin layer of Nafion (5 µL) showed improved sensitivity and hysteresis (Table 2) caused by slow proton transfer at high pH, which is in line with the findings of Kinlen *et al*. (Kinlen, Heider, and Hubbard 1994). In this work, Nafion reduced the disturbance caused by ascorbic acid and potassium permanganate, $KMnO_4$, with a thinner layer proving to be more protective than a much thicker and harder Nafion layer, which is consistent with the findings of Kinlen *et al*. (Kinlen, Heider, and Hubbard 1994). This phenomenon can be linked to the properties of Nafion, which upon hydration generates wrongly terminated channels that are strongly connected with cations. However, bigger channels might permit a slower migration of non-cationic species (Shylendra et al., 2020)

Table 2 - Nafion thickness investigation using optimized annealing time of 25 min and temperature of 150 °C as determined in Table 1.

Amount of Nafion (μL)	Sensitivity (mV/pH)	Hysteresis (mV)	Drift (mV/h)
50 (thick)	56 ± 0.92	56.1 ± 9.4	30.10
25	56.5 ± 0.88	34.5 ± 5.9	33.38
15	57.2 ± 1.7	10.7 ± 0.40	15.99
5 (thin)	58.5 ± 0.54	0.57 ± 0.29	0.920

As can be shown in Table 2, the sensor drift, hysteresis, and Nernstian sensitivity with standard deviation of 8 sensors in a group, were all improved by the thin layer of Nafion. This indicates that a TiN electrode modified with a thin coating of Nafion might be more suitable for applications in particular sample matrices; with "intermediate" amounts of disruptive redox chemicals, the thicker layers of Nafion displayed considerable hysteresis and drift values. The reaction time of the Nafion modified sensor is discussed in Section 5.3.4.

5.3.2   SEM analysis

Secondary electron images of the top surface morphology of the layers formed on TiN (85 nm) coatings with Nafion (5 μL) at different magnifications post-annealing are shown in Figure 4. The top surface view image of the Nafion layer on the TiN electrode shows a relatively uniform and smooth surface with only a few granular precipitates (Figure 4a, b) on the coating surface; however, as the magnification increased (Figure 4c, d) a more detailed morphology of the structure of the TiN with Nafion was visible, comprising many pillars, and in some areas, adjacent growths aggregated to form a clustered structure. Between the clusters, deep valleys can be observed in Figure 4c. According to the image in Figure 4d, the Nafion–TiN layer exhibits a rough sectional morphology. Cracks and defects can be observed in this image. This contrasts with what is observed for SEM images of pure TiN films, as shown by Nana Sun *et al*. (Sun et al., 2019), where the surface of the TiN film is a very smooth. Having the thicker Nafion film deposited on the TiN sensor significantly changes the sensor's behavior, as evident from the sensitivity results discussed in Section 5.3.1, and this could potentially be linked to the morphology of the Nafion film (Ramirez-Nava et al., 2021).
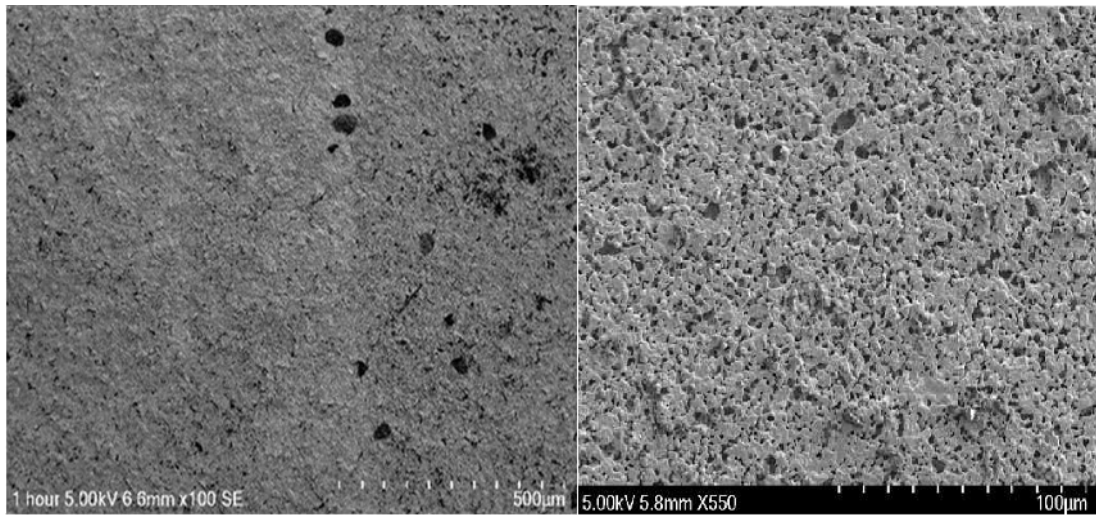
(a)

(b)
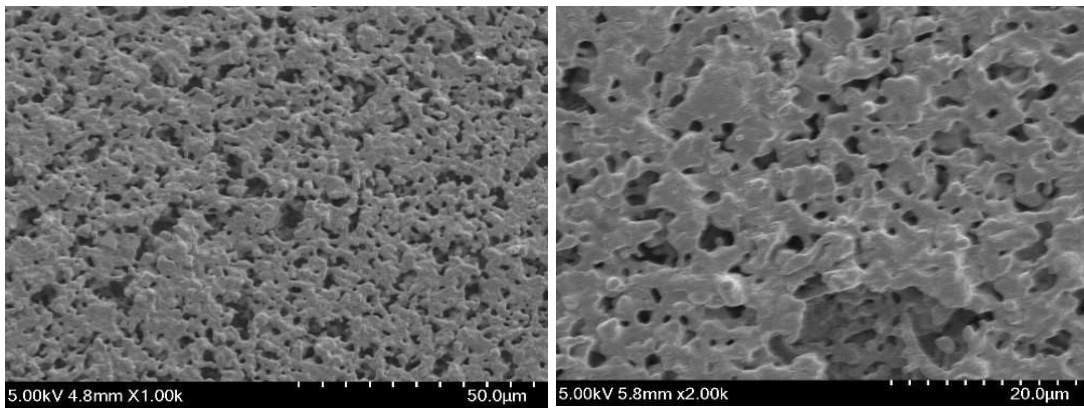
(c)

(d)

(e)

Figure 4 - SEM secondary electron images taken with Hitachi SU3500 of 4(a)-4(d) 85 nm TiN sensor modified with Nafion film at various magnifications, and 4(**e**) unmodified 85nm TiN sensor (Eastman et al., 2012).
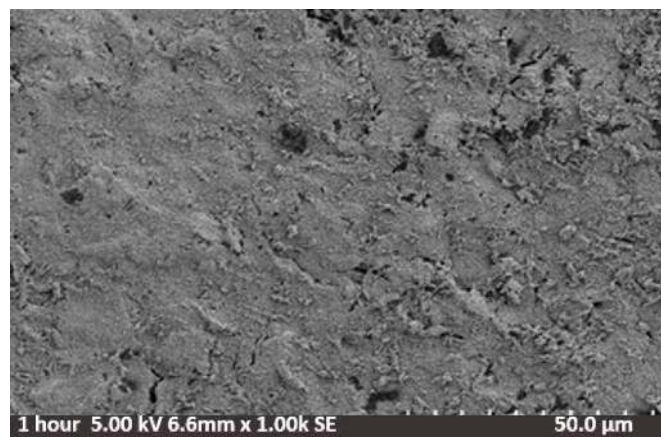
Annealing was found to be important, as the voltage readings were not available on air-treated electrodes, indicating that the complete layer of encapsulation, which occurs in water, was not performed over TiN. When annealed, an opaque white substance (when the electrode is dry) was formed, which is consistent with the fact that Nafion undergoes rapid polymerization when exposed to H_2O (Eastman et al., 2012). This showed that the annealing process caused Nafion to create a hollow structure that forms a proton transmission space.

5.3.3   Sensitivity testing

Three categories of the TiN with Nafion film were developed and tested, namely:

(i)   Pristine TiN (no layer of Nafion modification)
(ii)   TiN + N1 (N1—one layer of 5 µL of Nafion)
(iii)   TiN + N2 (N2—two layers of 5 µL of Nafion)
(iv)   TiN + N3 (N3—three layers of 5 µL of Nafion)

The properties of the Nafion membrane are affected by several variables, such as the deposition method, concentration, and volume of the applied solution, Nafion polymer properties (such as side chain length), solvent, deposition temperature, the number of applied layers (for multilayered films) and the time between layer depositions. Due to its simplicity and affordability, the drop-casting deposition process was chosen for this study, and a consistent Nafion volume and 5% Nafion concentration solution was applied. After the electrodes achieved stable sensitivity values, we compared the characteristics of electrodes containing TiN + N1, TiN + N2 and TiN + N3 layers of Nafion. After a month of conditioning in water, TiN + N1 electrodes were examined (Figure 5). The sensitivity response of all the produced electrodes were equivalent to the Nernstian response (58.4 mV/pH at 21 °C) and to a conventional glass electrode (58.8 mV/pH).

In addition to being comparable to a commercially available glass electrode, in terms of performance, the TiN + N1 and TiN + N2 electrodes revealed only minor differences in performance (Figure 5). An increase in hysteresis, a decrease in sensitivity, and a linear response were observed for TiN + N3 electrodes. As with previously fabricated unaltered TiN electrodes (Eastman et al., 2012), the sensitivity of Nafion-covered electrodes was comparable to and nearly equal to the theoretical value (58.8 mV/pH). With more Nafion layers present, there was also a minor drop in sensitivity; however, except for TiN + N3, it remained rather close to the Nernstain sensitivity.
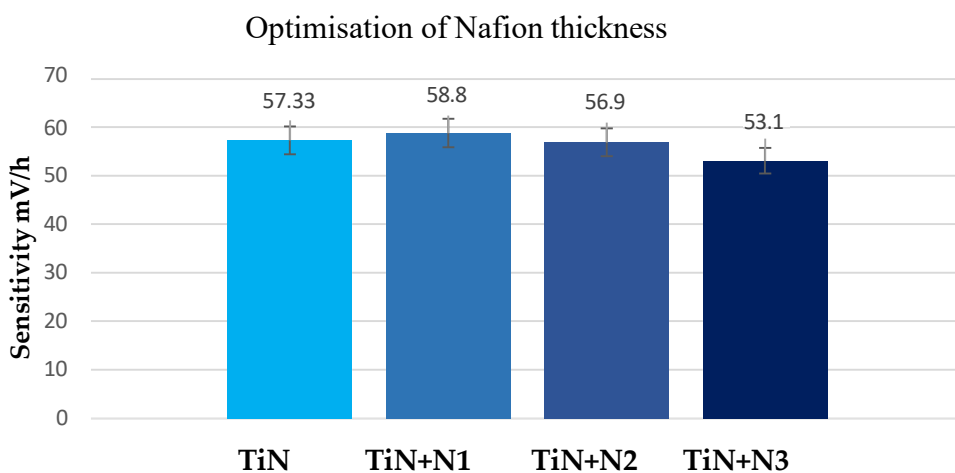
Figure 5 - Thickness optimization of Nafion on 85 nm TiN film by assessing the sensitivity as a key performance indicator.

5.3.4 Response time

When referring to electrochemical sensors, the response time is typically defined as the interval between the start of the measurement and the moment at which the sensory output reaches 90% of the measurement. The pH sensor response time was the amount of time needed after the sensor was submerged in the sample solutions for the sensor energy to reach 90% of the recorded voltage. The improved pH sensor was submerged in standard pH bath solutions with pH values of 4.33, 6.68 and 9.21 to measure the response time. Response times for the TiN sensor were discovered using an electrochemical field to record the sensor's output. All tests were completed in triplicate and the average reaction time is shown in Table 3. What is significant here is that the response time of the TiN/Nafion pH sensor is now only approximately 12 s in neutral solutions. This is a much shorter reaction time than for acidic and alkaline solutions (see Table 3), and more importantly, these response times are considerably shorter than for other solid-state sensors. For the $RuO_2/Ta_2O_5/Nafion$ sensor, the response time is 136 s at neutral pH, and longer for acidic and alkaline solutions, which would be inappropriate for some applications. The TiN/Nafion sensor, having such a short response time in various pH solutions compared to the $RuO_2/Ta_2O_5/Nafion$ sensor, is therefore very suitable for widespread applications.

Table 3 - TiN pH sensor response time for different pH solutions.

pH	Response Time (Sec)
4.33	35
6.68	12
9.21	21

5.3.5 Sensor stability

One of the most crucial indicators of a sensor is the stability of the pH sensor. All studies were carried out at room temperature to assess the stability of the TiN sensor (25 °C). The sensor was submerged in buffer solutions with pH standards of 2, 4 and 7. Each analysis took 10 min to complete, and an electro-chemical workstation logged the data every 30 s. The TiN pH sensor was cleaned in DI water and dried in a vacuum after each measurement. The outcomes are depicted in Figure 6.
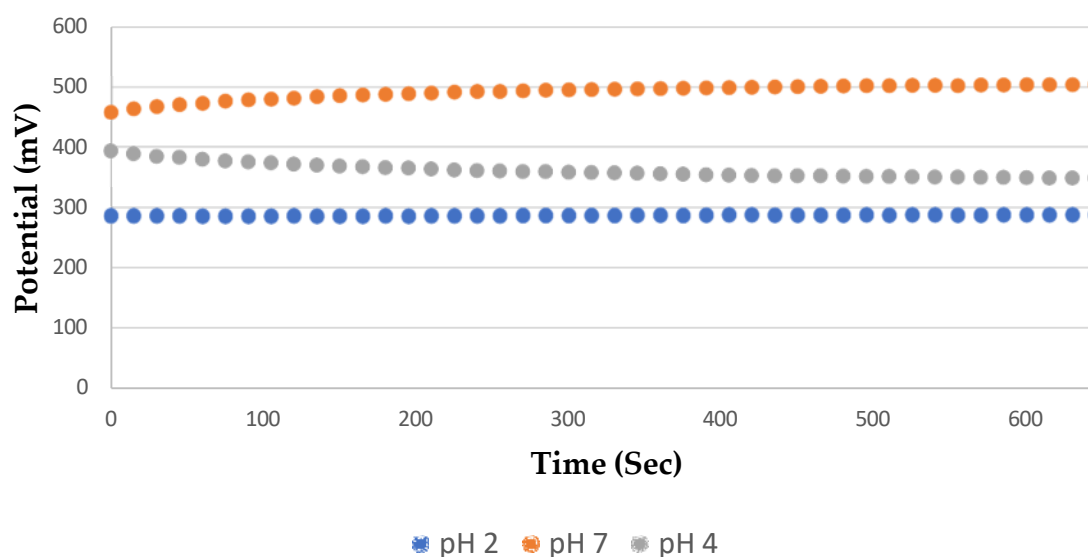
Figure 6 - Graphical representation of potential difference vs. time for pH 2, 4 and 7.

In this study, relative statistical analysis was used. The analysis's findings show that the observed output potential in pH 4 buffer solution had a standard deviation of 1.1 mV, compared to less than 1 mV for pH 7 and 2.1 mV for pH 2. As a result, throughout a 10-minutes period, the standard deviations in all three solutions were less than 2 mV. Additionally, a month-long study on the stability of the TiN pH sensor was conducted, with weekly measurements and

records of the solutions' pH levels and equilibrium potentials. Each measurement was carried out three times in a single day, and the mean linearity value was calculated as shown in Table 4 Linear fitting was used to determine the developed pH sensor's sensitivities for each measurement and reproducibility of the sensor was achieved for each of these stability tests. The sensitivities on the first, seventh, fourteenth, twenty-first and thirty-fifth days were 58.5 mV/pH, 55.8 mV/pH, 56.2 mV/pH, 56.5 mV/pH and 56.2 mV/pH, respectively. Less than 2.5 mV/pH represented the highest variation of the sensitivity.

Numerous research papers have investigated solid-state pH sensors, especially with magnetron sputtering. For example, Uppuluri *et al*. (Uppuluri, Lazouskaya, Szwagierczak, Zaraska, & Tamm, 2021) developed a pH sensor with RuO_2 electrodes deposited on screen-printed electrodes with a sensitivity of 56.1 mV/pH, and a response time of 2 s in less than pH 7. Xu *et al*. The author of (Xu, 2018) reported a RuO_2 pH sensor using RF sputtering, with a sensitivity of 54.5 mV/pH and potential drift of 2 mV/h, with a 20 s response time in the neutral region. Comparing the performance of the sensor developed here with the pH sensors reported by other scientists, the TiN/Nafion sensor displays better drift value of 0.93 mV/h (Table 2), and a stable Nernstian sensitivity (Table 4), but most importantly has a much shorter response time of 12 s in neutral solutions. Most importantly, there was no leaching of the modified membranes observed that can affect the sensitivity, which was an issue in previous modified pH sensors (Xu, 2018).

Table 4. - Linearity and sensitivity recorded over a period of 35 days.

	Interval at Which Linearity Was Measured (Days)					
	1st	**7th**	**14th**	**21st**	**28th**	**35th**
Linearity (R^2)	0.9999	0.9999	0.9998	0.9996	0.9991	0.9986
Sensitivity (mV/pH)	58.5	55.8	56.2	56.5	56.2	56.1

5.4   Conclusions

A solid-state TiN pH sensor was developed and tested. The TiN performance in redox samples was compared to a previously developed RuO_2 sensor. The potential value of the TiN (E^0) electrode varies significantly less (only 30 mV) in the reducing agents compared to the RuO_2

sensor, which displayed a tenfold variation (300 mV). This means that for the first time, accurate pH readings can now be obtained from samples such as wine and fresh orange juice, previously not possible with other metal-oxide pH sensors. This can be achieved by simply blocking a possible 30 mV variation with only a small amount of Nafion. Previously, Nafion was used successfully to prevent redox transfer in the RuO_2 sensor; however, a thick layer of Nafion was required to prevent the large 300 mV variation, and this in turn increased the response time of the sensor. However, with the TiN electrode, because only a small (30 mV) variation was required for blocking, a significantly thinner layer of Nafion was required. Experimental results showed that a 5 µL layer of Nafion not only was able to block the 30-mV variation, but also provided a significant reduction in reaction time, from 136 s to 17 s in a neutral pH, and in slightly acidic medium from 55 s to 20 s, and in basic regions from 38 s to 26 s. In addition, the TiN/Nafion sensor showed a much smaller drift (2 mV/h) than the RuO_2/Ta_2O_5/Nafion electrode (7.2 mV/h). This makes the TiN/Nafion electrode the best candidate for various matrix applications without any conditioning or matrix matching protocols. Future work in this field would comprise of interference testing by using potential species that can alter pH sensitivity, such as ascorbic acid, uric acid etc. That study would involve implementing profilometry or AFM characterization to investigate the surface and its porosity, to better understand the key factors that affect the capability to block interfering species.

5.5   References

1.   G. Nagy, L Nagy, *Potentiometric Sensors*; John Wiley & Sons, Inc.: New York, NY, USA, 2015. https://doi.org/10.1002/9781118684030.ch7.

2.   C. A. Li, K.N.; Han, X.H Pham, G.H Seong, A single-walled carbon nanotube thin film-based pH-sensing microfluidic chip. *Analyst* 2014, *139*, 2011–2015. https://doi.org/10.1039/c3an02195e.

3.   A. Kulasekaran, A. Gopal, R. Lakshimipathy, J. Alexander, Modification in pH measurements for getting accurate pH values with different pH meters irrespective of aging and drifts in the meters. *Int. J. ChemTech. Res*. 2015, *16*, 8–24.

4.   S. Romanenko, T Radenkov,.; E Newsky,.; A Kagirov,. Differential Sensor for PH Monitoring of Environmental Objects. *MATEC Web Conf.* 2016, *79*, 01008. https://doi.org/10.1051/matecconf/20167901008.

5.   Sagano, C Liao, R Liang, S Du, L Zhong, Y Tang, T Han, Y Bao, Z.; Y Sun, Ma, A Solid-Contact Reference Electrode Based on Silver/Silver Organic Insoluble Salt for Potentiometric Ion Sensing. *ACS Meas. Sci. Au* 2022, *2*, 568–575. https://doi.org/10.1021/acsmeasuresciau.2c00036.

6.   , C Manjarrés.; D Garizado, M Obregon, N Socarras, M; Calle, C; Jimenez-Jorquera, Chemical sensor network for pH monitoring. *J. Appl. Res. Technol*. 2016, *14*, 1–8. https://doi.org/10.1016/j.jart.2016.01.003.

7.   P.H Patil, V.V Kulkarni, S.A. Jadhav, An Overview of Recent Advancements in Conducting Polymer–Metal Oxide Nanocomposites for Supercapacitor Application. *J. Compos. Sci*. 2022, *6*, 363. https://doi.org/10.3390/jcs6120363.

8.   M.T Uddin, Y Nicolas, C Olivier, T; Toupance, M.M Müller, H.J; Kleebe, K.; Rachut, J Ziegler, A Klein, W, Jaeger Mann, Preparation of RuO_2/TiO_2 Mesoporous Heterostructures and Rationalization of Their Enhanced Photocatalytic Properties by Band Alignment Investigations. *J. Phys. Chem. C*. 2013, *117*, 22098–22110. https://doi.org/10.1021/jp407539c.

9.   K Wedege, E Dražević, D Konya, A. Bentien Organic Redox Species in Aqueous Flow Batteries: Redox Potentials, Chemical Stability and Solubility. *Sci. Rep*. 2016, *6*, 39101. https://doi.org/10.1038/srep39101.

10.   , A. T Pálla, A Mirzahosseini, B. Noszál, Species-Specific, pH-Independent, Standard Redox Potential of Selenocysteine and Selenocysteamine. *Antioxidants* 2020, *9*, 465. https://doi.org/10.3390/antiox9060465.

11. W Lonsdale, M Wajrak, K. Alameh, Manufacture and application of RuO2 solid-state metal-oxide pH sensor to common beverages. *Talanta* 2018, *180*, 277–281. https://doi.org/10.1016/j.talanta.2017.12.070.

12. D Maurya, A Sardarinejad, K Alameh,. Recent Developments in R.F. Magnetron Sputtered Thin Films for pH Sensing Applications—An Overview. *Coatings* 2014, *4*, 756–771. https://doi.org/10.3390/coatings4040756.

13. Y.L Chin, J.C Chou, Z.C Lei. T.P Sun,.; W.Y Chung,.; S.K Hsiung,. Titanium Nitride Membrane Application to Extended Gate Field Effect Transistor pH Sensor Using VLSI Technology. *Jpn. J. Appl. Phys*. 2001, *40*, 6311. https://doi.org/10.1143/JJAP.40.6311.

14. S.A Berlinger, B.D McCloskey, A.Z Weber, Inherent Acidity of Perfluorosulfonic Acid Ionomer Dispersions, and Implications for Ink Aggregation. *J. Phys. Chem. B*. 2018, *122*, 7790–7796. https://doi.org/10.1021/acs.jpcb.8b06493.

15. S Li, K.; *Terao*, T Sato, Colloidal Dispersion of a Perfluorosulfonated Ionomer in Water–Methanol Mixtures. *Polymers* 2018, *10*, 72. https://doi.org/10.3390/polym10010072.

16. F Yang, L Xin, A Uzunoglu, L Stanciu, J Ilavsky, S Son, J. Xie, Investigation of Solvent Effects on the Dispersion of Carbon Agglomerates and Nafion Ionomer Particles in Catalyst Inks Using Ultra Small Angle X-ray Scattering Method. *ECS Trans*.2016, *75*, 361–371. https://doi.org/10.1149/07514.0361ecst.

17. F Yang, L Xin, A Uzunoglu, Y Qiu, L Stanciu, J Ilavsky, W Li,.; J Xie,. Investigation of the Interaction between Nafion Ionomer and Surface Functionalized Carbon Black Using Both Ultrasmall Angle X-ray Scattering and Cryo-TEM. *ACS Appl. Mater. Interfaces*. 2017, *9*, 6530–6538. https://doi.org/10.1021/acsami.6b12949.

18. M Miranda, C Carvetta, N Sisodia, L Shirley, C.D Day, K.L McGuinness, J.D Wadhawan, N.S Lawrence, Nafion® Coated Electropolymerised Flavanone-based pH Sensor. *Electroanalysis* 2022, *34*, 1273–1279. https://doi.org/10.1002/elan.202100652.

19. L.Y Zhu, Y.C Li, J. Liu, J.; *He*, L.Y Wang, J.D Lei, Recent developments in high-performance Nafion membranes for hydrogen fuel cells applications. *Pet. Sci*. 2022, *19*, 1371–1381. https://doi.org/10.1016/j.petsci.2021.11.004.

20. A Buzid, G.P.; McGlacken, J.D.; J.H.T Glennon, Luong, Electrochemical Sensing of Biotin Using Nafion-Modified Boron-Doped Diamond Electrode. *ACS Omega* 2018, *3*, 7776–7782. https://doi.org/10.1021/acsomega.8b01209.

21. P Awasthi, R Mukherjee, R.; S.P.; *Okare*, S Das, Impedimetric blood pH sensor based on MoS$_2$ –Nafion coated microelectrode. *RSC Adv*. 2016, *6*, 102088–102095. https://doi.org/10.1039/C6RA17786G.

22. Z.; Chen, R Patel, J Berry, C Keyes, C Satterfield, C Simmons, A.; Neeson, X.; Cao, Q Wu,. Development of Screen-Printable Nafion Dispersion for Electrochemical Sensor. *Appl. Sci*. 2022, *12*, 6533. https://doi.org/10.3390/app12136533.

23. Y.C Tsai, S.C Li, J.M Chen, Cast Thin Film Biosensor Design Based on a Nafion Backbone, a Multiwalled Carbon Nanotube Conduit, and a Glucose Oxidase Function. *Langmuir* 2005, *21*, 3653–3658. https://doi.org/10.1021/la0470535.

24. N Stozhko, M Bukharinova, L Galperin, K. A: Brainina, Nanostructured Sensor Based on Gold Nanoparticles and Nafion for Determination of Uric Acid. *Biosensors* 2018, *8*, 21. https://doi.org/10.3390/bios8010021.

25. R.F.B Turner, D.J Harrison, R.V. Rojotte, Preliminary in vivo biocompatibility studies on perfluorosulphonic acid polymer membranes for biosensor applications. *Biomaterials* 1991, *12*, 361–368. https://doi.org/10.1016/0142-9612(91)90003-S.

26. H.S White, J Leddy, A.J. Bard, Polymer films on electrodes. 8. Investigation of charge-transport mechanisms in Nafion polymer modified electrodes. *J. Am. Chem. Soc*. 1982, *104*, 4811–4817. https://doi.org/10.1021/ja00382a013.

27. J.; Mettakoonpitak, J Mehaffy, J Volckens, C.S Henry, AgNP/Bi/Nafion-modified Disposable Electrodes for Sensitive Zn (II), Cd (II), and Pb (II) Detection in Aerosol Samples. *Electroanalysis* 2017, *29*, 880–889. https://doi.org/10.1002/elan.201600591.

28. V.; Myndrul, I. Iatsunskyi,; N.; Babayevska, M Jarek,.; T Jesionowski,. Effect of Electrode Modification with Chitosan and Nafion® on the Efficiency of Real-Time Enzyme Glucose Biosensors Based on ZnO Tetrapods. *Materials* 2022, *15*, 4672. https://doi.org/10.3390/ma15134672.

29. X.; Guimerà, Moya, A.Dorado, A.D.; Illa, X.; R Villa,.; D Gabriel,.; Gamisans, X.; Gabriel, G. A Minimally Invasive Microsensor Specially Designed for Simultaneous Dissolved Oxygen and pH Biofilm Profiling. *Sensors* 2019, *19*, 4747. https://doi.org/10.3390/s19214747.

30. T Miyake, M Rolandi, Grotthuss mechanisms: From proton transport in proton wires to bioprotonic devices. *J. Phys. Condens. Matter*. 2016, *28*, 023001. https://doi.org/10.1088/0953-8984/28/2/023001.

31. O Sofronov,O.; H.J Bakker,. Slow Proton Transfer in Nanoconfined Water. *ACS Cent. Sci.* 2020, *6*, 1150–1158. https://doi.org/10.1021/acscentsci.0c00340.

32. P.W. Majsztrik, Mechanical and Transport Properties of NafionRTM for Pem Fuel Cells; Temperature and Hydration Effects. Master's Thesis, Princeton University, Princeton, NJ, USA, 2008.

33. P.J.; Kinlen, J.E.; Heider, D.E Hubbard, A solid-state pH sensor based on a Nafion-coated iridium oxide indicator electrode and a polymer-based silver chloride reference electrode. *Sens. Actuators B Chem.* 1994, *22*, 13–25. https://doi.org/10.1016/0925-4005(94)01254-7.

34. L.; Yang, J.; *Zeng*, B Ding, C Xu, J.Y Lee, Lithium Salt Inclusion as a Strategy for Improving the Li^{+} Conductivity of Nafion Membranes in Aprotic Systems. *Adv. Mater. Interfaces* 2016, *3*, 1600660. https://doi.org/10.1002/admi.201600660.

35. A.G Ryder, S Power, T.J Glynn, Evaluation of Acridine in Nafion as a Fluorescence-Lifetime-Based pH Sensor. *Appl. Spectrosc.* 2003, *57*, 73–79. https://doi.org/10.1366/000370203321165232.

36. L Manjakkal, L Zaraska, K.; Cvejin, K.; Kulawik, J.; Szwagierczak, D. Potentiometric RuO_2–Ta_2O_5 pH sensors fabricated using thick film and LTCC technologies. *Talanta* 2016, *147*, 233–240. https://doi.org/10.1016/j.talanta.2015.09.069.

37. R Vaidya, P Atanasov, E.Wilkins, Effect of interference on the performance of glucose enzyme electrodes using Nafion$^{®}$ coatings. *Med. Eng. Phys.* 1995, *17*, 416–424. https://doi.org/10.1016/1350-4533(94)00006-U.

38. M Lazouskaya, O Scheler, V Mikli, K Uppuluri, K Zaraska, M Tamm, Nafion Protective Membrane Enables Using Ruthenium Oxide Electrodes for pH Measurement in Milk. *J. Electrochem. Soc.* 2021, *168*, 107511. https://doi.org/10.1149/1945-7111/ac2d3c.

39. B Wang, B Koo, H.G Monbouquette, Enzyme Deposition by Polydimethylsiloxane Stamping for Biosensor Fabrication. Electroanalysis 2017, 29, 2300–2306. https://doi.org/10.1002/elan.201700302.

40. B Wang, Biosensors Fabrication by Polydimethylsiloxane Stamping and Nanostructured Platinum for Construction of Improved Reference and Sensing Electrodes; University of California: Los Angeles, CA, USA, 2016.

41. S.G.A Flimban, S.H.A Hassan, M.M.; Rahman, Oh, S.E. The effect of Nafion membrane fouling on the power generation of a microbial fuel cell. *Int. J. Hydrogen Energy* 2020, *45*, 13643–13651. https://doi.org/10.1016/j.ijhydene.2018.02.097.

42. M.A Akl, An Improved Colorimetric Determination of Lead (II) in the Presence of Nonionic Surfactant. *Anal. Sci.* 2006, 22, 1227–1231. https://doi.org/10.2116/analsci.22.1227.

43. S.P Shylendra, M Wajrak, K Alameh, J.J Kang. Nafion Modified Titanium Nitride pH Sensor for Future Biomedical Applications. *Sensors* 2023, *23*, 699. https://doi.org/10.3390/s23020699.

44. W Lonsdale, M Wajrak, K Alameh, RuO2 pH Sensor with Super-Glue-Inspired Reference Electrode. *Sensors* 2017, *17*, 2036. https://doi.org/10.3390/s17092036.

45. S.; Paul Shylendra, W Lonsdale, M Wajrak, M Nur-E-Alam, K Alameh,. Titanium Nitride Thin Film Based Low-Redox-Interference Potentiometric pH Sensing Electrodes. *Sensors* 2020, *21*, 42. https://doi.org/10.3390/s21010042.

46. J.E Hensley, J.D Way, S.F Dec, K.D Abney, The effects of thermal annealing on commercial Nafion® membranes. *J. Memb. Sci.* 2007, *298*, 190–201. https://doi.org/10.1016/j.memsci.2007.04.019.

47. K Hongsirikarn, J.G Goodwin, S Greenway, S Creager, Effect of cations (Na+, Ca2+, Fe3+) on the conductivity of a Nafion membrane. *J. Power Sources* 2010, *195*, 7213–7220. https://doi.org/10.1016/j.jpowsour.2010.05.005.

48. N Sun, D Zhou, S Shi, F Liu, W Liu, Q Chen, P Zhao, S Li, J Wang, Superior-performance TiN films sputtered for capacitor electrodes. *J. Mater. Sci.* 2019, *54*, 10346–10354. https://doi.org/10.1007/s10853-019-03652-z.

49. J Ramirez-Nava, M Martínez-Castrejón, R.L.; García-Mesino, J.A López-Díaz, Talavera-Mendoza, O.; Sarmiento-Villagrana, A.; Rojano, F.; Hernández-Flores, G. The Implications of Membranes Used as Separators in Microbial Fuel Cells. *Membranes* 2021, *11*, 738. https://doi.org/10.3390/membranes11100738.

50. S.A.Eastman, S Kim, K.A Page, B.W Rowe, S Kang, C.L Soles, K.G Yage, Effect of Confinement on Structure, Water Solubility, and Water Transport in Nafion Thin Films. *Macromolecules* 2012, *45*, 7920–7930. https://doi.org/10.1021/ma301289v.

51. K Uppuluri, M Lazouskaya, D Szwagierczak, K Zara ska, Tamm, M. Fabrication, Potentiometric Characterization, and Application of Screen-Printed RuO2 pH

Electrodes for Water Quality Testing. *Sensors* 2021, *21*, 5399. https://doi.org/10.3390/s21165399.

52. K Xu, Development and Performance of an All-Solid-Stated pH Sensor Based on Modified Membranes. *Int. J. Electrochem. Sci*. 2018, *13*, 3080–3090. https://doi.org/10.20964/2018.03.04.

CHAPTER 6   NAFION MODIFIED TITANIUM NITRIDE pH SENSOR FOR FUTURE BIOMEDICAL APPLICATIONS

This chapter was published as an article in the journal MDPI *Sensors* 2023, Volume 23, Issue 2, 10.3390/s23020699. This article appears as it does in print except for the abstract being removed, minor changes to the layout, changed section numbers, font size and font style, which was implemented to maintain consistency in the formatting of this thesis.

This chapter reports the Nafion modified TiN pH sensor applied in real time complex matrices and reports the designed sensors exhibits Nernstian sensitivity and excellent linearity.

6.1   Introduction

pH monitoring and regulation is crucial in both biomedical and non-biomedical applications. In biological systems, pH maintenance is important to sustaining health and physiological equilibrium, and a disturbance in pH levels may reflect an underlying dysfunction or pathological process [1]. Certain examples of pH measurement include its use in detection of glioblastomas (type of brain tumor), monitoring of ischemic episodes, and testing of bodily fluids, such as urine, saliva, sweat and blood [2]. Non-medical applications include the use of pH monitoring in chemical industries, agriculture, water management, food safety control and the cosmetics industry.

In a specific application of pH in medical science, for instance, when labelling Prostate-specific membrane antigen (PSMA) peptide with lutetium-177 (Lu-177) or actinium-225 (Ac-225) in the radiopharmaceutical treatment of prostate cancer, the pH of the radioactive lutetium or actinium must be at pH = 9 to allow for complete binding of the peptide. Therefore, it is necessary to monitor the pH throughout the chemical reaction [3,4]. At present, a universal pH paper is used to monitor the pH of the Lu-177 and Ac-225 solutions, as glass pH electrodes cannot be placed into a 1 mL solution of radioactive substance. However, universal pH paper only provides a rough estimate of the pH and is prone to external factors, such as user error and lighting of test conditions due to the inability of the user to recognize color changes in the pH paper [5]. Consequently, a cheap, accurate and disposable pH solid-state electrode would be ideal for this situation. Another example of the importance of being able to accurately monitor pH is in the development of Covid-19 vaccines. Throughout the manufacturing process of the Covid-19 vaccines, the pH is required

to be maintained between 7.1 and 7.2 and, therefore, requires constant and accurate monitoring. Solid-state electrodes such as TiN can be ideal for such applications [6]. Although glass electrodes are the industry standard for measuring pH, they are not appropriate for all applications due to their fragility and size, limiting their use for medical purposes [7].

The pH sensors developed in this paper are evaluated in the various mediums and matrices for possible future medical, industrial, and environmental applications [8,9]. The two fundamental limits addressed in this work are the application of matrix and the microscopic size [10]. A smart sensor can be used to measure physiological characteristics, such as the acidity of drinking water at remote locations or in conflict zones, to overcome these restrictions. Soldiers in conflict zones will be able to keep track of their health conditions and issues with the use of convenient and accessible pH testing equipment. The most important discoveries and contributions of this work are that (1) thin TiN films have the potential for the development of miniaturized pH sensors and (2) Nafion-modified TiN electrodes have potential to be used for many new pH sensing applications.

Metal oxide pH electrodes were once an alternative to glass pH electrodes [11–14]. IrO_2-based pH electrodes and their less popular RuO_2-based counterparts have both been the subject of extensive research [12]. Metal oxides' primary flaw is their redox sensitivity [15]. This redox sensitivity has a negative impact on the electrode potential in the neutral region and, consequently, limits the use of these materials as sensors [16]. The disruption of reducing or oxidizing species causes this constraint to be most noticeable in potentiometric metal oxide electrodes. Fog and Buck [17] claim that RuO_2 exhibits significant changes in redox agents. However, they also state that other iron oxides, such as IrO_2, do not retain a Nernstian pH response above half the pH range when there are oxidizing or reducing agents [6,9]. It is interesting to note that this claim was only superficially addressed in their 1984 book and has not been adequately explored in the literature. To address this issue, other researchers investigated the use of Nafion to modify pH electrodes, such as an IrO_2 sensor [18], and they were successful in minimizing electrode potential shift in the neutral pH range. It was demonstrated in previously published work that adding protective layers of Ta_2O_5 [13] and Nafion [19,20] to a RuO_2 pH electrode lowers the redox interference and gives more accurate pH values of some samples, such as beer [11]. These modified electrodes, however, were still ineffective for samples such as wine and fresh citrus juice [11]. In this study, not only has it been possible to develop a sensor that is highly accurate in samples, but also has an improvement with a small potential shift of 2

mV, when compared to a RuO_2 sensor, has a shift of 300 mV, and an unmodified TiN sensor with a shift of 30 mV in reducing conditions [21,22]. Having overcome the redox interference in metal nitride pH sensors now allows for the possibility of replacing the glass electrode in applications where the size of the electrode and robustness are crucial, and where there is a need for low production costs [23– 27].

This work is a follow up study from previous studies conducted on metal oxides and nitrides, i.e., RuO_2 [7,11], RuN [23], Br-C-N [28], SiN [29], TiN [21,30], ZiN and HfN [31], as summarized in Table 1.

Table 1 - Comparison of current work on metal nitride-based pH sensors applied in redox matrix to previous work from the literature. * No conditioning protocol required for this sensor as compared to the RuO_2 sensor.

Application Matrix	pH Sensitive Material	Fabrication Method	Sensitivity (mV/h)	pH Range	Reference
Redox matrix	RuO_2	RF sputtering	−56.6	2–12	[7]
Biological and environmental application	RuN	Magnetron sputtering	−58.3	1–12	[23]
Phosphate buffer solution	Br-C-N	Dual gun sputtering	−46	1–13	[28]
Aquaculture	SiN	ISFET package	−53.6	4–10	[29]
Chemical applications	InN	ISFET	−58.2	2–12	[32]
Chemical application	IrO_2 + Nafion	Cryogenic sputtering	−60.2	2–12	[21]
Fresh orange juice	TiN	RF Magnetron sputtering	−59.1	2–12	[21] previous work
Common drinks with redox species	TiN + Nafion	RF Magnetron sputtering	−56.6	2–12	* This work

TiN is proven to be a biocompatible material for medical and chemical applications [33,34]. However, the reaction of the metal-oxide or metal-nitride film with the testing medium remains a gap in the literature. Interference of pH material with high-redox species, such as ascorbic acid and orange juice, is a major disadvantage with oxidation surfaces used as pH sensors [35]. To address this gap, TiN was modified with Nafion to protect the material from interacting with other species in the sample, which in turn affects the sensitivity of the sensor [36,37]. Overcoming this issue paves the path for the future development of a robust and reliable pH sensor for chemical and biological applications [38,39]. Experiments, analysis and applications of the TiN sensor with Nafion modification are presented in the following sections.

6.2 Materials and Methods

Working electrodes made of TiN that are pH sensitive were fabricated by sputtering TiN over an Al_2O_3 substrate that was 0.5 mm thick. A TiN target (99.95% purity) with 110 W of sputter power was used to deposit TiN, utilizing radio frequency magnetron sputtering (RFMS) at room temperature. Various gas pressures in the gas chamber and argon: oxygen gas ratios were tested, as described in previous publications [14,21]. In Figure 1, the TiN-sputtered layer created a vividly colored gold coating on a glass substrate [22]. A total of 5 µL of 5% Nafion 117 in a mixture of aliphatic alcohol and water from Sigma was spin coated on top of 85 nm TiN. It was then annealed for 25 min at 150 °C.
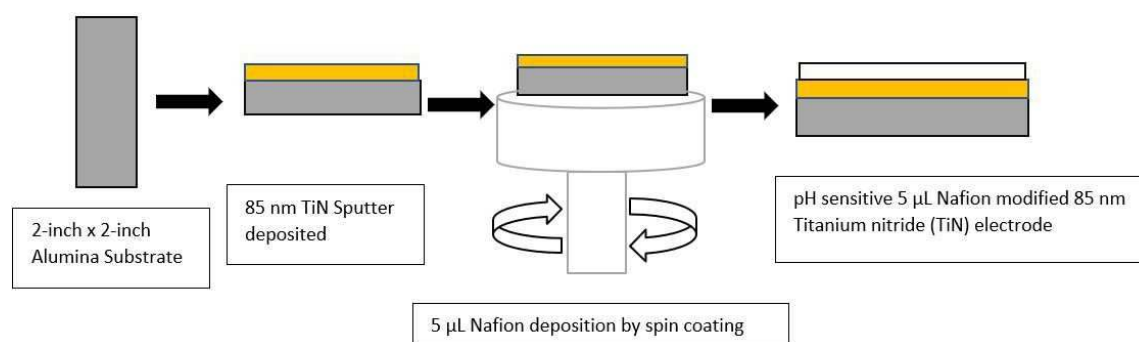

Figure 1 - Schematic representation of 85 nm TiN electrode modified with Nafion.

6.2.1 pH Measurements

Using a high impedance voltmeter (Agilent, Santa Clara, CA, USA), potentiometric measurements were recorded between the TiN + Nafion working electrode and a commercial Ag|AgCl|KCl glass, double-junction, reference electrode (Sigma-Aldrich, St. Louis, MO, USA). At 22 °C, commercial buffer solutions (Rowe Scientific, Minto, Australia) were used for the analysis. Each measurement was completed in five minutes. The movement of the potential in pH 7 buffer over the duration of the analysis time is given by the drift numbers, with error bars indicating the 95% confidence interval [10,23,24]. For each measurement, the last 30 s of analysis were averaged and used to calculate sensitivity, E°, and hysteresis.

The selective identification of H^+ ions present in the examined solution is necessary for potentiometric pH determination. A measurement device and an electrochemical cell make up the typical potentiometric configuration (potentiometer, voltmeter, multimeter, etc.). A pH-

sensitive sensor electrode and a reference electrode make up the electrochemical cell (usually silver chloride electrode). Electromotive force is an electrochemical cell's electrical characteristic (Emf). The difference in electrode potentials (E) of the two half-reactions occurring at the sensing and reference electrodes is used to determine the cell's Emf. The Emf of the cell is typically equal to the potential of the sensing electrode, and the reference electrode is grounded, with its potential regarded as equal to zero. The half-reaction occurs in response to detecting, where E^0 is the reference voltage:

$$E = E^0 - R·T \, n·F·ln \, [Red] \, [Ox] \tag{1}$$

where R is the universal gas constant, 8.314 J/Kmol; T is the temperature, K; and n is the quantity of electrodes involved in the redox reaction. The activities of the reduced and oxidized versions of the electrode material, respectively, are [Red] and [Ox], measured in mol/L, and F is the Faraday constant, which is equal to 96,485 C/mol.

The standard potential is a measurement of the equilibrium individual potential of the reversible electrode in the standard condition (1 mol/L concentration, 1 atm pressure and 25 °C temperature). The following simplified equation, which was proposed by [40,41], may be used to explain the pH-sensing mechanism for the TiN electrode:

$$Ti(III) + e^- + [H]^+ \leftrightarrow Ti(II) \tag{2}$$

The Nernst equation for this process takes the following form:

$$E = E^0 - \frac{RT}{zF} ln \frac{\alpha \, Ti[III]}{\alpha \, Ti \, [IV][H^+]} \tag{3}$$

where [Ti(III)], [Ti(II)] and [H$^+$] are activities. Equation (3) has the following form at room temperature (T = 22 °C), considering that the values of metal activities in solids are close to 1:

$$[Ti(III)/Ti(II)] \, 0.0583 \, log \, [H^+] + E = E^0 \tag{4}$$

Electrode sensitivity, or the theoretical Nernst response at 22 °C, is defined as the value of 58.3 mV. When n = 1 in Equation 3, all pH-sensitive electrodes at the specified temperature should

have the same sensitivity value; however, the theoretical response, in practice, will deviate from this value [33, 34].

Prior to the initial measurement, all electrodes underwent a conditioning routine that involved soaking them in distilled water for 24 h to hydrate pH-sensitive surfaces. The sensitivity of the manufactured electrodes was assessed by detecting the electrochemical cell's electromagnetic field (the potential difference between the reference electrode and the fabricated pH-sensitive electrode) as a function of pH. For that, electrodes were submerged into buffer solutions of pH range from 1 to 14. Every 10 s, data points were obtained while the Emf was recorded for 5 min. The average value of the previous 10 data points was used to calculate the Emf at that pH. By charting the electrode potential as a function of pH and figuring out the equation expressing this dependency, the electrode sensitivity, E^0, and linearity of the response were found, using the least-squares method. E^0 was estimated as the potential at pH $= 0$ by extrapolating the data, and the linearity of the electrode's response to pH change was calculated as the correlation coefficient. Electrode sensitivity was computed as the slope of the linear equation.

6.2.2 Response time, drift rate and hysteresis

The time required for the electrode potential to reach 90% of the stable value was used to calculate the response time. Electrodes were left in distilled water overnight to assess the drift of electrode response in time. The drift rate (in mV/h) was calculated using the slope of the line-of-best-fit method. The created electrodes were subjected to a variety of pH buffers to evaluate the hysteresis, or memory effect, of an electrode. The pH of the electrodes was first changed from 1.1 to 4.1 to 7.0 to 10.0 (acidic to basic), and then the pH was changed in the other direction. After dipping the electrode into a fresh buffer solution, the electrode response was monitored for three minutes. A solution of cleaned electrodes was washed with distilled water and dried with a pressure gun after each measurement.

6.2.3 Measurements of real samples

The fabricated TiN + Nafion electrodes were used to measure the pH values of different types of samples: cola, beer, red wine, white wine, orange juice, fresh lemon juice and iced tea. The glass commercial electrode was used to test all these samples as a reference to the TiN pH sensor.

6.3   Results and Analysis

This section records the detailed step-by-step fabrication process of TiN + Nafion electrodes. The key performance indicators of pH sensors, such as sensitivity, drift and hysteresis, are explained and reported in this section of the paper. Finally, the TiN + Nafion electrode was applied in real high-redox sample varieties to test the performance and validate the role of Nafion modification to TiN pH sensors.

6.3.1   Deposition Parameters

To find the best manufacturing conditions for all-TiN pH electrodes, the TiN sputter deposition gas pressure and Ar: N_2 gas ratio were briefly investigated. Two alternative substrates were tested: polished Al_2O_3 and glass at Ar: N_2 gas ratio of 1:9. By soaking samples in a deionized water ultrasonic bath for 10 minutes and putting them through a peel adhesion test using polyimide adhesive tape, samples were examined for adhesion. When the polyamide was evaluated for pH characteristics, it demonstrated greater adhesion. Using pH 2, 4, 7, 10 and 12 buffers, the pH sensitivity of the samples was assessed. All the TiN electrodes showed Nernst response, although electrodes with thicker than 5 µL of Nafion showed a significant amount of drift, as shown in Table 2.

| Resistivity (ohm)	Sputter Target	Gas Ratio (Ar:N_2)	Sputter Pressure (mTorr)	Nafion Thickness (µL)	Sensitivity (mV/pH)	Hysteresis (mV)	R^2	Drift (mV/h)
2.6	Ti	9:1	2	5	−56.4 ± 1.2	2.3 ± 1.2	0.9997	4.6 ± 1.2
4.1	Ti	9:1	2	10	−59.3 ± 3.2	84.7 ± 3.4	0.9341	78.48 ± 2.5
4.8	Ti	9:1	2	15	−56.2 ± 2.8	52.63 ± 1.2	0.9818	165.4 ± 6.7
4.9	Ti	9:1	2	20	−53.4 ± 4.2	55.17 ± 4.7	0.9698	210.56 ± 2.7
5.6	Ti	9:1	2	25	−53.1 ± 1.2	71.30 ± 7.8	0.9519	222.84 ± 3.8

Table 2 - Summary of the pH-sensing performance for TiN electrodes with various Nafion thickness ranging from 5 to 25 µL thickness, with TiN deposited using 2 m Torr pressure and 1:9 Ar: N_2 gas ratio.

Based on these results, the best electrode characteristics for TiN are when sensitivity is close to Nernstian, and hysteresis and drift are both low. It was found that an 85 nm TiN electrode exhibited Nernstian sensitivity of 56.4 mV/pH, 2.3 mV hysteresis, and had the lowest drift of of 4.6 mV/h when 5 mL of Nafion was applied. Hence, this thickness of Nafion was selected to spin coat on TiN to determine the sensing properties of the electrode.

In addition, this electrode, when left in pH 7 buffer for 4 months, maintained its sensitivity. This is a significant finding because other metal-oxide solid-state electrodes demonstrate signs of degradation in less than 4 months [20]. This is likely due to the specific construction of the TiN electrode, where the effects from electrical contact materials, such as carbon, platinum, or gold, are eliminated.

6.3.2   Sensing properties

The TiN + Nafion pH sensor was examined by looping pH from 2 to 12, as shown in Figure 2a. The developed sensor shows Nernstian sensitivity (−56.6 mV/pH) and a reaction time of less than 30 s, which is consistent with previous reports of pH sensors employing this type of working electrode [14,15]. As seen in Figure 2b, the pH response is linear (R^2 = 0.9999) and reproducible, as summarized in Table 2. The R square value is the correlation coefficient, which indicates the excellent linearity of the slope.

(a)
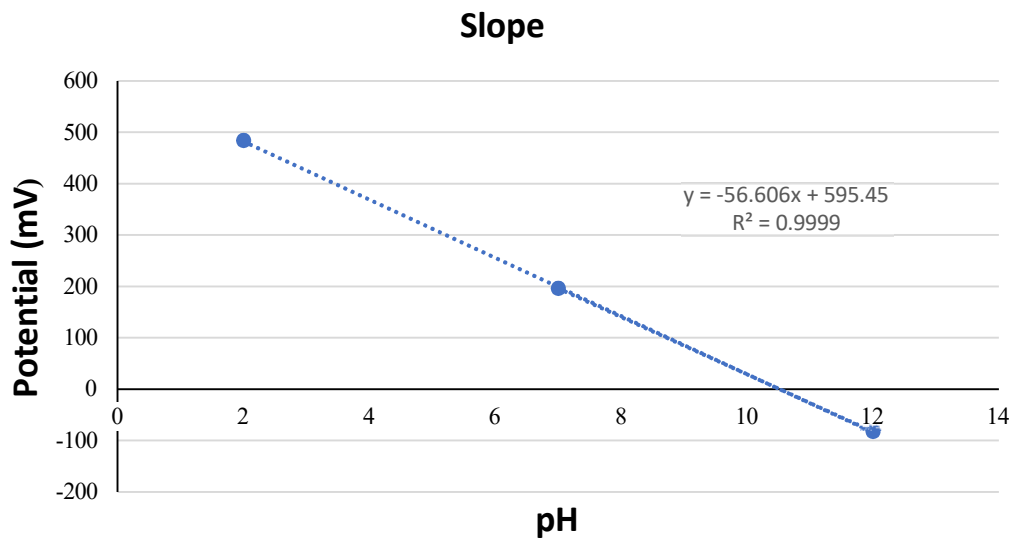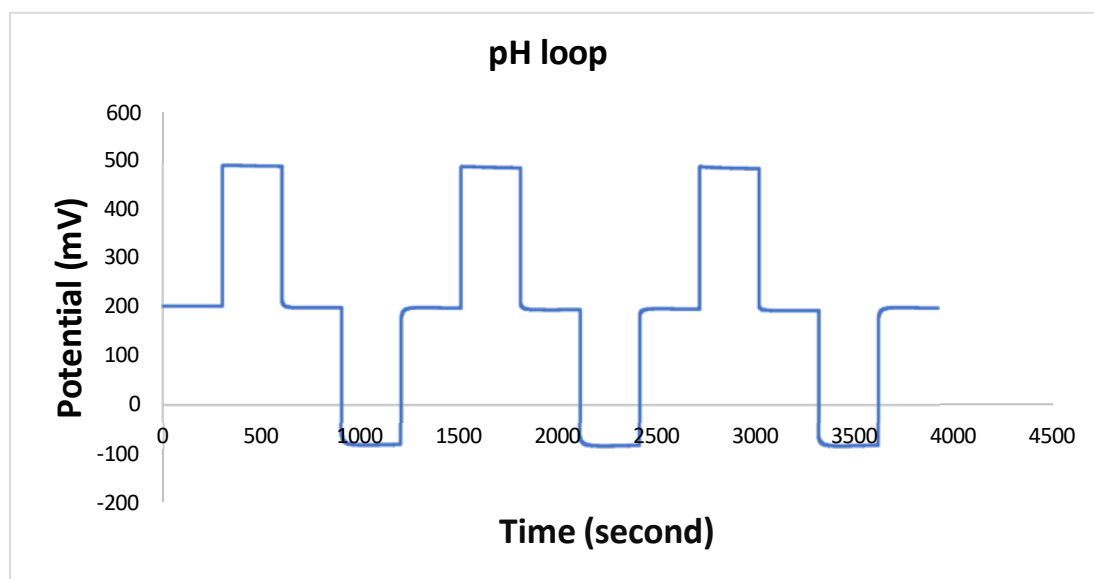
pH loop

(**b**)

Figure 2 - (a) Linear calibration plot for pH sensor from pH 2 to 12, (**b**) pH loop cycled 7-2-7-12-7 three times, using potential data versus time for TiN working electrode in pH 7 buffer vs. glass reference electrode.

The specific construction of the TiN + Nafion sensor reported here has resulted in several advantages compared to the solid-state electrodes previously reported [14]. The biggest advantage is that almost all the sputtered material is used, hence, there is no wastage, and this also allows for uniform production of bulk number of electrodes.

The 85 nm-thick TiN + Nafion pH-sensitive electrode was deposited at a pressure of 2 mT and a gas ratio of 1:9 Ar: N_2 to study the effects of redox agents. Then, 1 mM ascorbic acid or MnO_4 were added to buffer solutions. As shown in Figure 3, the electrode was calibrated at pH 7 (with a redox agent) for 15 min before pH was looped 3 times from 7-2-7-12. As shown in Figure 3, in neutral and reducing conditions, the shift in the redox potential has now been significantly minimized (2 mV) as an expected outcome. This is exactly the outcome we were hoping to achieve. Unfortunately, when pH measurements were performed in buffer solutions with oxidizing redox agents, there was still potential shift close to 45 mV. However, the good news is that the shift was stable over that range of pH values and, more importantly, the shift was smaller than for TiN without the Nafion protection.
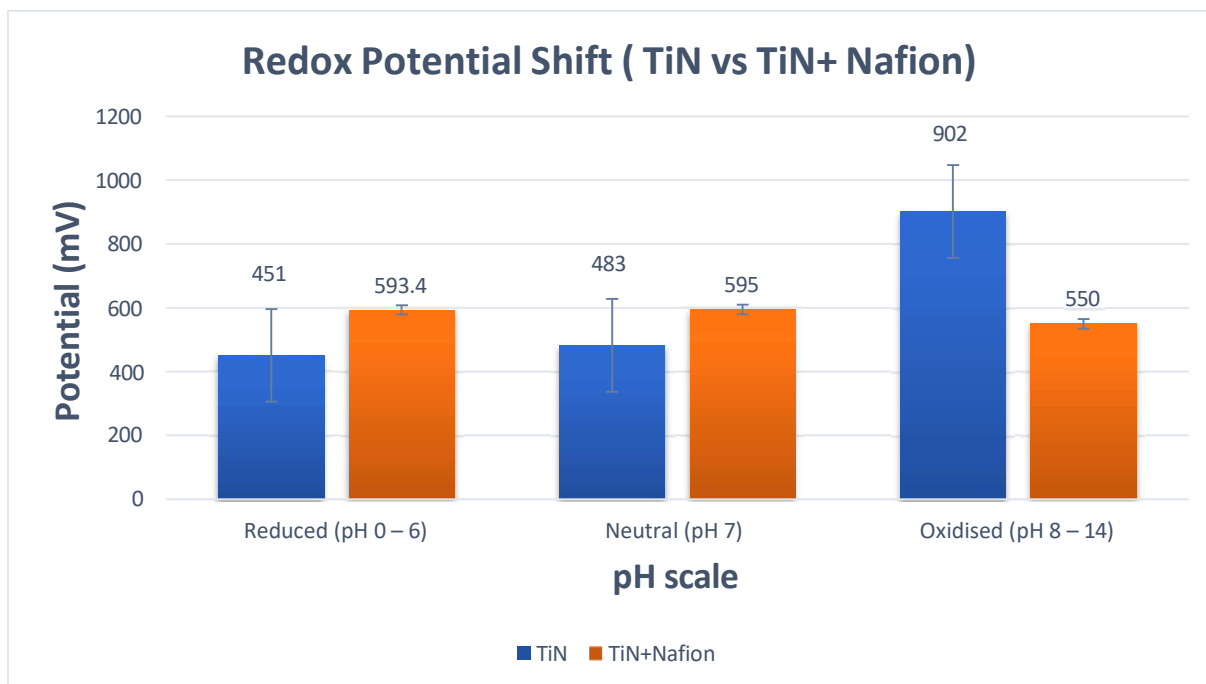
Figure 3 - Potential versus different matrices for TiN and TiN + Nafion working electrode.

Careful examination of the data in Figure 3 confirms that the TiN + Nafion electrode's behavior in different redox solutions corresponded to a change in the E* value while maintaining Nernstian sensitivity, as shown in Figure 2. When exposed to a new test solution, the potential for each pH measurement quickly changed and equilibrated within 30 s, after which the observed potential started to drift. The pH sensitivity of the electrode can be determined using the difference between the final reading from the previous measurement and the 30 s equilibrated value, as shown in Figure 2, assuming that this drift is caused by a shift in E* rather than sensitivity.

6.3.3 Drift rate

TiN + Nafion electrodes were subjected to various pH conditions, ranging from 2 to 12 for varied reaction periods (15, 60, 120, or 240 min), to investigate the drift effect. The drift of the electrodes obtained in pH = 2 and pH = 12 solutions showed an apparent decrease from 36.18 to 6.4 mV/h and 22.53 to 5.16 mV/h, respectively, as shown in Table 3, with an increase in reaction time from 15 to 240 min. The TiN electrode drifted considerably more than we expected, which may be attributed to the high resistance and inherent characteristics, such as the TiO_2 sheets [8]. Yusof [9] reported that TiO_2-sensing membrane fabricated using the RF sputtering method has a drift of 4.41 mV/h. However, when TiO_2 film was doped with ruthenium metallic ions, using a co-sputtering system to decrease the resistivity and increase its carrier mobility, that resulted in a very low drift effect of only 1.67 mV/h. In conclusion,

the TiN + Nafion electrode exhibits good stability with increased reaction time, which means that the sensor reaches its equilibrium when reaction time is increased, and hence, acceptable drift of 7 mV/h (average across pH 2 to 12) is achieved. The longevity of the sensor beyond 6 months remains a further area of study.

Table 3 - Drift of TiN electrodes treated using different pH parameters.

pH	Reaction Time (min)			
	15	60	120	240
2	36.16 mV/h	15.22 mV/h	9.32 mV/h	6.20 mV/h
4	18.26 mV/h	12.54 mV/h	10.33 mV/h	7.88 mV/h
7	15.33 mV/h	12.45 mV/h	9.44 mV/h	4.22 mV/h
10	42.56 mV/h	34.88 mV/h	19.73 mV/h	12.45 mV/h
12	22.43 mV/h	9.36 mV/h	7.11 mV/h	4.26 mV/h

6.3.4   Hysteresis

Previous work by Fog and Buck [17] showed the hysteresis width of the TiN pH sensors to be 30 mV in the cycle of 2-12-2. The hysteresis width of TiN pH electrodes has only been briefly described in previous research papers [30,32,39]. The TiN electrodes manufactured here have a comparatively high hysteresis. For 5 µL of Nafion, 60 min hysteresis was 17.6 mV to 19.3 mV, and for 120 min, hysteresis was 8.9 mV to 11.4 mV, and for 10 µL, 60 min hysteresis was 10 mV to 10.5 mV, and for 120 min, it was 7.3 mV to 9.5 mV [17]. This is higher when compared to other metal-oxide-based pH-sensitive electrodes. According to previous research [39], a magnetron-sputter-fabricated RuO_2 pH sensor has a hysteresis of 6.4 mV in the loop of 7-4-7-10-7 and 5.1 mV in the loop of 7-10-7-4-7, and for electrodeposited iridium oxide, the pH sensor ranges from 0.5 to 1.5 mV.

With repeatability based on the characterization studies, the ideal manufacturing parameters for the super-hydrophilic TiN pH electrode were determined to be 9.29 mV/h and 120 min. In addition, these conditions displayed the highest sensitivity of 54.13 mV/pH, the fastest response of 18.1 s in the pH range of 4 to 12, a tolerable drift of 9.29 mV/h, and the widest hysteresis at 11.4 mV. A new series of electrodes was then created to test the reproducibility of these electrodes. For each pH level, the new series of electrodes displayed steady and consistent response potentials and showed a comparable Nernstian response, with a sensitivity of 54.55 and 56.58 mV/pH. Thus, the discrepancy in the sensitivity for the various

manufactured electrodes was less than 1.95 mV/pH, indicating very good repeatability when compared with previously reported electrodes [38].

6.3.5 Real samples application

To determine the performance of the TiN + Nafion electrode in strong reducing and oxidizing matrices, various real samples were tested. Consequently, an 85 nm TiN + Nafion electrode (2 m Torr, 1:9 Ar: N_2) was tested in solutions such as coke, beer (Corona), white wine (McWilliams), red wine (McWilliams), iced tea (Lipton), orange juice (Golden circle) and fresh lemon juice. Firstly, the sensor was rinsed with deionized water and equilibrated in pH 4 or 7 buffer standard for 90 s to obtain a standard value for single-point calibration of the sensor's E* value [7]. Calculations were performed using the sensitivity of
−56.6 mV/pH, as determined previously. Sample pH values were calculated using the pH sample equation [11]. The equation and buffer standard were chosen to minimize the pH difference between the standard and sample tests to provide the highest accuracy of the single-point calibration [7].

Figure 4 compares the pH readings obtained using a commercial glass pH sensor and an 85 nm TiN electrode to those obtained using the TiN + Nafion. The results shown in Figure 4 illustrate that there is excellent consistency between the pH values obtained using this measurement methodology and those obtained using a commercial glass pH sensor (EU Tech). These experimental findings show that a variety of sample matrices can be used with TiN + Nafion electrodes. As mentioned earlier, the RuO_2 sensor exhibited ±300 mV shifts in potential and instability in many of the samples, resulting in a poor performance. The TiN + Nafion sensor developed here shows improved performance, with pH values on average within 0.25 pH units of the commercial glass electrode. In addition, the TiN + Nafion sensor outperforms the differential pH sensor developed by previous researchers because it exhibits significantly less potential shift of 2.1 mV (595 mV − 593 mV = 2 mV), as shown in Figure 3.
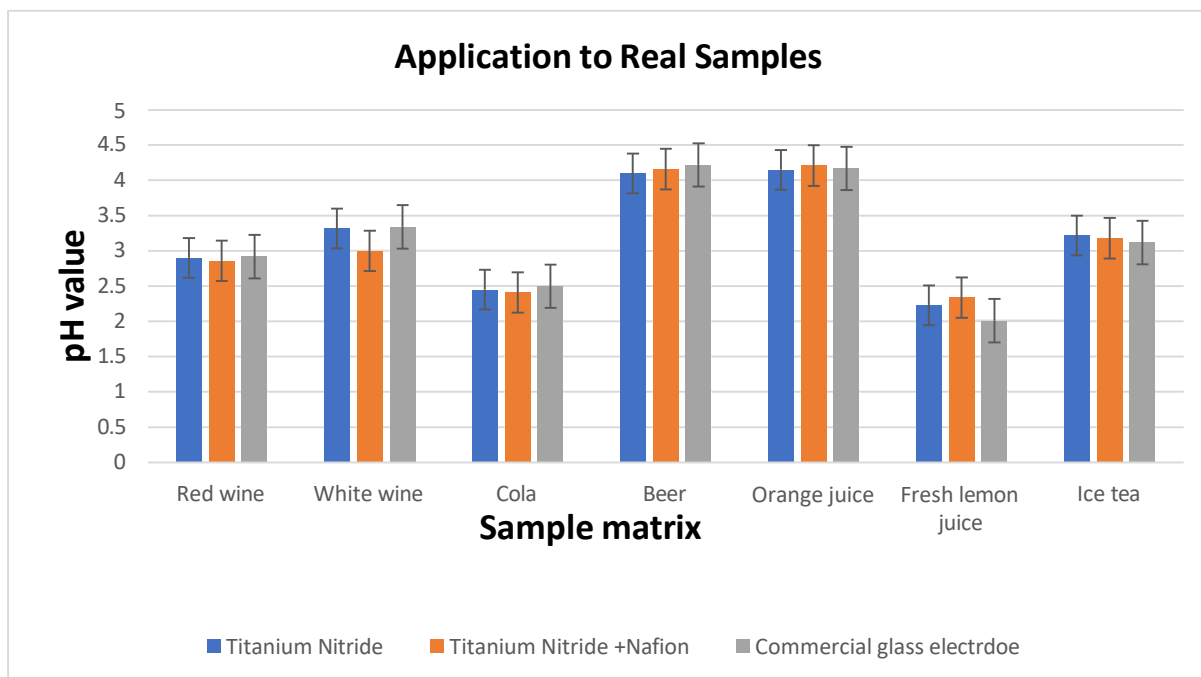
Figure 4 - pH values determined using 85 nm TiN electrode with the developed TiN + Nafion and using a commercial glass pH sensor for seven samples.

Accurate pH measurement of the samples, such as white wine and fresh citrus juice, using solid-state electrodes has not been feasible before due to the presence of ascorbic acid and other redox active compounds, such as preservatives. These types of samples cause large shifts in potential due to the oxidization/reduction of the working electrode [7]. The result of our work demonstrates that a differential pH sensor based on TiN film with Nafion coating can function as a reliable pH sensor in matrices that have been previously problematic [42].

6.4   Conclusions

An all-solid-state potentiometric pH sensor was successfully developed, which employs a thin-film sputter-deposited TiN + Nafion (spin coated) working electrode and an Ag|AgCl|KCl glass electrode as a reference. A durable pH-sensitive electrode has been manufactured entirely from sputter-deposited TiN using a TiN sputter target at 2 m Torr gas chamber pressure and with 1:9 Ar: O_2 gas ratio. It has been demonstrated here that the TiN/Nafion sensor can be used to overcome redox interference and can give accurate (precision of ±0.25 pH units) pH values in samples, such as wine and fresh citrus juice, where metal-oxide type pH sensors were previously unable to accurately measure. Experimental results have shown that the sensor we developed not only exhibits a Nerstian linear pH response (-56.6 mV/pH, $R^2 = 0.9999$), but

also has excellent reproducibility (hysteresis < 2 mV) without the need of sample calibration, unlike previous sensors. Additionally, only with a single-point calibration measurement protocol, the sensor can attain a moderate level of accuracy (±0.25 pH) when applied to cola, milk, yogurt, and beer samples.

Experimental results have demonstrated that, for orange juice and wine samples, with the TiN, the electrode potential shift is reduced and an improved accuracy of ±0.25 pH can be attained. Manufacturing of TiN is considerably cheaper than RuO_2 and Pt and Au electrodes, which are also robust, accurate and cheaper than standard glass electrodes. Additionally, the measurement protocol is well suited for low-throughput analysis, particularly by unskilled operators, which may be utilized for domestic applications. Further miniaturized development of this electrode and validation with biological samples could see this electrode be applied in the medical field, especially in situations where current glass electrodes cannot be used due to fragility and size constraints. For example, gastrointestinal reflux disease requires pH monitoring and currently diagnosis is conducted using endoscopy but developing this work into a nano capsule can help retrieve data by wireless signals from the sensor without any medical intervention.

6.5   References

1.   P. Kurzweil, Metal oxides and ion-exchanging surfaces as pH sensors in liquids: state-of-the-art and outlook, Sensors. 9 (2009) 4955–4985. doi:10.3390/s90604955.

2.   D. Maurya, A. Sardarinejad, K. Alameh, Recent Developments in R.F. Magnetron Sputtered Thin Films for pH Sensing Applications—An Overview, Coatings. 4 (2014) 756–771. doi:10.3390/coatings4040756.

3.   P. Riddle, pH meters and their electrodes: calibration, maintenance, and use, Biomed. Sci. April (2013) 202–205.
      https://www.ibms.org/includes/act_download.php?download=2013-apr-ph meters.pdf.

4.   K. Cheng, D. Zhu, On calibration of pH meters, Sensors. 5 (2005) 209–219. doi:10.3390/s5040209.

5.   S. Carroll, R. Baldwin, Self-calibrating microfabricated iridium oxide pH electrode array for remote monitoring, Anal. Chem. 82 (2010) 878–885. doi:10.1021/ac9020374.

6.   L. Manjakkal, B. Synkiewicz, K. Zaraska, K. Cvejin, J. Kulawik, D. Szwagierczak, Development and characterization of miniaturized LTCC pH sensors with RuO_2 based sensing electrodes, Sensors Actuators B Chem. 223 (2016) 641–649. doi: 10.1016/j.snb.2015.09.135.

7.   T. Nguyen, B. Journet, H. Takhedmit and G. Lissorgues, "Porous Titanium Nitride electrodes on miniaturised pH sensor for foetal health monitoring application," 2022 Symposium on Design, Test, Integration and Packaging of MEMS/MOEMS (DTIP), 2022, pp. 1-4, doi: 10.1109/DTIP56576.2022.9911738.

8.   W. Lonsdale, S. Shylendra, S. Brouwer, M. Wajrak, K. Alameh, Application of ruthenium oxide pH sensitive electrode to samples with high redox interference, Sensors Actuators, B. Chem. 273 (2018) 1222–1225. doi: 10.1016/j.snb.2018.07.022.

9.   L. Manjakkal, K. Cvejin, J. Kulawik, K. Zaraska, D. Szwagierczak, R. Socha, Fabrication of thick film sensitive RuO_2-TiO_2 and Ag/AgCl/KCl reference electrodes and their application for pH measurements, Sensors Actuators, B Chem. 204 (2014) 57–67. doi: 10.1016/j.snb.2014.07.067.

10.   L. Manjakkal, K. Cvejin, J. Kulawik, K. Zaraska, D. Szwagierczak, G. Stojanovic, Sensing of RuO_2–SnO_2 thick film pH sensors studied by potentiometric method and electrochemical impedance spectroscopy, J. Electroanal. Chem. 759 (2015) 82–90. doi: 10.1016/j.jelechem.2015.10.036.

11. W. Lonsdale, M. Wajrak, K. Alameh, Manufacture and application of RuO_2 solid-state metaloxide pH sensor to common beverages, Talanta. 180 (2018) 277–281. doi: 10.1016/j.talanta.2017.12.070.

12. Q. Dong; X. Sun; S. He, Iridium Oxide Enabled Sensors Applications. Catalysts (2021), 11, 1164. https://doi.org/10.3390/catal11101164

13. P. Awasthi, R. Mukherjee, S. P. O. Kare, S. Das, Impedimetric blood pH sensor based on MoS_2-Nafion coated microelectrode, RSC Advances 6 (2016) 102088 – 102095. doi:10.1039/c6ra17786g.

14. M. Lazouskaya, O. Scheler, V. Mikli, K. Uppuluri, K. Zaraska, M.Tamm, Nafion protective membrane enables using ruthenium oxide electrodes for pH measurement in milk. J Electrochem Soc 168 (2021) 107511-107522.

15. W. Lonsdale, M. Wajrak, K. Alameh, RuO_2 pH Sensor with Super-Glue-Inspired Reference Electrode, Sensors. 17 (2017) 2036-2047. doi:10.3390/s17092036.

16. I. Shitanda, H. Kiryu, M. Itagaki, Improvement in the long-term stability of screen-printed planar type solid-state Ag/AgCl reference electrode by introducing poly(dimethylsiloxane) liquid junction, Electrochim. Acta. 58 (2011) 528–531. doi: 10.1016/j.electacta.2011.09.086.

17. A. Fog, R. P. Buck, Electronic semiconducting oxides as pH sensors, Sensors and Actuators, 5 (1984), 137-146. doi:10.1016/0250-6874(84)80004-9.

18. P. Kinlen, J. Heider, D. Hubbard, A solid-state pH sensor based on a Nafion-coated iridium oxide indicator electrode and a polymer-based silver chloride reference electrode, Sensors Actuators B Chem. 22 (1994) 13–25. doi:10.1016/0925-4005(94)01254-7.

19. S. Chalupczok, P. Kurzweil, H. Hartmann, Impact of Various Acids and Bases on the Voltammetric Response of Platinum Group Metal Oxides, Int. J. Electrochem. 2018 10,1697956. doi:10.1155/2018/1697956.

20. E. Bakker, Hydrophobic Membranes as Liquid Junction-Free Reference Electrodes, Electroanalysis. 11 (1999) 788–792. doi:10.1002/(SICI)1521-4109(199907)11:10/11<788: AID-ELAN788>3.0.CO;2-4.

21. S. Paul Shylendra, W. Lonsdale, M. Wajrak, M. Nur-E-Alam, K. Alameh, Titanium Nitride Thin Film Based Low-Redox-Interference Potentiometric pH Sensing Electrodes. *Sensors, 21 (*2021) 42-59. https://doi.org/10.3390/s21010042.

22. G.V. Naik, J. L. Schroeder, X. Ni, A.V. Kildishev, T.D. Sands, A. Boltasseva, Titanium nitride as a plasmonic material for visible and near-infrared wavelengths Opt Mater Express, 2 (4) (2012), pp. 478-489.

23. H.-Y. Liao, J.-C. Chou, Fabrication and Characterization of a Ruthenium Nitride Membrane for Electrochemical pH Sensors. Sensors 9 (2009) 2478–2490.

24. J. H. Huang, K.-W. Lau, G.-P. Yu, Effect of nitrogen flow rate on structure and properties of nanocrystalline thin TiN films produced by unbalanced magnetron sputtering. Surf. Coat. Technol. 191 (2005) 17–24.

25. F.A. Sabah, N.M. Ahmed, Z. Hassan, M.A. Almessiere, Study effects of thin film thickness on the behavior of CuS EGFET implemented as pH sensor. DJNB 11 (2016) 787–93.

26. M. Nur-E-Alam, M.M. Rahman, M.K. Basher, M. Vasiliev, K. Alameh, Optical and Chromaticity Properties of Metal-Dielectric Composite-Based Multilayer Thin-Film Structures Prepared by RF Magnetron Sputtering. Coatings. 10 (2020) 251-265.

27. W.M. Mohammed, A.I. Gumarov, I.R. Vakhitov, I.V. Yanilkin, A.G. Kiiamov, S.S. Kharintsev, S.I. Nikitin, L.R. Tagirov, R.V. Yusupov, Electrical properties of titanium nitride films synthesized by reactive magnetron sputtering. J. Phys. Conf. Ser. 927 (2017) 012036 – 012036-5.

28. C.L. Li, B.R. Huang, S. Chattopadhyay, K.H. Chen, L.C. Chen, Amorphous boron carbon nitride as a pH sensor. Appl. Phys. Lett. 84 (2004), 2676–2678.

29. K.A. Yusof, N.I. Noh, S.H. Herman, A.Z. Abdullah, M. Zolkapli, W.F. Abdullah, pH sensing characteristics of silicon nitride thin film and silicon nitride based ISFET sensor. In Proceedings of the 2013 IEEE 4th Control and System Graduate Research Colloquium, IEEE, Shah Alam, Malaysia, 19–20 August (2013) 132–135.

30. Y.L. Chin, J.-C. Chou, Z.-C. Lei, T.-P. Sun, W.-Y. Chung, S.-K. Hsiung, Titanium Nitride Membrane Application to Extended Gate Field Effect Transistor pH Sensor Using VLSI Technology. Jpn. J. Appl. Phys. 40 (2001) 6311–6315.

31. D.I. Bazhanov, A.A. Knizhnik, A.A. Safonov, A. A. Bagatur'yants, M.W. Stoker, A.A. Korkin, Structure and electronic properties of zirconium and hafnium nitrides and oxynitrides. J. Appl. Phys. 97 (2005) 044108 – 044108-6.

32. Y.H. Chang, Y.-S. Lu, Y.-L. Hong, S. Gwo, J.A. Yeh, Highly Sensitive pH Sensing Using an Indium Nitride Ion-Sensitive Field-Effect Transistor. IEEE Sens. J. 11 (2011) 1157–1161.

33. Y.L. Jeyachandran, S.K. Narayandass, D. Mangalaraj, S. Areva, J.A. Mielczarski, Properties of titanium nitride films prepared by direct current magnetron sputtering. Mater. Sci. Eng. A 445-446 (2007) 223–236.

34. W. Lengauer, The Reactivity of Some Transition Metal Nitrides and Carbides; Wiley: Hoboken, NJ, USA, (2015) 1–24.

35. B.M. Gray, A.L. Hector, M. Jura, J.R. Owen, J. Whittam, Effect of oxidative surface treatments on charge storage at titanium nitride surfaces for supercapacitor applications. J. Mater. Chem. A 5 (2017) 4550–4559.

36. I. Shitanda, M. Komoda, Y. Hoshi, M. Itagaki, An instantly usable paper-based screen-printed solid-state KCl/Ag/AgCl reference electrode with long-term stability, Analyst. 140 (2015) 6481–6484. doi:10.1039/C5AN00617A.

37. L.J. Meng, M.P. dos Santos, Characterization of titanium nitride films prepared by d.c. reactive magnetron sputtering at different nitrogen pressures. Surf. Coat. Technol. 90 (1997) 64–70.

38. R.V. Babinova, V.V. Smirnov, A.S. Useenov, K.S. Kravchuk, E.V. Gladkikh, V.I. Shapovalov, I.L. Mylnikov, Mechanical properties of titanium nitride films obtained by reactively sputtering with hot target. J. Phys. Conf. Ser. 872 (2017) 012035-010235-3.

39. C.M. Zgrabik, E.L. Hu, Optimization of sputtered titanium nitride as a tunable metal for plasmonic applications.

40. M.K. Patan. Titanium nitride as an electrode material for high charge density applications (2007). Theses. 394. https://digitalcommons.njit.edu/theses/394.

41. C.M. Yang, H.N. Wang, S.F. Lu, C.X. Wu, Y.Y. Liu, Q.L. Tan, D.W. Liang, Y. Xiang, Titanium nitride as an electrocatalyst for V(II)/V(III)redox couples in all-vanadium redox flow batteries. Electrochemical Acta 182 (2015) 834–840. https://doi.org/10.1016/j.electacta.2015.09.155.

42. R. Umapathi, S.M. Ghoreishian, S. Sonwal, G.M. Rani, Y.S. Huh, Portable electrochemical sensing methodologies for on-site detection of pesticide residues in fruits and vegetables, Coord Chem Rev, 453 (2022).

CHAPTER 7   CONCLUSIONS AND FUTURE WORK

The first phase of this project (Chapter 4) reports a solid-state potentiometric TiN pH sensitive working electrode, which was developed and analysed by combining it with a commercial glass reference electrode. Various parameters, such as substrate type and film thickness of TiN were examined and optimized to improve the performance of the sensor. Four different substrates were tested by sputtering TiN using radio frequency magnetron on glass, silica, polyamide and alumina. Results have shown that alumina outperforms the other substrates by exhibiting the best adhesion and robustness in complex matrices. The optimised TiN film thickness has resulted in an 85 nm TiN film sensor exhibiting Nernstian sensitivity of -59.1 mV/pH, R^2 = 0.9997 and reproducibility of 1.2 mV. The sputtering parameters consisting of gas ratio, deposition time and sputter pressure have also optimised to achieve Nernstian sensitivity. The final optimized TiN electrode has been tested in highly redox media, exhibiting only a 30-mV potential shift which is almost four times less than the shift of previous solid state metal oxide electrodes, such as IrO_2. Testing the developed TiN sensor in real samples, such as wine and fresh orange juice, has demonstrated that this sensor is a potential candidate for overcoming redox interference.

In the second phase of the project (Chapter 5), a Nafion protection membrane was implemented to further minimise the redox shift of the TiN sensor. Previously, RuO_2 sensors needed to employ a thick Nafion membrane to reduce the redox shift, however, that considerably increased the reaction time to 136s of the sensor. Hence, this work examined a considerably thinner layer of Nafion by utilising a spin coating technique of applying only 5 μL of Nafion. This resulted in a sensor that was not only able to block the 30-mV redox shift from 115mV (RuO_2), but also decrease the reaction time from 136 s (RuO_2 with thick Nafion membrane) to 17 s in neutral pH, 38s in basic and 55 s in acidic solutions. Also, the Nafion membrane mitigated the potential shift to 2 mV/h. This makes the TiN/Nafion an excellent sensor for application in redox matrices without compromising the reaction time and Nernstian sensitivity. More importantly for the TiN/Nafion sensor there is no longer a need for any matrix matching method and lengthy calibration as required for other metal oxide sensors.

In the final part (Chapter 6) of the project, the successfully fabricated 85 nm TiN/Nafion pH electrode was tested in challenging matrices, such as wine and fresh orange juice. Previously, other solid-state sensors were unable to accurately measure pH in those samples. The Nafion

modified pH sensor was applied to real samples, such as cola, milk, yogurt, beer, red and white wine, orange juice and iced tea. The results showed that with only a single-point calibration measurement protocol, the sensor can attain a high level of accuracy of ±0.25 pH, which has not been achieved before with metal nitride sensors. The TiN/Nafion sensor exhibits a Nerstian linear pH response (-56.6 mV/pH, $R^2 = 0.9999$), and unlike previous sensors, achieved excellent hysteresis of 1.2 mV without the need for sample calibration. Manufacturing of TiN electrodes is considerably less expensive than conventional solid-state pH sensor electrode counterparts, such as RuO_2, Pt and Au.

The developed TiN/Nafion sensor is significantly advantageous compared to the traditional glass pH sensor, due to the solid-state structure, mechanical robustness, possibility of miniaturisation, reduced production cost, minimal maintenance, simple measurement protocol and good accuracy. Experimental results have shown that TiN/Nafion pH sensor outperforms other solid state sensor candidates with excellent pH characteristics even when applied to complex matrices. This broadens its application to operation in the pH range from 2-12, whilst maintaining Nernstian sensitivity.

Based on the findings from the research conducted throughout this PhD project, further improvements to the sensor could be made in the future, as follows:

1. The Nafion optimisation was carried out using only pH characteristics including sensitivity, linearity, and hysteresis. More precise techniques such as AFM and profilometry would provide a more detailed information regarding the precise thickness of the Nafion layer and surface roughness. This would help in understanding the relationship between Nafion layer and its performance in redox matrices.
2. The Nafion membrane could be further investigated by conducting more application specific interference studies in biological, environmental, and industrial samples.
3. Since pH sensitivity is dependent on temperature and humidity, further studies would be necessary to account for temperature and humidity fluctuations.
4. The current project focused on the development of solid-state titanium nitride pH working electrode using the standard Ag/AgCl glass electrode as the reference. Future studies could investigate other TiN compatible materials as reference, which are not as fragile as the glass electrode.

5. Ultimately, the gaol is to design a miniaturised pH capsule, which will comprise of both working and reference electrode, for wide range of applications. This project has paved the way towards this aim through the development of miniaturised solid-state sensor demonstrator.

APPENDIX

Statement of Contribution

To Whom It May Concern,

I Shimrith Paul Shylendra, conceived, designed, and undertook all experiments.
Shimrith Paul Shylendra analysed all data, interpreted results, and authored the publications.
Prof. Kamal Alameh, Dr. Magdalena Wajrak and Dr. Wade Lonsdale interpreted results and
edited the publications entitled:

- Paul Shylendra, S., Lonsdale, W., Wajrak, M., Nur-E-Alam, M., & Alameh, K. (2021).
  Titanium nitride thin film based low-redox-interference potentiometric pH sensing
  electrodes. *Sensors, 21*(1), article 42. https://doi.org/10.3390/s21010042
- Shylendra, S.P.; Wajrak, M.; Alameh, K.; Kang, J.J. Nafion Modified Titanium Nitride
  pH Sensor for Future Biomedical Applications. *Sensors* 2023, *23*, 699.
  https://doi.org/10.3390/s23020699
- Paul Shylendra, S.; Wajrak, M.; Alameh, K. Fabrication and Optimization of Nafion
  as a Protective Membrane for TiN-Based pH Sensors. Sensors 2023, 23, 2331.
  https://doi.org/10.3390/s23042331

Shimrith Paul Shylendra

I, as a Co-Author, endorse that this level of contribution by the Candidate indicated above is
appropriate.

Prof. Kamal Alameh
School of Science, Edith Cowan University, Joondalup, WA 6027, Australia

Dr. Magdalena Wajrak
School of Science, Edith Cowan University, Joondalup, WA 6027, Australia